Use of N_2O and its Isotopic Composition to Investigate Nitrogen Processes in Groundwater

by

Lin Li

A thesis
presented to the University of Waterloo
in fulfilment of the
thesis requirement for the degree of
Master of Science
in
Earth Sciences

Waterloo, Ontario, Canada, 2010

AUTHOR'S DECLARATION

I hereby declare that I am the sole author of this thesis. This is a true copy of the thesis, including any required final revisions, as accepted by my examiners.

I understand that my thesis may be made electronically available to the public.

ABSTRACT

This study explores the use of N_2O and its isotopic composition to investigate nitrogen processes in groundwater aquifers. Groundwater sampling was undertaken in 2008-2009 at two septic system sites (Long Point site and Lake Joseph site) and two agricultural sites (Strathroy site and Woodstock site). All of these four sites have been studied previously, and denitrification zones were identified by using NO_3^- isotopes. Extremely broad ranges of N_2O-N concentrations are present at septic system sites (1 to 1071 μg/L at Long Point and 0.1 to 106 μg/L at Lake Joseph). N_2O concentrations at the agricultural sites show lower levels and narrower ranges (0.1 to 3.3 μg/L at Strathroy and 14.6 to 40.5 μg/L at Woodstock site). However, N_2O-N concentrations at four sites except Strathroy are higher than the atmospheric equilibrium values (0.27 to 0.37 μg/L at 8 to 17°C) as well as N_2O-N values in surface water (0.2 to 1.2 μg/L, Grand River). This provides indication of N_2O production in subsurface in both septic system sites and agricultural sites. Using reported enrichment factors and measured ranges for NH_4^+ and NO_3^- isotopic values, ranges were calculated for the isotopic composition expected for N_2O produced by nitrification and denitrification.

At Long Point site, $\delta^{15}N$-N_2O and $\delta^{18}O$-N_2O ranging from -43.9 to +24.9 ‰ and +20.6 to +89.4 ‰ indicates that nitrification is mainly responsible for N_2O accumulation in both proximal shallow and deep zones while some N_2O at the bottom of the aquifer is presumably produced from denitrification. After N_2O is produced in the plume core, $\delta^{15}N$ and $\delta^{18}O$ in N_2O reveal that N_2O is further consumed to N_2. Also, N_2O isotopic values cleanly show seasonal N_2O production shifted from mostly nitrification in early season to primarily denitrification in late season.

At Lake Joseph, $\delta^{15}N\text{-}N_2O$ and $\delta^{18}O\text{-}N_2O$ varying from -4.4 to -43.2 ‰ and +24.7 to +56.7 ‰ reveal that nitrification N_2O was mainly present in aerobic zone whereas denitrification zone was found in downgradient anaerobic area.

At Strathroy site, $\delta^{15}N\text{-}N_2O$ (+1.7 to -29.7 ‰) and $\delta^{18}O\text{-}N_2O$ (+33 to +65 ‰) show that N_2O in shallow aquifer (< 5m depth) is presumably derived from atmosphere and nitrification whereas in deep aquifer (>5m depth), N_2O formation occurs during denitrification.

At Woodstock site, $\delta^{15}N\text{-}N_2O$ (-4.7 to -15.9 ‰) and $\delta^{18}O\text{-}N_2O$ (+30.7 to +37.1 ‰) at Woodstock provide indication of N_2O production from a mixing of denitrification N_2O and tropospheric N_2O.

N_2O isotopic signatures are highly useful to identify N_2O sources which include nitrification, denitrification, and dissolution of atmospheric N_2O at both septic system sites and agricultural sites. Further, at Lake Joseph site and Woodstock site, denitrification evidence from NO_3^- concentration/isotopes is lacking but N_2O isotopes suggest the occurrence of denitrification. At Long Point site, N_2O isotopes indicated N_2O production was by denitrification occurred early in the season; however, no NO_3^- isotopic enrichment was t that depth until in late season. These sites provide evidence that N_2O is an early and sensitive indicator of denitrification in groundwater at both septic system and agricultural sites. Additionally, N_2O isotopes are valuable for detecting N_2O consumption whereas NO_3^- isotopes cannot provide insight into this process.

ACKNOWLEDGEMENTS

I would like to thank my co-supervisors, Dr. William D. Robertson and Dr. John Spoelstra for their endless guidance and help during my graduate study. Special thanks to Dr. William D. Robertson who took me to the field sites to do groundwater sampling and helped me editing my thesis over and over again.

I would like to thank the members of my committee, Dr. Sherry Schiff and Dr. Ramon Aravena, for their suggestions and support.

Laboratory analysis support provided by Richard J. Elgood, Justin Harbin, Nicholas Flinn, Dave Dilworth, Brent Labenzy, Xu Zhang, and Yuxuan (Ariel) Guo, special thanks to Clarence Lo, who showed me how to extract N_2O and involved in collaboration in writing Method section (N_2O isotope analyses).

I would like to thank Adriana Rossi who provided geochemistry and isotope data from Lake Joseph to me.

I would like to thank my parents and all of my friends for everything they have done to support my graduate study

Funding for the study was provided by the Natural Sciences and Engineering Research Counsel of Canada (NSERC).

TABLE OF CONTENTS

LIST OF TABLES

LIST OF FIGURES

CHAPTER 1: INTRODUCTION

1.1 Nitrate contamination and Nitrification

Nitrate (NO_3^-) in groundwater, generated from the application of fertilizers and manure on agricultural fields and from waste water disposal via septic systems, has become one of the most common groundwater contaminants in Canada and elsewhere (Gillham and Cherry, 1978; Kreitler et al., 1979; Spalding and Exner, 1991; Bogardi et al., 1991; Komor and Anderson 1993; Wassenaar, 1995; Rudolph et al., 1998; Seiler, 2005). It is mobile and persistent in subsurface where oxygen is present (Robertson and Cherry, 1995). Shallow aquifer systems where sewage from septic systems is discharged often have high concentration of NO_3^--N (Aravena et al., 1993). This is because sewage which has elevated ammonium (NH_4^+-N) (~40 mg N/L) normally oxidizes to NO_3^- through nitrification in the unsaturated zone under septic system tile beds (Harman et al., 1996; Aravena and Robertson, 1998) as follows:

$$NH_4^+ + 2O_2 \rightarrow NO_3^- + 2H^+ + H_2O \qquad (1)$$

Septic system derived NO_3^--N in shallow aquifers can exceed the drinking water limit (10mg/L, Walker et al., 1973; Robertson and Cherry, 1995; Harman et al., 1996; Seiler, 2005). The application of fertilizers to the agricultural farms in the past decades significantly increases the nitrogen loading to groundwater systems. In Ontario, 14% of farm wells have NO_3^--N concentrations that exceed the drinking water limit (Goss et al., 1998). NO_3^--N concentrations in excess of this limit can cause methemoglobinemia (blue baby disease) (U.S. EPA, 1976). In aquatic environments, high concentrations of NO_3^- can initiate algal blooms in surface water, which is harmful to aquatic life (Vandenhoff, 2007). As a result of agricultural activity in the

US Midwest, Goolsby et al., (2001) has noted that the NO_3^- flux in the lower Mississippi River has more than doubled in the last several decades which has negatively affected the trophic status of the Gulf Mexico. In addition, nitrogen loading to groundwater in agricultural areas is continuing, thus NO_3^--N concentrations are increasing with time in many areas (Heagle, 2000). As a result, more and more drinking water wells could develop elevated levels of NO_3^--N in future if groundwater is not protected.

1.2 Denitrification

Denitrification is recognized as the most important microbial process that can attenuate nitrate contamination in groundwater. In anaerobic zones, when denitrifying bacteria and electron donors are present, NO_3^- is reduced to nitrite (NO_2^-), nitric oxide (NO), nitrous oxide (N_2O), and finally nitrogen gas (N_2). (Bremner 1997). The overall denitrification sequence of reactions is shown in Equation 2 (Appelo and Postma, 1996):

$$5CH_2O + 4NO_3^- + 4H^+ \rightarrow 5CO_2 + 2N_2 + 7H_2O \qquad (2)$$

However, denitrification does not occur in aerobic zones or when electron donors are inadequate and further, the rate of the process is often difficult to evaluate (Groffman, 2006). Consequently, a series of approaches have been developed to test for and measure denitrification. These include isotopic ^{15}N-enriched tracer methods, N_2 quantification, molecular biochemical methods, mass balance approaches, use of in situ environmental tracers (e.g. ^3H, CFCs), and natural abundance stable isotope methods (Groffman, 2006). However, use of stable isotopes (^{15}N and ^{18}O) in NO_3^- is

considered a specialized technique to identify denitrification in groundwater environments (Amberger and Schmidt, 1987; Mariotti et al., 1988; Böttcher et al., 1990; Aravena and Robertson, 1998). During the process of denitrification, enrichment of both ^{15}N and ^{18}O occurs in the residual nitrate because of a kinetic isotope effect; NO_3^- containing the lighter isotopes, ^{14}N and ^{16}O is preferentially consumed (Böttcher et al., 1990; Granger et al., 2004; Granger et al., 2008). In groundwater studies, denitrification enrichment factors ($\varepsilon_{(NO_3^- - NH_4^+)}$) in the range of -13.9 to -30 ‰ have been reported for nitrogen. The enrichment factor $\varepsilon_{(product - substrate)}$, is calculated using the following equation (Kendall and Aravena, 2000):

$$\varepsilon_{(product - substrate)} = \delta_{product} - \delta_{substrate} \qquad (3)$$

where $\delta_{product}$ and $\delta_{substrate}$ are isotopic values of product and substrate, respectively. It has been observed that, as denitrification progresses, $\delta^{15}N$ and $\delta^{18}O$ values of the residual NO_3^- increase in ratio of approximately 2:1 as NO_3^- concentrations decrease (Vogel et al., 1981; Bottcher et al., 1990; Aravena and Robertson, 1998; Mengis et al., 1999; Granger et al., 2008).

1.3 N_2O

N_2O is one of the greenhouse gases (GHG) involved in global warming (Russow and Neue, 1999). It has a global warming potential approximately 300 times that of carbon dioxide (CO_2) (IPCC 2007). The level of N_2O in the atmosphere in 1999 was 320ppb (v/v) and continues to increase at a rate of 0.25 % per year (Denman et al., 2007). N_2O sources are both anthropogenic and natural (Table.1.1). Among anthropogenic sources, agricultural activities are responsible for ~36 % of total N_2O production. N_2O generated naturally from ocean and soils accounts for ~20 % and ~40 %, respectively. Production data from various sources in 1994 showed a

clear trend that anthropogenic sources were becoming increasingly important compared with previous measurement in 1990 (Olivier et al., 1998; Mosier et al., 1998; Kroeze, 1999; Stein and Yung, 2003).

The atmospheric equilibrium N_2O concentrations can be calculated using henry's law. The calculation method is provided in detailed in Table 1.2. The groundwater temperature ranges from 8 to 15 °C in southern Ontario, and calculated N_2O concentrations in groundwater in equilibrium with atmosphere vary from at 0.37 μg/L at 8 °C to 0.27 μg/L at 17 °C (Table 1.2)

N_2O can be produced during the processes of both denitrification and nitrification (Russow and Neue, 1999), (Fig. 1.1). During the process of nitrification, NH_4^- is oxidized first to hydroxylamine (NH_2OH) by nitrifying microorganisms in presence of O_2 (Thuss, 2008). Most NH_2OH is further oxidized to NO_2^-; however, a small fraction can also be oxidized to N_2O. During the process of denitrification, N_2O can be formed by two separate mechanisms: nitrifier-denitrification and dissimilatory denitrification (Snider et al. 2008). The reduction of NO_2^- to N_2O is called nitrifier-denitrification (Fig. 1.1). Dissimilatory denitrification refers to the reduction of NO_3^- to N_2 with N_2O as an intermediate and alternate product (Equation 2). The ratio of N_2: N_2O production during dissimilatory denitrification can vary with temperature, NO_3 concentration, availablility of electron donors (e.g. DOC), etc, and also only certain types of denitrifying microorganisms have the ability to convert N_2O into N_2 (Bouwan, 1990). Once produced and released into the environment, N_2O can persist as a reaction by-product that dissolves in groundwater and can be then released to the atmosphere upon groundwater discharge or it can be further reduced to N_2 (Thuss, 2008).

1.4 Stable Isotopes of N_2O

Stable isotopes of N_2O can be used to provide evidence for the source of N_2O production (Thuss, 2008). Average tropospheric $\delta^{15}N\text{-}N_2O$ and $\delta^{18}O\text{-}N_2O$ values are reported as +6.72 ‰ and +44.62 ‰, respectively (Kaiser et al., 2003; Snider et al., 2008). When N_2O is produced from nitrification, the $\varepsilon_{(N_2O\text{-}NH_4^+)}$ ranges from -45 to -66 ‰ (Shearer and Kohl, 1986; Yoshida, 1988; Kendall, 1998; Pérez et al., 2001; Stein and Yung, 2003; Sutka et al. 2006), indicating that a large depletion of ^{15}N occurs in the produced N_2O relative to the NH_4^+ source. However, when N_2O is formed in the process of dissimilatory denitrification, reported nitrogen fractionation factors $\varepsilon_{(N_2O\text{-}NO_3^-)}$ are substantially lower varying from -9 to -37 ‰ (Martiotti et al. 1982); -20 to -29 ‰ (Snider et al., 2008); and -30 to +10 ‰ (Perez et al. 2001). The ^{18}O fractionation factor is not as well documented, however, Casciotti et al. (2002) report an $\varepsilon_{(N_2O\text{-}NO_3^-)}$ value of +40 ‰ and Snider et al. (2009) determine a range of $\varepsilon_{(N_2O\text{-}NO_3^-)}$ values from +37 to +43 ‰. In a laboratory experiment conducted by Menyailo and Hungate (2006), it was found that the ratio of $\delta^{18}O$: $\delta^{15}N$ for N_2O production through denitrification varied from 1.6 to 2.7, depending on soil type. The process of further reduction of N_2O to N_2 is referred to as N_2O consumption. During N_2O consumption, $\varepsilon_{(N_2O\text{-}N_2)}$ ranges from -1 to -27 ‰ (Yoshida, 1984) whereas the ratio of $\delta^{18}O$:$\delta^{15}N$ is relatively constant at 2.5 (Mandernack, 2000; Menyailo and Hungate 2006; Viten et al. 2007).

1.5 Research Objectives

The principle research objective for this study is to explore the use of N_2O and its isotopic composition to sort out nitrogen cycles in groundwater. Previous studies have not yet explored the use of N_2O for this purpose in groundwater systems. The

understanding of N_2O concentrations and isotopic composition in groundwater is currently very limited. Measuring $\delta^{18}O\text{-}NO_3^-$ and $\delta^{15}N\text{-}NO_3^-$ values is the widely used approach to test for denitrification (e.g. Mengis et al., 1999). However, substantial NO_3^- loss (greater than about 25 %) may be necessary before the change of isotopic composition in the residual NO_3^- is sufficient to be definitive of denitrification. In contrast, dissolved N_2O analyses by headspace gas chromatography has a detection limit about (~0.1 μg/L) and are therefore approximately 5,000 times more sensitive than that of nitrate. Almost as early as denitrification starts, very small amount of N_2O produced from denitrification can be detected. This is much earlier than the detection from NO_3^- tools. For these reasons, assessing accumulation of N_2O could be a more sensitive method for determining denitrification activity in groundwater than analyzing for NO_3^- loss. Though both nitrification and denitrification can produce N_2O, isotopic composition of N_2O can be used to distinguish these two pathways because N_2O formed during nitrification is more depleted (Thuss, 2008; sutka et al., 2006).

The objective of the current study is to determine the usefulness of N_2O and its isotopic composition assessing nitrogen processes in groundwater at four different NO_3^- - impacted field sites in Ontario. The Long Point and Lake Joseph sites are impacted by on-site wastewater disposal in septic systems; the Strathroy and Woodstock sites are impacted by agricultural activity. All of these sites have been investigated previously using NO_3^- isotopic methods (Aravena and Robertson, 1998; Heagle, 2000; Sebol et al., 2007; Rossi, 2010) and in each case, zones of denitrification are indicated. The current study presents new field data from each of these sites, particularly measurements of N_2O concentrations in and around these known areas of groundwater NO_3^- loss, and accompanied by isotopic characterization

of such N_2O where present. This data provides a preliminary indication of whether or not N_2O can be used as a tool to investigate nitrogen processes in groundwater.

CHAPTER 2: METHODS

2.1 Field Methods

Prior to groundwater sampling, all of the piezometers were purged with a peristaltic pump, an amount at least three volumes of the sampling tubing to get rid of stagnant water. Before sample collection in most cases, groundwater temperature (T), electrical conductance (EC), pH and dissolved oxygen (DO) were measured before groundwater was exposed to atmosphere. EC and T were measured using an Oakton Acorn CON 6 Conductivity/ºC meter (Oakton Instruments, Vernon, IL). Measurement of pH was performed using a Barnant 20 digital pH meter (Barnant, Barrington, IL) calibrated using buffers of pH 4 and 7. DO was measured in field using HQ20d Dissolved Oxygen meter (Hach Company, Loveland, CO). All groundwater and tank samples for chemical and isotope analyses were filtered inline (0.45 μm) with the exception of NH_4^+ concentration and isotope ($\delta^{15}N$) samples, which were unfiltered.

Groundwater samples for dissolved N_2O concentration and isotope analyses were collected in 60 mL and 160 mL serum bottles, respectively. Bottles were filled with groundwater to overflowing, and then a rubber stopper (Vaccutainer ^{TM}) with a hypodermic needle inserted was put into the bottle to release excess air and water as well as prevent atmospheric exposure (Vandenhoff, 2007; Thuss, 2008). Needles were then subsequently removed and stoppers were sealed with tape. N_2O samples were preserved immediately by injecting 0.2 mL and 0.4 mL of saturated $HgCl_2$ solution for concentration and isotope analyses, respectively.

Groundwater samples were collected in three identical 30 mL plastic bottles for cations, NH_4^+ and anions+DOC analyses. Samples for cations and NH_4^+ were acidified with HNO_3 and H_2SO_4 to pH< 2 and pH 5-6, respectively. Anions+DOC samples were left untreated.

1L plastic bottles were filled with groundwater for NO_3^- isotope analyses. Samples were filtered (0.45 μm) in the field but were not preserved.

All groundwater samples once collected and preserved were placed in cooler filled with ice and transported back to the lab. Samples for NO_3 isotope analyses were then frozen until analysis. Other samples were kept in cold room (4 ºC) until analysis.

2.2 Laboratory Methods

2.2.1 Cation Concentrations

Major cations (Al^{3+}, Ca^{2+}, K^+, Mg^{2+}, Na^+) were analyzed at Canadian Centre for Inland Waters (CCIW), Burlington, Ontario, utilizing an Inductively Coupled Plasma (ICP) technique, which provided a detection limit of 0.005 – 0.01 mg/L for each of these cations.

2.2.2 Anion Concentrations

Major anions (NO_3^-, Cl^-, SO_4^{2-}, Br^-, PO_4^{3-}, F^-) were analyzed by ion chromatography using a Dionex ICS-90 (Dionex, Sunnyvale, CA) in the Environmental Geochemistry Laboratory (EGL), University of Waterloo. The detection limit was <0.5 mg/L for each of those anions.

2.2.3 NH_4^+ Concentrations

NH_4^+ concentrations were completed using an automated colorimetric technique with a Technicon TRAACS-800 auto-analyzer (Technicon Instruments, Tarrytown, NY), which provided a detection limit of 0.02 mg/L (Robertson et al., 2008). NH_4^+ analyses were performed both in the EGL, University of Waterloo, and at the Soil and Nutrient Laboratory, University of Guelph.

2.2.4 DOC Concentrations

Dissolved organic carbon (DOC) analysis was performed at the EGL, using a Dorhman DC-190 High Temperature Total Carbon analyzer (Rosemount Analytical Inc. Santa Clara, CA) which provides a detection limit of 0.5 mg C/L. Samples were first acidified by adding 20 % phosphoric acid and sparging with oxygen to remove inorganic carbon (Thuss, 2008). DOC was then measured as CO_2 on a non-dispersive infrared (NDIR) spectrum after combustion at 680 ^{o}C. DOC concentrations were calibrated using a set of three potassium hydrogen phthalate (KPH) standards.

2.2.5 Dissolved N_2O Concentrations

N_2O analyses were performed in the EGL using a headspace equilibrium technique and a gas chromatograph (Thuss 2008). In brief, a pressurized headspace was created inside bottles by injecting 10ml of He into the samples while removing 5ml of water. The sample bottles were then shaken for about 90 minutes, allowing the dissolved N_2O to equilibrate with the headspace. The N_2O concentrations were then determined with an Electron Capture Detector (ECD) on a Varian CP 3800 greenhouse gas analyzer (Varian Canada, Inc.). Dissolved N_2O concentrations were then calculated according to Henry's Law (Thuss, 2008; Sander, 1999; Lide and Fredrikse, 1995). Given the analytical detection limit (100 ppbV) associated with the GC analysis, the detection limit and precision for dissolved N_2O analysis for this study was 0.1 μg N/L and ±0.2 μg N/L, respectively.

2.2.6 NO_3^- Isotope Analyses

NO_3^- isotopic values were determined in the EGL and EIL (Environmental Isotope Laboratory) using the technique described by Silva et al. (2000). $BaCl_2$ was first added to the sample to precipitate sulphate, and $BaSO_4$ was filtered out the day after addition of $BaCl_2$, after that, NO_3^- was then extracted from the samples by passing through Bio Rad AG 1-X8 anion resin columns (Aravena and Robertson, 1998). NO_3^- was removed from the resin columns by eluting with 15mL of 3M HCl solution and then converted to $AgNO_3$ by addition of Ag_2O, additional AgCl was removed by filtering, and solution was frozen to dry (Silva et al. 2000). $AgNO_3$ was then combusted to N_2 gas and CO_2 for $\delta^{15}N\text{-}NO_3^-$ and $\delta^{18}O\text{-}NO_3^-$ analyses, respectively (Silva et al., 2000). $\delta^{15}N\text{-}NO_3^-$ values were determined using a Carlo Erba 1108 CNOS Elemental Analyzer coupled to a Fisons Instrument Isochrom-EA mass spectrometer (GV Instruments, Manchester, UK); $\delta^{18}O\text{-}NO_3^-$ values were measured by breakseal combustion using a VG PRISM Series II mass spectrometer (GV instruments, Manchester, UK) (Spoelstra et al., 2001; Robertson and Schiff, 2008). The isotopic values are reported in the standard delta(δ) notationin units of per mil (‰) relative to the reference standards of atmospheric N_2 for $\delta^{15}N$ and Vienna Standard Mean Ocean Water (VSMOW) for $\delta^{18}O$ (Robertson and Schiff, 2008). The analytical precision for $\delta^{15}N\text{-}NO_3^-$ and $\delta^{18}O\text{-}NO_3^-$ are ± 0.1 ‰ and ± 0.2 ‰, respectively (Spoelstra et al., 2001).

2.2.7 NH_4^+ Isotope Analyses

The technique used for the isolation of NH_4^+ for N stable isotope analysis is a modified version of the acidified disk diffusion method (Brooks et al., 1989; Sørensen and Jensen, 1991). In brief, dissolved NH_4^+ in the sample was converted to NH_3 gas

in a sealed bottle. The NH_3 was subsequently trapped on an acidified quartz disk enclosed in a gas permeable, polytetrafluoroethylene (PTFE) membrane. The N isotopic composition of the diffusion disks containing the NH_4^+ as $(NH_4)_2SO_4$ were analyzed using a Carlo Erba 1108 Elemental Analyzer interfaced with a Thermo Instruments Deltaplus – IRMS (Thermo Fisher Scientific, Milan Italy). NH_4^+-N isotope ratios are reported in delta (δ) notation relative to atmospheric N_2. The uncertainty associated with the ^{15}N-NH_4^+ analysis was generally better than ± 0.3‰.

2.2.8 N_2O Isotope Analyses

Samples were preconcentrated using a purge and trap device (Thuss, 2008), in which samples were sparged with helium, and then gas passed through 20mL headspace vials, packed with glass beads and pyrex wool, while submersed in liquid nitrogen. The glass beads and pyrex wool were used to increase the surface area, and consequently increase the efficiency of cryo-trapping N_2O (Thuss, 2008). The vials were then over pressurized with helium and the extracted N_2O samples were then analyzed for $\delta^{15}N$ and $\delta^{18}O$ on an IsoPrime mass spectrometer, coupled with a Micromass TraceGas Pre-concentrator (GV instruments, Thermo Electron Corp., Manchester, UK), corrected and calibrated using an internal N_2O isotope standard (EGL-5) (Thuss, 2008). Again, ^{15}N and ^{18}O values are reported relative to atmospheric N_2 and VSMOW, respectively. The analytical precision for $\delta^{15}N$-N_2O and $\delta^{18}O$- N_2O are ± 0.4 ‰ and ± 0.2 ‰, respectively (Snider et al, 2008).

CHAPTER 3: LONG POINT SITE

3.1 Site Description

The Long Point study site is a conventional septic system that provides service for a campground in a provincial park situated on the north shore of Lake Erie, in southern Ontario, Canada. The campground has approximately 200 overnight campsites and opens seasonally from early May to late October (Aravena and Robertson, 1998; Robertson et al. 2000; Robertson, 2008,). All the effluent from a single comfort station with toilet, showers and laundry facilities drain into a septic tank and is then discharged to two different but similar-sized tile beds; tile bed 1 and tile bed 2 (approximately 290m^2 each) that discharge to an unconfined sand aquifer (Aravena and Robertson, 1998; Robertson, 2008). Tile bed 1 was used before 1990, then after that, all the sewage flow was directed into tile bed 2 during 1990-2007 except for 1995 and 1996, when effluent was diverted back to tile bed 1 (Robertson, 2008; Robertson *et al*., 2008). After 2007, flow was alternated between the two tile beds. The unconfined sand aquifer is 6m thick and sits on a silt layer (Aravena and Robertson, 1998). The sand aquifer has a carbonate mineral content of 18.5 wt% and a hydraulic conductivity of approximately 2×10^{-2} cm/s (Aravena and Robertson, 1998; Robertson, 2008, Stafford, 2008). During peak use in summer (late June to end of August), sewage loading to the tile bed was about 10 cm/day prior to 2007. Recently, loading has decreased to about 4 cm/day due to new water conservation measures. In 1990, prior to tile bed 2 commissioning, eight piezometer bundles were installed near tile bed 2 (Aravena and Robertson, 1998). Most of the piezometer bundles used in the current study (LP120-138) were installed along the section A-A' (Fig. 3.1) during 2003-2004 (Robertson, 2008). Site investigation and piezometer installation techniques are described in more detailed by Robertson and Cherry

(1992), Aravena and Robertson (1998) and Robertson (2008). In the previous study, Aravena and Robertson (1998) found that denitrification occurred naturally in the bottom part of the sand aquifer near tile bed 2 based on the complete attenuation of NO_3^--N concentrations of 50-100 mg/L accompanied by isotopic enrichment of δ^{18}O-NO_3^- and δ^{15}N-NO_3^- as the NO_3^--N concentrations decreased with depth. SO_4^{2-} concentrations increased and δ^{34}S-SO_4^{2-}, δ^{18}O-SO_4^{2-}, and δ^{13}C-DIC signatures suggested that pyrite and sediment organic carbon acted as electron donors for denitrification (Aravena and Robertson, 1998).

Groundwater samples were collected at septic tank and piezometer nests LP 120, LP 121, LP 122, LP 123, LP 124, LP 125, LP 135, LP 136, and LP 138 for major anions (NO_3^-, Cl^-, SO_4^{2-}, Br^-, PO_4^{3-}, F^-), cations (Al^{3+}, Ca^{2+}, K^+, Mg^{2+}, Na^+), NH_4^+, DOC, dissolved N_2O concentrations and isotopic analyses (NO_3^-, N_2O, NH_4^+) on June 17 and September 11, 2008. Br tracer was injected on July 4, 2008. In 2009, groundwater sampling was undertaken at septic tank and piezometer nest LP 100 (June 2, June 24, July 23 and October 13) for the same laboratory analyses as that of 2008.

3.1.1 Groundwater Flow System

The Long Point septic system is located within the small scale groundwater flow system associated with the Long Point sand spit which extends outward into Lake Erie for about 20 km and is ~500 m wide. The tile bed is positioned about 150 m from the southern (windward) shoreline of the sand spit, thus the groundwater flow direction is southward toward the southern shoreline, within the 6 m thick unconfined aquifer of medium sand. The horizontal groundwater velocity at the downgradient side of the tile bed was estimated previously at 23 m/yr based on EC breakthrough measurements over the 2004 summer season (Robertson, 2008). This velocity is

relatively low and stems from the location of the tile bed close to the groundwater flow divide, which runs along the spine of the sand spit. As a consequence of this location and the resulting weak horizontal velocities, the substantial wastewater loading to the tile bed (4-10 cm/day during peak use), produces vertical flow that is dominant and allows the plume to penetrate to the full 6 m depth of the aquifer (Aravena and Robertson, 1998). In the area downgradient of the tile bed, recharge rates are driven by natural precipitation and are much lower than for the tile bed. Based on the thickness of the clean water wedge overlying the plume in the downgradient area, vertical velocity from precipitation has been estimated previously at ~50 cm/yr at this site (recharge of ~20 cm/yr) (Robertson, 2008). The area around the tile bed consists of sand dunes and naturally vegetated grasslands with relatively pristine groundwater present.

3.2 Results

3.2.1 Cl^-

Cl^-, as a conservative tracer, is useful for distinguishing the plume from background groundwater at this site. Cl^- concentrations in the area below tile bed 2 (LP 120, LP 121, LP 122, LP 123) ranged from 43 to 75 mg/L in June, 2008 (Fig. 3.2a) and from 46 to 71 mg/L in September, 2008 (Fig. 3.2b). The distribution of Cl^- in the area about 10- 20 m down gradient from tile bed 2 (LP 138, LP 136, LP 135, LP 124) shows a much broader range of values (1 to 63 mg/L June, 2008 Fig. 3.2a; 6 to 62 mg/L September, 2008 Fig. 3.2b). The low values occur along the upper fringe of the plume and represent clean recharge from precipitation occurring downgradient of the tile bed.

3.2.2 Groundwater Age, Dissolved Oxygen (DO) and Groundwater Temperture

The plume age at Long Point is well constrained based on measurements of EC breakthrough and from two NaBr tracer tests undertaken previously (Robertson et al., 2010). The plume varies in age from approximately 7 days in the shallow water table zone under the tile bed during peak loading to about 130 days at the bottom of the plume and to ~ 300 days at the most distal monitoring location (LP 124), 17m from the edge of the tile bed (Fig. 3.3a). Dissolved oxygen (DO) concentrations below ~2m depth are consistently < 1mg/L, suggesting that the plume core zone below that depth is under anaerobic conditions (Fig 3.3b, Robertson et al., in prep.). Groundwater temperatures below the Long Point tile bed were consistently in the range of 12-14^{o}C during sampling in the summer and fall of 2009 (Robertson et al., in prep.; Robertson per comm).

3.2.3 NO_3^-

Figure 3.4a and 3.5a show NO_3-N distribution along section A-A' in June, 2008 and September, 2008, respectively. Both figures show high concentrations of NO_3-N below the tile bed (25-127 mg/L) but then values decrease abruptly at the depth of ~5m to <10 mg/L near the bottom aquifer. Also, in June 2008, a NO_3^--N "hole" with low NO_3^--N concentrations (0.1 to 4 mg/L) was evident at mid-depth (2.5-3.0m) in the two proximal nests LP 122 and LP 123. Background groundwater outside the plume boundary has NO_3^--N concentrations less than 5 mg/L. During four sampling profiles completed at nest LP 100 in 2009, there was again a mid-depth (2.6-4.5m) zone with low NO_3^--N concentrations in each case and in many cases NO_3^--N was fully disappeared in this zone (Fig. 3.6). The tank has very low NO_3^--N with values less than 0.1 mg/L (Robertson, et al., in prep.).

3.2.4 NO_3^- Isotopes

Figure 3.5b shows $\delta^{15}N\text{-}NO_3^-$ distribution on section A-A' in September, 2008. $\delta^{15}N\text{-}NO_3^-$ signatures can be roughly divided into two zones: a) proximal shallow zone (depth< 4m in plume core zone) with generally lower $\delta^{15}N\text{-}NO_3^-$ values ranging from +9 to +27 ‰, b) a proximal deep zone (depth> 4m) with more enriched $\delta^{15}N\text{-}NO_3^-$ signatures changing from +14 to +91 ‰. The four sampling profiles completed at nest LP 100 in 2009 (Fig 3.6) revealed that the most depleted $\delta^{15}N\text{-}NO_3^-$ values were observed in the shallow proximal zone (1.8-2.4m) and ranged from +1.5 to +12.6 ‰, with a mean of +6.3 ± 1.0 ‰ (n=13). Similarly, $\delta^{18}O\text{-}NO_3^-$ was also depleted in these samples and ranged from -4.8 to -2.1‰, with a mean of -3.5 ± 0.5 ‰ (n=5) (Fig. 3.6). These shallow $\delta^{15}N\text{-}NO_3^-$ signatures are comparable to $\delta^{15}N\text{-}NO_3^-$ values (approximately +6 ‰) reported in this zone previously (Aravena and Robertson, 1998). There is then an overall trend showing $\delta^{15}N\text{-}NO_3^-$ and $\delta^{18}O\text{-}NO_3^-$ becoming gradually enriched with depth. Substantial enrichment of both $\delta^{15}N\text{-}NO_3^-$ and $\delta^{18}O\text{-}NO_3^-$ occurs in the deepest piezometers at 5-6m depth (Fig. 3.4-3.6), with $\delta^{15}N\text{-}NO_3^-$ varying from +21.1 to +46.9 ‰; and $\delta^{18}O\text{-}NO_3^-$ varying from +6.9 to +18.3 ‰.

3.2.5 N_2O

N_2O distribution can be roughly divided into two zones. In June 2008, the bottom of the aquifer and the distal plume had low N_2O-N (< 84 μg/L) with the exception of LP 124-4.5m which had higher N_2O concentrations of 314 μg/L (Fig. 3.4b). The shallow proximal zone below the tile bed had relatively high concentrations of N_2O-N (242 to 798 μg/L) except for the NO_3^--N "hole" zone (2.6-3.4m b.g.s) which had lower N_2O-N levels of only 1-21 μg/L. N_2O-N distribution in

September, 2008 was quite different from that of June (Fig. 3.5c). The N_2O plume extended over a much larger area into the downgradient distal zone. The centre of the September N_2O plume had some very high N_2O-N levels of up to 1071 μg/L. The bottom of the aquifer remained depleted in N_2O-N (< 40 μg/L) during both 2008 sampling events. Profiling below the tile bed in 2009 N_2O also showed a N_2O pattern correlated to the NO_3-N distribution (Fig. 3.6). Peak N_2O-N values occurred at both the top and bottom of the mid depth NO_3-N depleted zone during each sampling event (e.g. 600-800 μg/L N_2O-N during the June 2 sampling. Again much lower values (<7 μg/L) were noted in the core of the NO_3-N depleted zones. N_2O-N concentrations decreased abruptly in the deepest zones during all four sampling events.

3.2.6 N_2O Isotopes

N_2O isotopic distribution in 2008 is shown in Fig.3.4Ec and Fig. 3.5Ed. In June, 2008, the proximal shallow zone had depleted $\delta^{15}N$-N_2O of -42 to -19 ‰ and $\delta^{18}O$-N_2O of +20 to +61 ‰. The proximal deep zone and the distal plume zone showed a general trend of more enriched $\delta^{15}N$-N_2O and $\delta^{18}O$-N_2O signatures (up to +31 ‰ and +96 ‰, respectively). A similar pattern was observed in September, 2008 (Fig. 3.5Ed). In the 2009 sampling profiles isotopic signatures are variable in the proximal shallow zone but then again below 4m depth, there is a clear trend of $\delta^{15}N$-N_2O and $\delta^{18}O$-N_2O enrichment.

3.2.7 SO_4^{2-}

In the shallow plume core zone during 2009 sampling episodes, SO_4^{2-} concentrations ranged from 14- 60 mg/L (Fig. 3.6). Substantially higher SO_4^{2-}

concentration with values as high as 152 mg/L occurred at the bottom of the aquifer in the basal denitrification zone (Fig. 3.6).

3.2.8 NH_4^+

Figure 3.4d and 3.5e show NH_4^+-N distribution during June and September, 2008, respectively. The tank has the highest concentration of NH_4^+-N (106 ± 17 mg/L, n=13, Sept 2007- Sept 2010) (Fig. 3.4d and Fig. 3.5e). During the June sampling episode, relatively high levels of NH_4^+-N up to 63 mg/L were observed in the proximal shallow zone below the tile bed, but NH_4-N values then decreased rapidly to 0.2 mg/L at bottom of the aquifer. Another area of relatively high levels of NH_4^+-N (1 - 10 mg/L) was found in the distal plume zone centred at nest LP 138. Groundwater outside the plume had low values of NH_4^+-N (~0.1 mg/L). Generally, much lower NH_4^+-N values were observed during the September event, particularly below the tile bed (generally < 1mg/L) (Fig. 3.5e). During sampling in 2009, similar trends were observed from June to October (Fig. 3.6); a mid-depth zone (~2.5 - 4 m) consistently had elevated NH_4^+-N of up to 70 – 110 mg/L (Fig. 3.6), but much lower values occurred below this depth.

3.2.9 DOC

Figs 3.4e and 3.5f show DOC distribution during June and September, 2008. In June, high concentrations up to 39.4 mg C/L were present at LP 122-mid depth coinciding with the NH_4^+- rich zone, whereas much lower values (about 2- 5 mg C/L) were present at greater depths (Fig. 3.4e). During September 2008, DOC concentrations throughout the transect were low (about 2- 7 mg C/L, Fig. 3.5f). DOC distribution in 2009 exhibited a pattern similar to June, 2008 with an elevated DOC

zone (about 10- 20 mg C/L) present at mid-depth (2.2 – 3.5m) below the tile bed (Fig. 3.6), and again, coinciding with the NH_4^+- rich zone.

3.3 Discussion

3.3.1 Plume Seasonal Transience

The Cl^- concentration of 30 mg/L is useful for outlining the boundary of the plume (Fig. 3.2). Seasonally, the plume in September, 2008 was increased in size, compared to June 2008, particularly along the upper fringe. This is due to the higher loading of sewage that occurs during the peak use in July and August.

3.3.2 Nitrification

There are two main processes that could lead to the loss of NH_4^+, which is the dominant form of nitrogen present in the raw septic system tank effluent. The first pathway is NH_4^+ nitrification to NO_3^- in presence of oxygen; the other pathway is through anaerobic ammonium oxidation (anammox) (Robertson et al., in prep.). NH_4^+-N concentrations in the tank are always much higher than it in the plume. NH_4^+-N concentrations in the shallowest piezometers close to water table show very low NH_4^+-N concentrations (0.1-0.3 mg/L, Fig. 3.5e). Thus, it is likely that most NH_4^+ is oxidized to NO_3^- in unsaturated zone during downward migration from the tile bed. However, on the Victoria Day weekend, sewage pulse started loading to the tile bed, nitrifiers were not active enough to nitrify NH_4^+; therefore, some of this initial NH_4^+ slug passed the nitrifiers and moved downward into the groundwater. The anammox reaction, however, requires an absence of oxygen, thus, if anammox is also active, this reaction most likely occurs in the deeper saturated zone which is suboxic (< 1 mg/L DO, Robertson et al., in prep.).

3.3.3 Denitrification

Substantial NO_3^--N decrease to < 10 mg/L is evident at the bottom of the plume below the tile bed (Fig. 3.4a, 3.5a and 3.6) and is accompanied by enrichment of $\delta^{15}N\text{-}NO_3^-$ and $\delta^{18}O\text{-}NO_3^-$ values. The isotope enrichment ratio of $\delta^{15}N\text{-}NO_3^-$ to $\delta^{18}O\text{-}NO_3^-$ is approximately 1.8:1 (Fig 3.9), which is close to the expected ratio of 2:1 for denitrification (Vogel et al., 1981; Bottcher et al., 1990; Aravena and Robertson, 1998; Mengis et al., 1999; Granger et al., 2008). A similar ratio (2.1:1) was reported at this site previously (Aravena and Robertson, 1998). It has been established previously that both pyrite and organic carbon act as electron donors during denitrification at Long Point (Aravena and Robertson, 1998). An abrupt increase in SO_4^{2-} at the bottom of LP 100 to approximate 150 mg/L (Fig. 3.6) correlates to zone where NO_3^--N is generally attenuated to < 10mg/L. This confirms that pyrite continues to act as an important electron donor for denitrification in the deep aquifer zone. Below 3m depth, elevated DOC concentrations of up to 14 mg/L gradually decline to about 2-4 mg/L indicating that DOC may also be contributing to denitrification (Fig. 3.6).

3.3.4 N_2O Concentrations and Isotopic Values in Long Point Groundwater Compared to Other Sites

Dissolved N_2O-N concentrations in groundwater at different field sites show extremely broad ranges (Table. 3.1); generally several orders of magnitude varying from 0.4 to up to 1071 μg/L at Long Point and 0.8 up to 1100 μg/L at the Putnam site, which is a field used for corn production and poultry manure composting in Ontario, Canada (McLean, 2007; Vandernhoff, 2007). The atmospheric equilibrium values at these two sites where groundwater temperatures are in the range of 8-17°C, should be only in the range of 0.27- 0.37 μg/L. Thus, in-situ N_2O production is clearly indicated

in the groundwater zone at these sites. The exception to these high values is Von der Heide et al. (2008) who reported a relatively narrow range of only 3 to 13 μg/L at Fuhrberger Feld catchment in Northern Germany. Groundwater sampling depths ranged from 2.0 to 6.3 m at Long Point, and from 1.2 to 4.0 m depth at Putnam site, but were shallower (0 to 3.4 m) at the Fuhrberger Feld catchment. N_2O-N concentrations vary significantly with depth at both Long Point and Putnam indicating that the amount of N_2O accumulated in the subsurface is sensitive to variable environmental factors. In addition, the isotopic values of N_2O ($\delta^{15}N$ and $\delta^{18}O$) also have substantially wide ranges at each site (e.g. at Long Point, $\delta^{15}N$-N_2O ranged from -42 to +31 ‰ and $\delta^{18}O$-N_2O ranged from +20 to +96 ‰) (Table 3.1). In contrast to these groundwater studies, N_2O-N concentrations and isotopic signatures in surface water have much smaller ranges, (e.g. in Grand River, N_2O-N concentrations ranged from 0.2 to 1.2 μg/L; $\delta^{15}N$-N_2O ranged from -5 to +6 ‰ and N_2O-$\delta^{18}O$ ranged from +38 to +49 ‰ Thuss, 2008). Thus, $\delta^{15}N$-N_2O and $\delta^{18}O$-N_2O signatures in groundwater appear to be more variable than in surface water and thus have the potential to be useful in indentifying sources and processes affecting N_2O accumulation and consumption in groundwater. However, the lack of N_2O isotopes variability in surface water does not mean studying N_2O is not valuable and useful in the surface water environment.

3.3.5 Factors and Processes Affecting N_2O Concentrations

A series of factors influence N_2O production. Those factors can be further divided into two groups: positive factors (increase N_2O concentrations) and negative factors (decrease N_2O concentrations). During the process of N_2O production from nitrification, NH_4-N and DO concentrations, as well as temperature increase the

nitrification rates (Strauss et al., 2002; Kemp and Dodds, 2002; Strauss and Lamberti, 2000). However, lower DO concentrations increase the N_2O: NO_3^- ratio of nitrification (i.e. more N_2O produced per NH_4^+ oxidized); therefore, DO can be positively and negatively correlated to N_2O production by nitrification, depending on the situation (Spoelstra, per comm). During the process of N_2O production from denitrification, positive factors include NO_3^--N concentrations (Kemp and Dodds, 2002; Garcia-Ruiz et al., 1998; Richardson et al., 2004), DOC concentrations (Richardson et al., 2004) and temperature (Garcia-Ruiz et al., 1998). Generally, presence of DO (Kemp and Dodds, 2002) is a negative factor that inhibits denitrification. However, when DO concentrations are low, denitrification can be incomplete and stop at N_2O phase because the redox is not low enough to allow N_2O production to N_2. In this case, the N_2O:N_2 ratio for denitrification increases (Spoelstra, per comm). Those factors have been studied in surface water systems, particularly in aquatic sediments, but little is known about how these environmental factors influence groundwater N_2O production. In groundwater systems, DO and temperature are relatively stable compared to surface water systems and thus may have more limited influence on N_2O-N variability. Rather, the extremely broad range of N_2O-N formed in groundwater systems indicates that N_2O-N accumulation is very sensitive to the other environmental situations. In 2008 and 2009 sampling profiles (Fig. 3.4, Fig. 3.5 and Fig. 3.6), N_2O-N distributions had very similar patterns to NO_3^--N and DOC distributions and showed an opposite pattern to NH_4^+-N distribution. This suggests that the presence of NO_3^- and NH_4^+ both contribute to N_2O accumulation in groundwater systems. In this case, N_2O is most elevated immediately above and below the mid-depth zone with substantially low NO_3^--N concentrations. The complete attenuation of NO_3^--N in this zone to < 0.1 mg/L provides strong

evidence that denitrification is active in this zone, presumably stimulated by the high DOC concentrations. Thus, the N_2O accumulation occurring immediately above and below this zone is very likely a consequence of denitrification rather than nitrification actively. The increase in SO_4^{2-} in the basal zone confirms that to denitrification is occurring in the deeper zone as well, using pyrite as an electron donor. This zone is also characterized by increased N_2O concentrations (e.g. 198-314 μg/L, nest LP 124, deep) (Fig 3.4b, 3.5c and 3.6).

The N_2O-N vs. NO_3^--N plots shown in Fig 3.7 do not indicate any simple clear trend of correlation. This is because N_2O can be produced from both nitrification and denitrification and further, N_2O is not the final product of those two processes, it can be consumed to N_2 depending on redox conditions (Spoelstra, per comm.). Therefore, it is reasonable that N_2O-N and NO_3^--N are not correlated directly to each other.

The $\delta^{15}N$- NO_3^- vs. NO_3^--N plots shown in Fig. 3.8a has an overall trend that isotopic enrichments related to decrease of NO_3^--N concentrations. A similar pattern is also shown in the $\delta^{18}O$- NO_3^- vs. NO_3^--N plots (Fig 3.8b). However, plots of N_2O isotopic values vs. N_2O-N do not reveal such correlation (Fig. 3.8c and 3.8d). This indicates that there is no direct relationship between N_2O isotopes and N_2O-N concentrations.

3.3.6 N_2O Isotope Data at Long Point

As N_2O can be generated from both nitrification and denitrification, it is important to distinguish these two processes. Stable isotope analysis of N_2O can be used to help distinguish N_2O production processes (Perez et al., 2001).

3.3.6.1 N_2O Production by Nitrification

The $\delta^{15}N$ isotopic enrichment factor $\varepsilon_{(N_2O\text{-}NH_4^+)}$, where the product here is N_2O and the substrate is NH_4^+ in the process of nitrification, is reported to be in the range of -45 to -66 ‰ (Stein and Yung, 2003) (Table. 3.2). The average $\delta^{15}N\text{-}NH_4^+$ value from tank at Long Point is +5 ‰ (n=7) (Robertson et al., 2010 in preparation). Using these reported enrichment factors and known ranges for the NH_4^+, ranges can be calculated for the isotopic composition expected for N_2O produced by the nitrification pathway using the following equation:

$$\varepsilon^{15}N_{(N_2O\text{-}NH_4^+)} = \delta^{15}N\text{-}N_2O - \delta^{15}N\text{-}NH_4^+ \qquad (4)$$

Assuming $\delta^{18}O\text{-}N_2O$ values are within a range of +23.5 ± 5 ‰ (Spoelstra, per comm), when N_2O is produced from nitrification, the nitrification "box" has hypothetical $\delta^{15}N\text{-}N_2O$ ranging from -61 to -40 ‰, and $\delta^{18}O\text{-}N_2O$ varying from +18.5 to +28.5 ‰ (Table 3.2, Fig. 3.9-3.11).

3.3.6.2 Vadose N2O values at Long Point

The N_2O concentrations in the vadose zone ranged from 1.3×10^5 ppb to 3.8×10^5 ppb (Table E3.3), three orders of magnitude higher than the average level of N_2O in the atmosphere (320 ppb). The N_2O concentrations at 1.8-2.0m depth on June 24, 2009 (the same date soil N_2O samples were taken) range from 112 to 193 μg/L in groundwater, which equates to 1.1×10^5 to 1.9×10^5 ppb air-equilibrium values when considering Henry's law. As vadose N_2O concentrations are higher, up to 3.8×10^5 ppb, more likely, N_2O production occurred in the vadose zone. Further, since there is almost no DO present in the groundwater, if any nitrification is involved to produce N_2O, it must be in the vadose zone. $\delta^{15}N\text{-}N_2O$ and $\delta^{18}O\text{-}N_2O$ from soil gas were measured 0.3 -1.0 m below ground surface on June 24, 2009 with mean values of -

20.85±0.09‰ (n=7) and +20.84±0.17‰ (n=7), respectively (Table E3.3, Fig. 3.11b). The soil $\delta^{15}N\text{-}N_2O$ and $\delta^{18}O\text{-}N_2O$ values are substantially different from the average tropospheric $\delta^{15}N\text{-}N_2O$ and $\delta^{18}O\text{-}N_2O$ signatures (+6.72‰, +44.62‰) (Kaiser et al., 2003), however, they are very close to the N_2O isotope values present at 1.8 to 2.0m depth (-20‰ for $\delta^{15}N\text{-}N_2O$ and +25‰ for $\delta^{18}O\text{-}N_2O$). Therefore, soil gas N_2O is more likely produced from nitrification within unsaturated zone and N_2O diffusion from groundwater. For this reason, the $\delta^{15}N\text{-}N_2O$ range expected for N_2O produced by the nitrification is adjusted to -21 to -61‰ (-21‰ is the average soil $\delta^{15}N\text{-}N_2O$ value in the vadose zone) (Table E3.3). This broadens the nitrification source ranges in ^{15}N which makes an overlap between nitrification and denitrification source boxes. If the soil N_2O information was not available, the $\delta^{15}N\text{-}N_2O$ ranges would be narrower. In this case, the wider range causes some data points to fall out of the nitrification source box..

3.3.6.3 N_2O Production by Denitrification

In the process of denitrification, the $\delta^{15}N$ isotopic enrichment factor $\varepsilon^{15}N_{(N_2O\text{-}NO_3^-)}$ has a range of values between -20 to -29 ‰ based on laboratory tests (Snider et al. 2008). $\varepsilon^{18}O_{(N_2O\text{-}NO_3^-)}$ varies from +32 to +48 ‰ (Table. 3.2) (Spoelstra, per comm). For denitrification, Fig. 3.9 illustrates that the $\delta^{15}N\text{-}NO_3^-$ at Long Point site has a range from 0 to 48 ‰ while the $\delta^{18}O\text{-}NO_3^-$ varies between -12 to +25 ‰. Using the measured NO_3^- isotope ranges (Fig 3.9) and the enrichment factors (Table 3.2), following the equation:

$$\varepsilon^{15}N_{(N_2O\text{-}NO_3^-)} = \delta^{15}N\text{-}N_2O - \delta^{15}N\text{-}NO_3^- \qquad (5)$$

the calculated range for the isotopic composition of N_2O produced by denitrification at Long Point site is -29 to +28 ‰ and +20 to +73 ‰ for $\delta^{15}N\text{-}NO_3^-$ and $\delta^{18}O\text{-}NO_3^-$, respectively (Table 3.2, Fig. 3.9-3.11).

3.3.6.4 N_2O Produced from Nitrification and Denitrification at Long Point Site

Plotting field $\delta^{15}N$ vs. $\delta^{18}O$ of N_2O on a diagram which contains expected nitrification and denitrification ranges can help in identifying the different possible sources of N_2O production. Three aquifer zones, the proximal shallow zone (< 4m in depth), the proximal deep zone (> 4m in depth) and the distal plume zone along the transect section A-A' further distinguish the N_2O isotopic data (Fig 3.4Ec and Fig. 3.5Ed). In late May to early June, wastewater loading was initiated to the tile bed and nitrification in the vadose zone was presumably active. Once produced, N_2O in the vadose zone can dissolve to groundwater and move downward to the saturated zone. Fig. 3.10a shows that early in the 2008 season, about half of the N_2O samples within the proximal shallow zone exhibit a nitrification signature. At greater depth under anaerobic conditions, N_2O then appears to be consumed as indicated by an enrichment ratio of $\delta^{15}N$:$\delta^{18}O$ close to 1:2.5 with N_2O-N concentrations decreased with depth (Fig. 3.4b and 3.10a). In the proximal deep zone, plotting of $\delta^{15}N$ vs. $\delta^{18}O$ indicated some N_2O was produced from nitrification. However, most of the N_2O isotopic values in proximal deep zone suggested that N_2O produced from nitrification was subsequently consumed and move along the 1:2.5 slope. (Fig. 3.10a) Figure 3.10b shows that late in the 2008 season, N_2O from nitrification moves outside of the source range along 1:2.5 slope by subsequent N_2O consumption. However, some data points within the denitrification box that do not follow 1:2.5 slope suggest that some N_2O is likely has an origin of NO_3^- from denitrification. This is consistent with the NO_3^-

evidence indicating occurrence of denitrification. To show seasonal trends of N_2O production in more temporal detail, four sampling snapshots from nest LP 100 (June 2-Oct 13, 2009) are shown on Fig. 3.11. Early June isotopic data from the shallow piezometers show clear nitrification-derived N_2O (Fig. 3.11a). In late June, nitrification still produces N_2O in the shallow zone, and in deeper aquifer zone, N_2O also appears to be formed from nitrification as most of N_2O isotopic data points move out of the nitrification box along N_2O consumption slope 1: 2.5, indicating that N_2O is being reduced to N_2 (Fig. 3.11b). Later in the season (July-October), denitrification continues to play an increasingly dominant role in producing N_2O and samples are almost absent from the nitrification box (Fig. 3.11c and 3.11d).

The large range in nitrification and denitrification boxes and the overlap between those two boxes are due to the large ranges of enrichment factors $\varepsilon^{15}N_{(N_2O\text{-}NO_3^-)}$ and $\varepsilon^{15}N_{(N_2O\text{-}NH_4^+)}$ reported in literature and the large measured NO_3^- isotope ranges (0 to 48‰). In addition, N_2O consuming to N_2 can cause the movement of isotopic values out the original source box (at Long Point site, this refers to nitrification box) into the denitrification box.

3.4 Conclusions

NO_3^--N concentrations that dropped abruptly from 70mg/L to < 0.1 mg/L indicate NO_3^- attenuation in proximal deep zone. Significant enrichment of $\delta^{15}N$ and $\delta^{18}O$ values of NO_3^- as NO_3^--N concentrations decrease, as well as a ratio of $\delta^{15}N$:$\delta^{18}O$ that is close to 2:1, suggest denitrification occurs actively. SO_4^{2-} values that increase by a factor of 2 to approximately 140 mg/L in the proximal deep zone and DOC values that decrease from 40 to 2 mg C/L suggest that during denitrification, pyrite

and organic carbon are used as electron donor. N_2O-N concentrations at this site with an extremely wide range from 1 μg/L in the proximal shallow zone to 1071 μg/L in the proximal deep zone are substantially higher than the atmospheric equilibrium values (0.27 to 0.37 μg/L at 8 to 17°C) (Fig. 3.4b and 3.5c Table 1.2) as well as N_2O-N values in surface water (0.2 to 1.2 μg/L, Grand River, Thuss, 2008). This provides strong evidence of N_2O production in subsurface. In addition, in early season (June, 2009), at 2.6 to 4m depth, NO_3^--N concentrations decreased from 125 to 30 mg/L whereas N_2O-N increased from 239 to 485 μg/L. This suggested that N_2O production by denitrification was presumably occurring at mid-depth of the plume early in the season; however, no NO_3^- isotopic enrichment was observed at that depth in early season (Fig.3.6). This provides a preliminary indication that N_2O has the potential to be a more sensitive indicator of denitrification than NO_3^- isotopes in groundwater. $\delta^{15}N$ and $\delta^{18}O$ in N_2O show that both nitrification and denitrification are involved in production of N_2O; however, nitrification is mainly responsible for N_2O accumulation in both proximal shallow and deep zones while N_2O at the bottom of the aquifer is also produced from denitrification where oxygen is absent (Fig 3.10a and 3.10b). N_2O isotopic values also show seasonal N_2O production shifted from mostly nitrification in early June to primarily denitrification in October (Fig. 3.11). In addition, after N_2O is produced in the plume core zone, $\delta^{15}N$ and $\delta^{18}O$ in N_2O reveal that N_2O is further consumed to N_2 under anaerobic conditions (Fig. 3.10 and 3.11). Theses evidence indicates that N_2O isotopes are particularly useful for sorting out the N-cycling (N_2O production from nitrification vs. denitrification, N_2O consumption) in septic system plume. Most of the N_2O isotope data points have $\delta^{18}O$-N_2O values higher than the calculated range for N_2O production by denitrification suggesting that possible ^{18}O enrichment factor for denitrification can be higher than literature values.

CHAPTER 4: LAKE JOSEPH SITE

4.1 Site Description

The Lake Joseph site is situated in Seguin Township in central Ontario (Fig.4.1). It has a seasonal use (from May to September) campground serviced by a single septic system (Robertson, 2003). During peak-use (July to August), the campground accommodates approximately 85 people daily (Robertson, 2003). The infiltration bed of the septic system was commissioned in the early 1990s and is approximately 1500 m^2 in area (Robertson, 2003). Detailed site monitoring began in 1998 when a series of 21 multi-level piezometer bundles (114 monitoring points) were installed beneath the tile bed and up to 30m downgradient (Fig. 4.1) (Robertson, 2003). Previous studies (Robertson, 2003) revealed that the sand aquifer at the site was unconfined and consisted of homogeneous medium sand with hydraulic conductivity of ~0.01 cm/s. The plume core zone could be easily identified by high EC values and high Cl^- concentrations, which distinguished it from background groundwater. However, the winter application of road salt to a highway 69, which is situated only 50m away from the infiltration bed, produces another high EC, Cl^--rich plume that underlies the septic system plume. Separating these plumes is a 0.5-2m thick downgradient area with lower EC and Cl^- values (Robertson, 1999). In June 2009, an assessment of the fate of NO_3^- in the plume was initiated which included NO_3^- isotope analyses to test for possible zones of denitrification (Rossi, 2010). A local anaerobic core zone was indentified with lower NO_3-N values (< 2 mg/L) exhibiting isotopic enrichment suggesting a zone of denitrification was present. The current study, focusing on N_2O behaviour, was then initiated in July 2009 based on the indicated presence of a denitrification zone.

Groundwater samples were collected at septic tank and piezometer nests CB 1, CB 2, CB 3(R), CB 13, CB20, CB 21, CB 22, and CB 23 for major anions (NO_3^-, Cl^-, SO_4^{2-}, Br^-, PO_4^{3-}, F^-), cations (Al^{3+}, Ca^{2+}, K^+, Mg^{2+}, Na^+), NH_4^+, DOC, dissolved N_2O concentrations and isotopic analyses (NO_3^-, N_2O, NH_4^+) on June 9, July 27 and September 20, 2009. In order to measure NH_4^+-N concentrations with associated isotopic measurements, a more limited groundwater sampling was undertaken at septic tank and piezometer nest CB 13, CB 20 and CB 22 on August 30, 2009 which also included the same laboratory analyses as that of earlier samples. Detailed groundwater sampling information is described in Rossi (2010).

4.1.1 Groundwater Flow System

The shallow groundwater flow system at Lake Joseph originates in forested terrain lying north of the study site and migrates within the surficial sand aquifer southward toward Lake Joseph, located 200 m south of the tile bed. The horizontal groundwater velocity near the tile bed has been estimated previously at 70 m/yr based on calculations using the Darcy equation (Robertson, 2003). Groundwater recharge in sandy forested terrain in this region has been measured to be in the range of 15 cm/yr (Sturgeon Falls site, Robertson and Schiff, 1994) which leads to a vertical velocity of ~40 cm/yr assuming porosity of 0.35. Recharge to the tile bed (1500 m^2) during peak seasonal usage (85 persons/day, assuming 200 L/day/person water usage) is only ~1 cm/day at this site, much less than at Long Point, which leads to vertical velocities in the shallow water table zone below the tile bed of only about 3 cm/day (10 m/yr). Thus, the groundwater flow direction, at this site, is dominantly horizontal even below the tile bed, whereas Long Point has a much more prominent vertical component of flow below the tile bed.

4.2 Results

4.2.1 K^+, Cl^- and EC Distributions and Groundwater Temperature

Figure 4.2 and 4.3 show K^+, Cl^- and EC distributions along the plume core centreline (section A-A') in July and September, 2009. K^+ was relatively consistent in the plume core varying from 5 to 8 mg/L in late July and 7 to 22 mg/L in September similar to the septic tank values (Fig. 4.2a and 4.3a). Cl^- exhibited similar consistently high concentrations in the plume core (24-107mg/L July; 76-127 mg/L September) and were similar to the septic tank effluent value (107±5 mg/L, n=3). The upgradient well (CB1) had very low Cl^- concentration (< 1 mg/L) during both sampling events (Fig 4.2b and 4.3b). A thin layer with lower Cl^- values (10-28 mg/L) occurred at 5-6 m depth during the July sampling (Fig 4.2b) and was underlain by the road salt plume (Cl^-, up to 107 mg/L, Fig. 4.2b). EC distribution minored Cl^- distribution (Fig 4.2c, 4.3c). Although all three parameters (Cl^-, EC, K^+) successfully identified the plume core zone, K^+ was selected as the primary identifier of the plume boundary (3 mg/L concentration) because K^+ remained low (< 1 mg/L) in the underlying road salt plume.

Groundwater temperatures below the Lake Joseph tile bed decreased with depth, ranging from 9 in shallow zone to 17^{o}C in deep zone during sampling in the summer and fall of 2009.

4.2.2 Nitrogen Goechemistry Data

Dissolved oxygen (DO) distribution in the plume was closely correlated to NO_3^- distribution. A DO depleted zone (DO < 1mg/L) was found in the area where low NO_3-N occurred, whereas much higher DO of up to 11 mg/L was present elsewhere in the plume where NO_3-N concentrations were higher (Fig 4.4a and 4.5a).

Figure 4.4 and 4.5 show detailed groundwater nitrogen data and N isotopic data for July and September 2009. NO_3^--N concentrations were highest at nest CB 23 both in July (up to 28 mg/L) and in September (up to 23 mg/L) (Fig 4.4b and Figure 4.5b). However, a zone with low NO_3-N concentrations (<3 mg/L) was observed in the downgradient area at CB 13 and CB 20 in July and at CB 22 and CB 13 in September.

N_2O-N distribution exhibited a pattern similar to NO_3-N distribution. In July 2009, nest CB 23 had highest levels of N_2O-N (up to 54 μg/L) (Fig. 4.4e) in the same zone where NO_3^--N was highest (up to 28 μg/L, Fig. 4.4b). A N_2O-N depleted zone occurred downgradient of the high N_2O-N zone and coincidences with the anaerobic zone where NO_3^--N is also low (Fig 4.4a, 4.4c and 4.4e). N_2O-N distribution in September, 2009 was generally similar (Fig 4.5d).

Figure 4.4d and 4.5c show NH_4^+-N distribution in July, 2009 and September, 2009. The highest concentrations of NH_4-N can be found in the septic effluent tank (31± 7mg/L, n=3). In July, the septic system plume was almost entirely depleted in NH_4^+-N (0.02-3 mg/L), however in September 2009, two small zones with elevated NH_4^+-N (2-12 mg/L) were observed in shallow aquifer at nests CB 23, CB 13 and CB 20 (Fig. 4.5c).

The ratio of total inorganic nitrogen to Cl^- (TN/Cl^-) in the tank with a mean of 0.24±0.08 (n=3) was substantially lower than that in the plume (0.01 to 0.2 in July and 0.01 to 0.2 in Septmber) (Fig. 4.4g and 4.5f). In addition, this ratio within the plume was varied with nests and seasons. In July, nests CB 23 and CB 22 had higher ratios (0.01 to 0.3) than that of nests CB 13, CB 20 and CB 21 (0.01 to 0.2). In late September, nest CB 22 still had the high ratios (0.2) whereas other nests had much lower ratios (0.0004 to 0.2).

4.2.3 NO_3^- and N_2O Isotope Data

$\delta^{15}N\text{-}NO_3^-$ values ranged from +1 to +10 ‰ and $\delta^{18}O\text{-}NO_3^-$ varied from -7 to 1 ‰ throughout the transect in July, 2009 (Fig. 4.4c). The tank had an average $\delta^{15}N\text{-}NH_4$ of 6±0.5‰ (n=5). No clear trend of $\delta^{15}N\text{-}NO_3^-$ and $\delta^{18}O\text{-}NO_3^-$ enrichment with depth was observed.

Figure 4.4Ef and 4.5Ee show N_2O isotopic distribution. During July 2009, CB 23 had more depleted $\delta^{15}N\text{-}N_2O$ (-14 to -27 ‰) compared with other piezometer nests which had $\delta^{15}N\text{-}N_2O$ of -5 to -18 ‰ and $\delta^{18}O\text{-}N_2O$ varied from +25 to +43 ‰ (Fig. 4.4Ef).. In September, $\delta^{15}N\text{-}N_2O$ values were somewhat more depleted (-16 to -31 ‰) while $\delta^{18}O\text{-}N_2O$ varied between +30 to +33 ‰ (Fig. 4.5Ee). In addition, groundwater samples were also taken for N_2O isotopic analyses in June, 2009 (Rossi, 2010). The results indicate that $\delta^{15}N\text{-}N_2O$ values ranged from -4.4 to -43.2 ‰ and $\delta^{18}O\text{-}N_2O$ varied from +32.6 to +56.7 ‰ at this time (Fig 4.7a).

4.3 Discussion

4.3.1 Nitrification and Denitrification

Cl^- is highly conservative in the groundwater; therefore, the ratio of total inorganic nitrogen to Cl^- is used to calculate the total inorganic nitrogen loss in the plume as follows:

$$\text{Nitrogen loss \%} = (1 - \text{TIN}/Cl^- \text{ in the plume} / \text{TIN}/Cl^- \text{ in tank}) \times 100\% \quad (6)$$

TIN/ Cl^- ratios shown in Fig 4.6 a and 4.6b reveal that in Lake Joseph septic system, up to 99.8% of the total nitrogen loss occurred in anaerobic core zone and in aerobic zone, there is almost no inorganic nitrogen loss at CB 23 in late September. In July 2009, wastewater discharged to tile bed was nitrified from NH_4^+ to NO_3^- in the unsaturated zone. High levels of NO_3^--N, N_2O-N and DO at CB 23 (Fig 4.4a, 4.4b and

4.4e) indicated that as NO_3^- migrated downward in the saturated zone, it remained as NO_3^-. However, further downgradient in the anaerobic core zone, much lower concentrations of NO_3^--N, N_2O-N and DO values suggested that significant NO_3^- attenuation have occurred in this zone. Similar NO_3^--N N_2O-N and DO distribution were observed during the September sampling (Fig 4.5a, 4.5b and 4.5d). Again, N_2O-N concentrations at this site (up to 106 μg/L) are substantially higher than the atmospheric equilibrium values (0.27 to 0.37 μg/L at 8 to 17°C) (Fig. 4.4e and 4.5d Table 1.2) indicating N_2O production in the plume core. Two small shallow zones with higher NH_4^+-N concentrations (2-12 mg/L) were present in September, indicating that, during the late summer, sewage oxidation in the vadose zone was incomplete (Fig 4.5c). Also, note that NH_4^+ migration rate is normally retarded by a factor of 2-4 as a result of sorption processes whereas NO_3^- is not (Dance and Reardon, 1983; Nicholson et al., 1983; Bolhke et al, 2006).

The average δ^{15}N-NH_4^+ value in the septic system tank effluent (6±0.5‰, n=5) at Lake Joseph is similar to that at Long Point (4.4‰, Robertson, et al., in prep.), No clear trend of ^{15}N-N_2O and ^{18}O-N_2O enrichment of N_2O corresponding to the NO_3^- attenuation zone was observed. In addition, a plot of δ^{18}O-NO_3^- versus δ^{15}N-NO_3^- for July (Fig. 4.7b) did not show an apparent denitrification trend as expected (ratio of 1:2). However, the June data did show a clear denitrification trend with of δ^{18}O-NO_3^- versus δ^{15}N-NO_3^- close to 1:1.8 (Fig. 4.7a) suggests denitrification did occur in some areas of the septic system plume at that time. Other than denitrification, anaerobic ammonium oxidation (anammox) reaction is also a potential mechanism for N attenuation at this site because NH_4^+ and NO_3^- do occur together, but NH_4^+-N values are generally too low (< 1mg/L) in most areas of the plume.

The overall range of $\delta^{15}N\text{-}NO_3^-$ and $\delta^{18}O\text{-}NO_3^-$ values at the Lake Joseph site ranged from -1 to +14 ‰ and -12 to +5 ‰, respectively (Fig. 4.7c), while $NH_4^+\text{-}\delta^{15}N$ in the tank ranges from +5 to +9 ‰ (Rossi, 2010). With these NO_3^- isotopic values and using reported isotopic enrichment factors (Chapter 3), the expected isotopic composition for N_2O produced by denitrification and nitrification can be calculated. Table 4.1 shows that the theoretical ranges for $\delta^{15}N\text{-}N_2O$ and $\delta^{18}O\text{-}N_2O$ when N_2O is produced from denitrification are -6 to -30 ‰ and +20 to +53 ‰, respectively (Table 4.1, Fig. 4.7). When N_2O is formed during the process of nitrification, the ranges should be -36 to -61 ‰ for $\delta^{15}N\text{-}N_2O$ and +18.5 to +28.5 ‰ for $\delta^{18}O\text{-}N_2O$ (Table 4.1, Fig. 4.8). The July and September $\delta^{18}O\text{-}N_2O$ versus $\delta^{15}N\text{-}N_2O$ values suggest that both of the two processes are involved in N_2O production (Fig 4.8a and 4.8b). In July 2009, N_2O isotope data values from CB 13, CB 22 and CB 23 were within the denitrification source range, suggesting that N_2O was formed during denitrification (Fig. 4.8a). In September 2009, N_2O isotope data from CB 23 on the edge of the two source ranges indicates that N_2O in the area around CB 23 was originated from nitrification and then moves out of the original nitrification range into the denitrification range by subsequent N_2O consumption (Fig 4.8b). N_2O isotopic data from CB 13 suggest that N_2O at this well originated from denitrification. This further confirms that N_2O produced from nitrification in the area at CB 23 and as groundwater travels downgradient to the anaerobic zone, NO_3^- was reduced to N_2O through denitrification.

Usually light $\delta^{15}N\text{-}NO_3^-$ (~ 6 ‰, $\delta^{15}N\text{-}NH_4^+$ in the tank) were present at each piezometer nest at Lake Joseph in July. A possible reason for these depleted $\delta^{15}N\text{-}NO_3^-$ signatures is nitrifier-denitrification involvment accompanied by denitrification and denitrification. Nitrifier-denitrification occurs when NH_4^+ is oxidized to NO_2^- and

then NO_2^- is subsequently reduced to N_2O through NO (Wrage et al., 2001). During this process, large ^{15}N fractionation was observed in laboratory experiments, and the reported fractionation factors $\varepsilon_{N2O\text{-}NO2^-}$ range from -24 to -38 ‰ (Sutka et al., 2003, 2004 and 2006). Usually, when NO_3^- produced from nitrification, similar or higher $\delta^{15}N\text{-}NO_3^-$ values can be expected compared to original $\delta^{15}N\text{-}NH_4$, therefore, the usually light $\delta^{15}N\text{-}NO_3^-$ values at this site possibly indicate that nitrifier-denitrification is involved in oxidizing NH_4^+ (Spoelstra, per comm). However, most of the NO_2^- concentrations at this site are lower than the detection limit (0.01mg/L) with exception of a couple of shallow piezometers having concentrations ranging from 0.07 to 0.48 mg/L (Appendix B2 and B4). NO_2^- released from cells can result in more exchange with water oxygen (Spoelstra, per comm). $\delta^{18}O\text{-}NO_3^-$ (-7 to +1 ‰) were also substantially light throughout the transect in July. These depleted $\delta^{18}O\text{-}NO_3^-$ values are presumably affected from N_2O exchange with H_2O during nitrification, considering a typical value for $^{18}O\text{-}H_2O$ (-10‰) (Snider et al., 2008).

4.4 Conclusions

TN/Cl^- ratios in plume core reveal that up to 99.8% of the nitrogen is attenuated in anaerobic core zone whereas in aerobic zone, this ratio is as low as 17%. NH_4^+-N concentrations in the septic tank was 31± 7mg/L, (n=3). The downgradient anoxic zone, NO_3^--N concentrations ranged from less than detection limit to 3mg/L and NH_4^+-N varied from 0.002 to 6 mg/L. N_2O-N concentrations at this site (up to 106 µg/L) are substantially higher than the atmospheric equilibrium values (0.27 to 0.37 µg/L at 8 to 17°C) (Fig. 4.4e and 4.5d Table 1.2) provide evidence for N_2O production. Further, N_2O isotopic signatures reveal that both nitrification and denitrification play a role in nitrogen attenuation (Fig 4.8a and Fig 4.8b). However, nitrification was mainly found at nest CB 23 in aerobic zone whereas denitrification

zone (nest CB 23) was present in downgradient anaerobic area. The denitrification zone suggested by N_2O isotopic values coincidences with the zone that has relatively low concentrations of N_2O-N (0.1-3 μg/L) and NO_3^--N values (0.2 to 2 mg/L) in anaerobic core. At this site, isotopic signatures of the NO_3^- in July did not provide evidence of denitrification (Fig. 4.7b) but N_2O isotopic values show clear evidence of N_2O produced by denitrification (Fig. 4.8a and 4.8b) which suggests that N_2O is a sensitive indicator in identifying denitrification in groundwater. In addition, similar to Long Point site, N_2O isotopes are useful for sorting out N_2O production from nitrification or denitrification in septic system plume.

CHAPTER 5: STRATHROY SITE

5.1 Site Description

The Strathroy site is located near the town of Strathroy, in southern Ontario (Sebol, 2004; Sebol et al., 2007). The area has a homogeneous unconfined sand aquifer that acts as regional water supply aquifer (Sebol et al., 2007). However, this aquifer is heavily impacted by agricultural NO_3^- from fertilizer use (Sebol, 2004). The sand aquifer is more than 10m thick and the depth to the water table throughout the area varies from 1.5m to 4.5m (Ryan et al., 2000). The water table depth at West Fence monitoring site (Fig. 5.1), which is the focus of this study, is in the range of 2.5-3.3m (Sebol, 2004). The land was originally used for dairy operations until 1970s, when it was switched to corn production. In 1989, no-till management practices were initiated by Middlesex Country Soil and Crop Improvement Association at this site (MSCIA) (Sebol, 2004). Detailed groundwater monitoring was initiated in 1997 and involved installation of multi-level piezometer bundles (P83-P89) to a maximum depth of 5.8m for NO_3^- studies. This included a bromide tracer test that allowed age dating of the shallow aquifer zone (Ryan et al., 2000, Sebol et al., 2007). Additional monitoring wells, including the five nests of multi-level bundle piezometers SR1-SR5 were installed in 2000 to a depth of 14.8m for groundwater age dating studies (Sebol, 2004). Previous studies indicated that occurrence of almost complete NO_3-N depletion at 6 m depth resulted from abrupt denitrification using pyrite as electron donor (Ryan, et al., 2000; Sebol, 2004).

This study focuses on the single nest SR3, and sampling was undertaken during a single site visit for major anions (NO_3^-, Cl^-, SO_4^{2-}, Br^-, PO_4^{3-}, F^-), DOC, dissolved N_2O concentrations and isotopic analyses (NO_3^- and N_2O) (October 15, 2009). No NH_4^+ was present in previous studies (Sebol, 2004).

5.1.1 Groundwater Flow System

The surficial unconfined sand aquifer at the Strathroy site is ~ 18 m thick and groundwater flow is southeastward toward a series of municipal water supply wells that are located ~ 1 km from the study site (Ryan et al., 2000). Ryan et al. (2000) reported hydraulic conductivity (K) of 1.5×10^{-2} cm/s and Sebol (2004) reported a similar average hydraulic conductivity of 1.9×10^{-2} cm/s at the West Fence. The horizontal groundwater velocity has been estimated previously at 50 m/yr based on calculations using the Darcy equation (Ryan et al., 2000). Groundwater vertical velocity was measured precisely at this site during 1997-2002 using a Br tracer test (Sebol et al., 2007). The vertical velocity measured in the shallow table zone (0.63 m/yr) implies a recharge rate of 23 cm/yr assuming porosity of 0.35. The tracer test also proved that the recharge area for the shallow groundwater to ~6 m depth at SR3 was the West field which extents 300 m upgadient (north) of the nest (Fig. 5.1). Groundwater below 6 m depth is presumed to have been recharged north of the West field, which is also an agricultural area. Groundwater flow is dominantly horizontal at this site.

5.2 Results

Groundwater temperatures at Strathroy site were consistently in the range of 9.6-11.6^{o}C during groundwater sampling in the fall of 2009.

The NO_3-N depth profile (Fig.5.2) shows that concentrations near the water table are 4.6 mg/L and then increased to 11.5 mg/L at 5.6m depth. Concentrations then declined abruptly to ≤0.02 mg/L at a depth of 7.7m. DO shows a very similar pattern of decline at 6m depth (Fig. 5.2). Below 6.7m, the groundwater is anaerobic. N_2O-N concentrations of ~1 μg/L occurred at 3-4m depth but then higher values up to

3 μg/L occurred at 5-6m depth. N_2O values then dropped rapidly to 0.1 μg/L at 7.7m. SO_4 values increased abruptly from ~6mg/L at 3-5m depth to ~60 mg/L below 7.7m depth. The zone of SO_4^{2-} increase coincidences with the zone of NO_3^- depletion, reflecting denitrification that occurs at this site, using pyrite in the aquifer sediments as the electron donor (Sebol, 2004). DOC concentrations varied from 0.7 to 3.4 mg C/L with the maximum value observed at 11.8m depth.

$\delta^{15}N\text{-}NO_3^-$ and $\delta^{18}O\text{-}NO_3^-$ signatures (Fig. 5.2) ranged from +2.2 to +3.5 ‰ and -0.03 to -3.0 ‰ respectively in the shallow zone (3-5m depth) but then abrupt isotopic enrichment with $\delta^{15}N\text{-}NO_3^-$ increasing to +25.4 ‰ and $\delta^{18}O\text{-}NO_3^-$ increasing to +15.5 ‰ occurred at 6.7m depth. $\delta^{15}N\text{-}N_2O$ decrease with depth from -0.6 to -29.7 ‰ whereas $\delta^{18}O\text{-}N_2O$ values increase with depth from +33 to +65 ‰ (Fig. 5.2).

5.3 Discussion

In the anaerobic zone below about 7m depth, complete NO_3^- depletion coinciding with significant $\delta^{15}N\text{-}NO_3^-$ and $\delta^{18}O\text{-}NO_3^-$ enrichment provide strong evidence that denitrification is occurring. Increased SO_4^{2-} suggests that pyrite is the electron donor for denitrification.

The depth profiles of $\delta^{18}O\text{-}NO_3^-$ versus $\delta^{15}N\text{-}NO_3^-$ with a ratio of 1:1.3 (Fig. 5.3) shows a clear trend of isotopic enrichment as NO_3^- is decreasing. The ranges for $\delta^{18}O\text{-}NO_3^-$ (-3 to +16 ‰) and $\delta^{15}N\text{-}NO_3^-$ (+3 to +26 ‰) in Strathroy plume are indicated in Table 5.1 and shown in Fig. 5.3. At this site, fertilizer would be the main source of NH_4^+, therefore 0 to +2‰ (Spoelstra, per comm) was used as $\delta^{15}N\text{-}NH_4^+$ ranges to determine the nitrification source range. The calculated ranges for N_2O produced from denitrification are -4 to -32 ‰ for $\delta^{15}N\text{-}N_2O$ and +35 to +74 ‰ for $\delta^{18}O\text{-}N_2O$. For N_2O production by nitrification, the ranges are -43 to -66 ‰ for $\delta^{15}N$-

N_2O and +18.5 to +28.5 ‰ for $\delta^{18}O$-N_2O (Table. 5.1 and Fig. 5.3). In shallow aquifer, above 5m depth, N_2O-N concentrations ranged from 0.5 to 0.9 μg/L (Fig. 5.2). This is slightly higher than N_2O-N concentration in water in equilibrium with atmosphere (0.27-0.37 μg/L at 8-17°C, Table 1.2). This suggests that N_2O in the zone above 5m depth is likely derived from a mix of atmospheric N_2O and nitrification N_2O in the vadose zone. Since the reported range in groundwater is close to atmospheric values, tropospheric N_2O is presumably responsible for most of the N_2O present above 5m depth. Further, $\delta^{15}N$-N_2O and $\delta^{18}O$-N_2O values are close to atmospheric values ($\delta^{15}N$-N_2O = +6.72 ‰; $\delta^{18}O$-N_2O = +44.62 ‰) (Kaiser et al., 2003) (Fig. 5.3). This indicates that N_2O from the atmosphere enters the vadose zone and dissolved in groundwater recharging the saturated zone. However, below 5m depth, N_2O originating from denitrification increases in concentrations and is accompanied by distinctive enrichment of N_2O-$\delta^{15}N$ and N_2O-$\delta^{18}O$ (Fig. 5.2 and 5.3).

.

5.4 Conclusions

The occurrence of NO_3^- attenuation can be found below a depth 6.7m (Fig. 5.2). Below that depth, almost no oxygen is present and NO_3-N concentrations dropped rapidly from 10.2 mg/L to ≤ 0.02 mg/L. Also in this anaerobic zone, significant enrichment of $\delta^{18}O$-NO_3^- and $\delta^{15}N$-NO_3^- (Fig. 5.2) as well as high levels of SO_4^{2-} (~60 mg/L) suggests that denitrification occurs actively using pyrite as electron donor. N_2O-N distribution exhibits a pattern that is closely related to NO_3-N distribution (Fig. 5.2). Above 5m depth, N_2O-N concentrations (0.5 to 0.9 μg/L) are slightly higher than N_2O-N concentration in water in equilibrium with atmosphere (0.27-0.37 μg/L at 8-17°C, Table 1.2). This suggests that N_2O in the zone above 5m depth is presumably derived from a mix of atmospheric N_2O and nitrification N_2O.

More importantly, $\delta^{15}N\text{-}N_2O$ and $\delta^{18}O\text{-}N_2O$ values (Fig. 5.3) provide evidence that N_2O in shallow aquifer (< 5m depth) is likely derived from the atmosphere whereas in deep aquifer (>5m depth), N_2O is formed during denitrification. This further confirms that in anaerobic zone below ~5m depth, denitrification plays an important role in NO_3^- loss. Therefore, although NO_3^- isotope values at this site provide strong evidence of denitrification, N_2O is still useful to sort out the N_2O sources (nitrification, denitrification and atmospheric N_2O). N_2O increase precedes the decrease in NO_3^- concentration and large change in NO_3^- isotopes (Fig. 5.2) – therefore N_2O a sensitive indicator of the start of denitrification. Also, N_2O isotopes from denitrification change as the NO_3^- isotopes change (as predicted).

CHAPTER 6: WOODSTOCK SITE

6.1 Site Description

The Thornton Well Field yields 2-4 million m^3 of water every year, and is the major drinking water supply system for the city of Woodstock, Ontario (Heagle, 2000; Koch, 2009). The heterogeneous and complicated glacial outwash stratigraphy at this site has been described previously (Heagle, 2000; Sebol, 2004; Koch, 2009). This aquifer is vulnerable to surface contamination because of the highly permeable sand and gravel sediments are unconfined in some areas (Heagle, 2000; Robertson, et al., 2005). Due to fertilizer applications in this agricultural area, NO_3^- is one of the main contaminants of concern for the aquifer (Heagle, 2000). However, Heagle (2000) reported that denitrification using pyrite as the electron donor was a key process for attenuating NO_3^- in the aquifer. However, this was not apparent in the main part of the aquifer, but only in basal zones and in areas to the north. Previous monitoring work at this site included installation of 25 multi-level monitoring wells in 1997 (Heagle, 2000) and additional well installations during 2005 to 2008 (Koch, 2009).

This study considers groundwater samples collected from two multi-level nests, WO 11 and WO 74 (Fig. 6.1), during a single sampling event, July 4, 2009. Samples were analyzed for major anions (NO_3^-, Cl^-, SO_4^{2-}), dissolved N_2O concentrations and isotopic analyses (NO_3^- and N_2O).

6.1.1 Groundwater Flow System

Groundwater flow within the heterogeneous glacial outwash aquifer at the site is toward a group of municipal water supply wells which lie ~ 300-500 m east of the study wells (Heagle, 2000). Previous borehole dilution tests conducted in the shallow

water table zone at a location ~100 m east of well WO 74 revealed a relatively fast mean horizontal groundwater velocity of ~ 180 m/yr (Robertson, 2005). Although vertical recharge rates (and velocities) were not measured directly in this study it is reasonable to assume recharge rates and vertical velocities are similar to that of the Strathroy site (recharge of 23 cm/yr and vertical velocity of 63 cm/yr), which is located only 100 km to the west in similar flat lying sandy agricultural terrain. Groundwater flow is thus dominantly horizontal at this site.

6.2 Result and Discussion

Although groundwater temperatures were not measured directly in this study, it is reasonable to assume that temperatures in the shallow aquifer at Woodstock are similar to those at the Strathroy site (9-12 ^{o}C), which is located only 100 km to the west.

6.2.1 Piezometer Nest WO 11

Cl^- concentrations in nest WO 11 vary between 15-54 mg/L (Fig 6.2). In the shallow aquifer (above the depth of 10m), SO_4^{2-} concentrations increase at 13m depth from approximately 40 to 86.4 mg/L, at the same depth where NO_3^--N decreases abruptly to 0.1 mg/L indicating a basal denitrification zone. However, $\delta^{15}N\text{-}NO_3^-$ varied from +4 to +7 ‰ but does not show any evidence of isotopic enrichment (Fig 6.2). Again, fertilizer would be the main source of NH_4^+, therefore 0 to +2‰ (Spoelstra, per comm) was used as $\delta^{15}N\text{-}NH_4^+$ ranges to determine the nitrification source range. Table 6.1 and Fig. 6.3 show the calculated ranges for N_2O produced from denitrification (-13 to -24 ‰ for $\delta^{15}N\text{-}N_2O$ and +31 to +50 ‰ for $\delta^{18}O\text{-}N_2O$) and from nitrification (-43 to -66 ‰ for $\delta^{15}N\text{-}N_2O$ and +18.5 to +28.5 ‰ for $\delta^{18}O\text{-}N_2O$).

The field N_2O isotopic values show that N_2O at WO 11 is primarily composed of both denitrification N_2O and tropospheric N_2O. However, at the N_2O concentrations measured (ranged from 19.9 to 49 μg/L at 6 to 13m depth), the isotopic signal from atmospheric N_2O at about 0.27-0.37 μg/L at 8-17°C (Table 1.2) would be masked and not a factor on overall N_2O isotopic composition in groundwater.

6.2.2 Piezometer Nest WO 74

$\delta^{15}N\text{-}NO_3^-$ signatures vary from +5 to +7 ‰ and are relatively stable (Fig. 6.2). $\delta^{18}O\text{-}N_2O$ (+34.3 to +37.1‰) and $\delta^{15}N\text{-}N_2O$ (-4.7 to -15.1‰) values show an opposite trend to the concentration data. A plot of $\delta^{18}O\text{-}N_2O$ vs. $\delta^{15}N\text{-}N_2O$ (Fig. 6.3) suggests that N_2O at WO 74 below 4m depth with concentrations ranged from 39.1 to 40.5 μg/L is likely composed of both denitrification N_2O and tropospheric N_2O, but denitrification is the major source, since the N_2O-N ranges are two orders of magnitudes higher than the atmospheric equilibrium ranges (0.27-0.37 μg/L at 8-17°C, Table 1.2). The $\delta^{15}N\text{-}N_2O$ and $\delta^{18}O\text{-}N_2O$ values at WO 11 (3.96m depth) are -4.74 ‰ and +37.05 ‰, close to the atomospheric N_2O isotope values (+6.72 ‰ for $\delta^{15}N\text{-}N_2O$ and +44.62 ‰ for $\delta^{18}O\text{-}N_2O$, Kaiser et al., 2003), however, N_2O-N concentration at that depth is 14.57 μg/L, substantially higher than N_2O-N concentration in water in equilibrium with atmosphere (0.27-0.37 μg/L at 8-17°C, Table 1.2). This suggests that N_2O at 3.96m depth is likely derived from a mix of atmospheric N_2O and nitrification N_2O, but the nitrification is mainly responsible for the N_2O formation since the high N_2O-N value (14.57 μg/L) is present. However, NO_3^--N, SO_4^{2-} and $\delta^{15}N\text{-}NO_3^-$ values do not show any evidence of denitrification.

6.3 Conclusions

NO_3^- attenuation occurred naturally below 10m depth at piezometer nest WO 11, but $\delta^{15}N\text{-}NO_3^-$ does not provide further evidence of denitrification (Fig. 6.2). For piezometer nest WO 74, the occurrence of NO_3^- attenuation is not evident (Fig. 6.2). N_2O distribution at both wells is somewhat correlated to NO_3^- distribution and does not show clear evidence of nitrogen loss (Fig. 6.2). N_2O-N concentrations at this site ranged from19.9 to 49 μg/L, are substantially higher than N_2O-N concentration in water in equilibrium with atmosphere (0.29-0.37 μg/L at 8-15°C, Table 1.2). This confirms N_2O production in the groundwater. $\delta^{18}O\text{-}N_2O$ and $\delta^{15}N\text{-}N_2O$ values shown in Fig. 6.3 indicate that most of N_2O at WO 11 and WO 74 is a mixing of denitrification N_2O and tropospheric N_2O with exception of N_2O in a shallow zone (~4m depth) at WO 74 that is derived from atmosphere and nitrification. At this agricultural site, denitrification evidence from NO_3^- concentration/isotopes is lacking but N_2O indicates it is occurring (Fig. 6.3). This again provides indication that N_2O is a sensitive indicator of denitrification and is able to sort out N_2O sources.

CHAPTER 7: CONCLUSIONS AND RECOMMENDATIONS

Groundwater sampling was undertaken in 2008-2009 at four different field sites. Those four study sites can be divided into two groups: septic system sites (Long Point site and Lake Joseph site) and agricultural sites (Strathroy site and Woodstock site). The overall N_2O-N concentrations vary from 1 to 1071 μg/L at Long Point site, and range from less than 0.1 to 106 μg/L at Lake Joseph site. Compared with the broad range present at septic system sites, N_2O concentrations at the agricultural sites exhibit lower levels and narrower ranges. The N_2O concentrations at Strathroy range from 0.1 to 3.3 μg/L and at Woodstock site, 14.6 to 40.5 μg/L. Vandenhoff (2007) reported the N_2O-N concentrations in groundwater at Putnam, a compost manure field, ranged from 0.8 to 1044 μg/L, which is very close to the N_2O-N range at Long Point site. Critchley (2010) measured N_2O-N concentrations in groundwater from ML-8 at Woodstock site, ranging from 35.5 to 41.0 μg/L which is similar to the ranges at WO 11 and WO 74 (14.6 to 40.5 μg/L). Previously (Hiscock, 2003) compared N_2O-N concentrations in various types of aquifers that were affected by different types of land use. In the sand aquifers which were affected by sewage effluent disposal (similar to Long Point and Lake Joseph site), the reported range is 53.2 to 252 μg/L, which is within reported the ranges from two septic system sites at this study. In cropped field soils (similar to Strathroy site), N_2O-N concentrations are shown within the range of 0.4 to 198 μg/L, much wider than the reported ranges at Strathroy. These comparisons provide a general idea that N_2O-N concentrations are particularly site specific. Even for the similar type of aquifers with similar land use, N_2O-N concentrations at different depths can be orders of magnitude different. Even within the same study site, the N_2O-N concentrations exhibit seasonal transient effects both specially and quantitatively. For example, at Long Point, the highest

concentrations (739 μg/L) was observed in very shallow zone early in the season while late in the season, the highest concentration (1071 μg/L) was found in the centre of the plume. Lake Joseph site has a similar situation. In July, the highest value of 54 μg/L was present at a shallow depth (3.7m) at CB 23 while in late September, 106 μg/L was observed in a deeper zone (4.9m) at CB 23. This suggests that N_2O is accumulated and migrates in groundwater over time.

Relatively high N_2O concentrations occurred at each of these four sites with measured values 1-3 orders of magnitude higher than atmospheric equilibrium values. Considering this groundwater will eventually discharge to surface water courses where excess N_2O that is still present, will diffuse to the atmosphere, it is of interest to speculate how important such a groundwater component could be to the global GHG budget. Although highest concentrations occurred at the two septic system sites, the agricultural sites also exhibited high values and represent much more extensive source areas. The Woodstock site is of particular interest, because it represents the downstream end of a vigorous regional groundwater flow system where depth profiles should represent recharge that has originated over a wide area that is dominantly agricultural. Expect for the shallowest points, relatively uniform (and high) N_2O concentrations occurred at the two nests WO 11 and WO 74 (~40 ug/L). Considering a reasonable rate of water table recharge in sandy agricultural terrain in southern Ontario (~10-20 cm/yr), these groundwater values suggest N_2O production of about 4000 ug N/m^2/yr (0.04 kg N m^2/yr). Remarkably, this value is identical to the mean groundwater production value estimated by Hiscock et al. (2003) for the Chalk aquifer in the UK (0.04 kg N m^2/yr), based on a moderately detailed (23 wells), but regionally extensive sampling program in 2001. This comparison suggests that the Woodstock N_2O concentrations could be quite typical of shallow groundwater in

agriculturally impacted terrain. However, Hiscock et al. also note that soil zone N_2O production was much higher in the agricultural areas included in the UK study (2.1-5.8 kg N m^2/yr), thus groundwater production represented only 1-2 % of the soil zone production.

NO_3^- loss is obvious at all study sites. At Long Point, $\delta^{15}N$-N_2O and $\delta^{18}O$-N_2O range from -43.9 to +24.9 ‰ and +20.6 to +89.4 ‰ respectively, and at Lake Joseph, $\delta^{15}N$-N_2O and $\delta^{18}O$-N_2O vary from -4.4 to -43.2 ‰ and +24.7 to +56.7 ‰. At Strathroy, $\delta^{15}N$-N_2O ranges from +1.7 to -29.7 ‰ and from -4.7 to -15.9 ‰ at Woodstock whereas $\delta^{18}O$-N_2O ranges from 33 to +65 ‰ at Strathroy and from +30.7 to +37.1 ‰ at Woodstock. The N_2O isotope values provide insight into the pathways of groundwater N_2O accumulation. At septic system sites, N_2O isotopic values indicate that in both proximal shallow and deep zones at Long Point and in aerobic core at Lake Joseph, N_2O is formed during the process of nitrification. However in proximal deep zone at Long Point and in anaerobic core at Lake Joseph, denitrification is responsible for N_2O production. Further, after N_2O is produced at Long Point site, N_2O isotopic signatures also demonstrate that N_2O is further reduced to N_2 in groundwater. Therefore, N_2O isotopes are useful for detecting N_2O consumption whereas NO_3^- isotopes are not able to determine whether the denitrification process is completed or stops at N_2O stage. At agricultural sites, the N_2O isotopes suggest that N_2O accumulation is the result of the following three processes; tropospheric N_2O is dissolved in the shallow groundwater; denitrification occurs in the deep aquifer where oxygen is absent; and nitrification occurs in the vadose zone.

Overall, assessment of N_2O concentrations and isotopic composition appears to be a potentially valuable tool in identifying N_2O produced by nitrification,

denitrification, and dissolution of atmospheric N_2O at both septic system sites and agricultural sites. Further, at Lake Joseph site and Woodstock site, denitrification evidence from NO_3^- concentration/isotopes is absent but N_2O isotopes suggest the occurrence of denitrification. At Long Point site, N_2O isotopes indicated N_2O production by denitrification occurred early in the season; however, no NO_3^- isotopic enrichment was observed at that depth until in late season. This provides indication that N_2O is an early and sensitive indicator of denitrification in groundwater at both septic system sites and agricultural sites.

Future studies should put efforts on resolving the cause of the NO_3^- attenuation evident at the field sites evidence from NO_3^- concentration/isotopes is lacking. Anammox reaction and denitrification are both able to cause NO_3^- loss, but distinguishing these two processes can be difficult. NH_4^+, NO_3^- and N_2O isotopic signatures can provide crucial evidence to determine which processes are responsible for observed N attenuation.

REFERENCES

Anderson, L.J., and H. Kristiansen. 1984. Nitrate in groundwater and surface water related to land use in the Karup Basin, Denmark. *Environmental Geology*. 5: 207-212.

Appelo, S.J., and R.R. Parizek. 1995. Dilution of nonpoint-source nitrate in groundwater. *J. of Environ. Qual.* 24: 707-718.

Aravena, R., M.L. Evans, and J.A. Cherry, 1993. Stable isotopes of oxygen and nitrogen in source identification of nitrate from septic systems. *Ground Water.* 31: 180-186.

Aravena, R., and W.D. Robertson. 1998. Use of multiple isotope tracers to evaluate denitrification in ground water: study of nitrate from a large-flux septic system plume. *Ground Water.* 36: 975-982.

Bogardi, I., R.D. Kuzelka, and W.G. Ennenga. 1991. *Nitrate Contamination: Exposure, Consequence and Control. Berlin Heidelberg: Springer-Verlag*.

Böhlke, J.K., L.S. Richard and N.M. Daniel. 2006. Ammonium transport and reaction in contaminated groundwater: application of isotope tracers and isotope fractionation studies. Water Resources Research. 42: W05411, doi:10.1029/2005WR004349.

Böttcher, J., O. Strebel, S. Voerkelius, and H.L. Schmidt. 1990. Using isotope fractionation of nitrate-nitrogen and nitrate-oxygen for evaluation of microbial denitrification in a sandy aquifer. *J. Hydrol.* 114: 413-424.

Bremner, J.M., 1997. Sources of nitrous oxide in soils. *Nutrient syscling in Agroecosystems.* 49: 7-16.

Brooks, P.D., J.M. Stark, B.B. McInteer, and T. Preston. 1989. Diffusion method to prepare soil extracts for automated nitrogen-15 analysis. Soil Sci. Soc. Am. J. 53: 1707.

Bouwman, A.F., 1990. Exchange of greenhouse gases between terrestrial ecosystems and atomosphere. In: Bouwman, A. F. (Ed.), *Soils and the Greenhouses Effect.* Wiley, New York. 61-127.

Carrara, C., C.J. Ptacek, W.D. Robertson, D.W. Blowes, M.C. Moncur, E. Sverko, and S. Backus. 2008. Fate of pharmaceutical and trace organic compounds in three septic system plumes, Ontario, Canada. *Environ. Sci. Technol.* 42: 2805-2811.

Casciotti, K.L., D.M. Sigman, H.M. Galanter, J.K. Böhlke, and A. Hilkert. 2002. Measurement of the oxygen isotopic composition of nitrate in seawater and freshwater using the denitrifier method. *Analytical Chemistry.* 74: 4905-4912.

Critchley, C. E. 2010. Stimulating in situ denitrification in an aerobic, highly conductive municipal drinking water aquifer. M.Sc. thesis, Department of Earth Sciences, Univ. of Waterloo, Waterloo, Ont. 249 pp.

Dance, J.T. and E.J. Reardon. 1983. Migration of contaminants in groundwater at a landfill: a case study, 5. Cation migration in the dispersion test. J. Hydrol. 63, no. 1-2: 109-130.

Denman, K.L., G. Brasseur, A. Chidthaisong, P. Ciais, P.M. Cox, R.E. Dickinson, D. Hauglustaine, C. Heinze, E. Holland, D. Jacob, U. Lohmann, S. Ramachandran, P.L. da Silva Dias, and S.C. Wofsy. 2007. In *Climate Change 2007: The Physical Science Basis. Contribution of Working Group I to the Fourth Assessment Report of the Intergovernmental Panel on Climate Change*, Soloman S, Qin D, Manning M, Chen Z, Marquis M, Averyt KB, Tignor M (eds). Cambridge University Press.: New York. 143-145, 544 – 546.

Elgood, Z., W.D. Robertson, S.L. Schiff, and R. Elgood. In Press. Nitrate removal and greenhouse gas production in a stream-bed denitrifying bioreactor. *Ecological Engineering.* ×××: ×××- ×××.

Forster, P., V. Ramaswamy, P. Artaxo, T. Berntsen, R. Betts, D.W. Fahey, J. Haywood, J. Lean, D.C. Lowe, G. Myhre, J. Nganga, R. Prinn, G. Raga, M. Schulz and R. Van Dorland. 2007. Changes in atmospheric constituents and in radioactive forcing. *In: Climate Change 2007: The physical Science Basis. Comtribution of Working Group I to the Fourth Assessment Report of the Intergovernmental Panel on Climate Change* [Solomon, S., D. Qin, M. Manning, Z. Chen, M. Marquis, K.B. Averyt, M. Tignor and H.L. Miller (eds.)]. Cambridge, United Kingdom and New York, NY, USA: Cambridge University Press.

Garcia-Ruiz, R., S.N. Pattinson and B.A. Whitton. 1998. Denitrification and nitrous oxide production in sediments of the Wiske, a lowland eutrophic river. *Science of the Total Environment*. 20, no.1-6: 307-320.

Gillham, R.W., and J.A. Cherry. 1978. Field evidence of denitrification in shallow groundwater flow systems. *Water Pollution Res. Can. 13*, no. 2: 53-71.

Goolsby, D.A., W.A. Battaglin, B.T. Aulenbach, and R.P. Hooper. 2001.Nitrogen input to the Gulf of Mexico. *J. Environ. Qual*. 30:329–336.

Goss, M.J., D.A.J. Barry, and D.L. Rudolph, 1998. Contamination in Ontario Farmstead Domestic Wells and Its Association with Agriculture: 1. Results from Drinking Water Wells. *Journal of Contaminant Hydrology.* no. 32: 269-293.

Granger, J., D.M. Sigman, J.A. Needoba, and P.J. Harrison. 2004. Coupled nitrogen and oxygen isotope fractionation of nitrate during assimilation by cultures of marine phytoplankton. *Limnology & Oceanography*. 49, no. 5: 1763-1773.

Granger, J., D.M. Sigman, M.F. Lehmann, and P.D. Tortell. 2008. Nitrogen and oxygen isotope fractionation during dissimilatory nitrate reduction by denitrifying bacteria. *Limnology & Oceanography.* 53, no. 6: 2533-2545.

Groffman, P.M., M.A. Altabet, J.K. Böhlke, K. Butterbach-bahl, M.B. David, M.K. Firestone, A.E. Giblin, T.M. Kana, L.P. Nielsen, and M.A. Voytek. 2006. Methods for

measuring denitrification: diverse approaches to a difficult problem. *Ecological applications.* 16, no. 6: 2091-2122.

Harman, J., W.D. Robertson, J.A. Cherry and L. Zanini. 1996. Impacts on a sand aquifer from an old septic system: nitrate and phosphate. *Ground Water*. 34: no.6: 1105-1114.

Heagle, D. J. 2000. Nitrate geochemistry of a regional aquifer in an agricultural landscape, Woodstock, Ontario. M.Sc. thesis, Department of Earth Sciences, Univ. of Waterloo, Waterloo, Ont. 97 pp.

Heaton, T.H.E. 1986. Isotopic studies of nitrogen pollution in the hydrosphere and atmosphere: A review. *Chemical Geology* (Isoot. Geosc. Section). 59: 87-102.

Henry's law Source: http://en.wikipedia.org/w/index.php?oldid=386577429

Hiscock, K.M., A.S. Bateman, Muhlherr, I. H., T. Fukada and P.R. Dennis. 2003. Indirect Emissions of Nitrous Oxide from Regional Aquifers in the United Kingdom. *Environ. Sci. Technol.* 37: 3507-3512.

Intergovernmental Panel on Climate Change. 2007. Climate Change 2007: the Physical Science Basis – Summary for Policymakers.

Kaiser, J., T. Rockmann and C. Brenninkmeijer. 2003. Complete and accurate mass spectrometric isotope analysis of tropospheric nitrous oxide. *J. Geophys. Res.* 108, no. 15: 4476. doi:10.1029/2003JD003613.

Kemp, M.J., and W.K. Dodds. 2002. The influence of ammonium, nitrate, and dissolved oxygen concentrations on uptake, nitrification, and denitrification rates associated with praire stream substrata. *Limnology and Oceanography*. 47, no.5: 1380-1393.

Kendall, C., 1998. Tracing nitrogen sources and cycling in catchments. In: C. Kendall and J.J. McDonnell, Eds. Isotope tracers in catchment hydrology. *Elsevier Science B. V.*, Amsterdam, The Netherland. 519-576.

Kendall C., and R. Aravena. 2000. Nitrate isotopes in groundwater systems. *Environmental Tracers in Subsurface Hydrology*. Cook, P., Herczeg, A.L. (eds). Kluwer Academic Publishers: Massachusetts, 261-297.

Koch, J. T., 2009. Evaluating regional aquifer vulnerability and BMP performance in an agricultural environment using a multi-scale data integration approach. M.Sc. thesis, Univ. of Waterloo, Waterloo, Ont. 279 pp.

Komor, S.C., and H.W. Anderson. 1993. Nitrogen isotopes as indicators of nitrate sources in Minnesota sand-plain aquifers. *Ground Water* .31: 260-270.

Kreitler, C.W., S.E. Ragone, and B.G. Kratz. 1979. $^{15}N/^{14}N$ ratios of ground-water nitrate, Long Island, New York. *Ground Water*. 16: 404-409.

Kroeze, C. 1999. Closing the global N_2O budget: a retrospective analysis 1500–1994. *Global Biogeochem. Cycles.* 13: 1–8.

Lide, D.R., Frederiskse, H.P.R. (eds.), 1995. *CRC Handbook of Chemistry and Physics*, 76th Edition. CRC Press, Inc, Boca Raton, FL

Mandernack, K.W., T. Rahn, C. Kinney, and M. Wahlen. 2000. The biogeochemical controls of the $\delta^{15}N$ and $\delta^{18}O$ of N_2O produced in landfill cover soils. *Journal of Geophysical Research.* 105, no.D14: 17709-11720.

Mariotti, A., J.C. Germon and A. Leclerc. 1982. Nitrogen isotope fractionation associated with the $NO_2^- \rightarrow N_2O$ step of denitrification in soils. *Canadian Journal of Soil Science.* 62: 227-241.

Mclean, N., 2007. Use of drains for passive control of flow through a permeable reactive barrier. M.Sc. thesis, Department of Earth Sciences. Univ. of Waterloo, Waterloo, Ont. 129 pp.

Mengis, M., S.L. Schiff, M. Harris, M.C. English, R. Aravena, R.J. Elgood, and A. McLean. 1999. Multiple geochemical and istopic approaches for assessing groundwater NO_3^- elimination in a riparian zone. Ground Water. 37, no.3: 448-457.

Menyalio, O.V., and B.A. Hungate. 2006. Stable isotope discrimination during soil denitrification: Production and consumption of nitrous oxide. *Global Biogeochemical Cycles.* 20, 10 pp., Doi: 10. 1029/200GB002527.

Mosier, A.R., C. Kroeze, C.D. Nevison, O. Oenema, S. Seitzinger, and O. van Cleemput. 1998. Closing the global N_2O budget: nitrous oxide emissions through the agricultural nitrogen cycle-OECD/IPCC/IEA phase II development of IPCC guidelines for national greenhouse gas inventory methodology. *Nutr. Cycl. Agroecosyst.* 52: 225–48.

Nicholson, R.V., J.A. Cherry and E.J. Rearson. 1983. Migration of contaminants in groundwater at a landfill: a case study, 6. Hydrogeochemistry. J. Hydrol. 63, no. 1-2: 131-176.

Olivier, J.G.J, A.F. Bouwman, K.W. van der Hoek, and J.J.M. Berdowski. 1998. Global air emission inventories for anthropogenic sources of NOX, NH_3, and N_2O in 1990. Environ Poll. 102: 135-148.

Pérez, T., S.E. Trumbore, S.C. Tyler, P.A. Matson, I. Ortiz-Monasterio, T. Rahn, and D.W.T. Griffith. 2001. Identifying the agricultural imprint on the global N_2O budget using stable isotopes. *Journal of Geophysical Research.* 106, no.D9: 9869-9878.

Richardson, W.N., E.A. Strauss, L.A. Bartsch, E.M. Monroe, J.C. Cavanaugh, L. Vingum and D.M. Soballe. 2004. Denitrification in the upper Mississippi River: rates, controls, and contribution to nitrate flux. *Canadian Journal of Fisheries and Aquatic Sciences*. 61, no.7: 1102-1112.

Robertson, W.D., J.A. Cherry and E. A. Sudicky. 1991. Ground-water contamination from two small septic systems on sand aquifers. *Ground Water.* 29: 1097-1109.

Robertson, W.D., and J. A. Cherry. 1992. Hydrogeology of an unconfined sand aquifer and its effect on the behaviour of nitrogen from a large-flux septic system. *Applied Hydrogeol.* 1: 32-44.

Robertson, W.D**.** and S.L. Schiff, 1994. Fractionation of sulphur isotopes during biogenic sulphate reduction below a sandy forested recharge area in south-central Canada. *J. Hydrol*. 158: 123-134.

Robertson, W.D. 1999. Enhanced attenuation of septic system phosphate in non-calcareous sediments. Technical report prepared for CRESTech. Department of Earth Sciences, University of Waterloo, Waterloo, ON.

Robertson, W.D., D.W. Blowes, C.J. Ptacek, and J.A. Cherry. 2000. Long-term performance of in situ reactive barriers for nitrate remediation. *Ground Water*. 38: 689-595.

Robertson, W.D. 2003. Enhanced attenuation of septic system phosphate in noncalcareous sediments. *Ground Water*. 41, no.1: 48-56.

Robertson, W.D., Yeung, N., vanDriel, P.W. and Lombardo, P.S., 2005. High-permeability layers for remediation of ground water; Go wide, not deep. Ground Water, 43:574-581.

Robertson, W.D., J.V. Vogan, and P.S. Lombardo. 2008. Nitrate removal rates in a 15-year-old permeable reactive barrier treating septic system nitrate. *Ground Water Monit. and Remed.* 28, no.3: 65-72.

Robertson, W.D., 2008. Irreversible P sorption in septic system plumes? *Ground Water.* 46:51-60.

Robertson, W.D., and S.L. Schiff. 2008. Persistent elevated nitrate in a riparian zone aquifer. *J. Environ. Qual.* 37: 669-679.

Robertson, W.D., J. Spoelstra, L. Li, R. Elgood, I.D. Clark, S.L. Schiff, R. Aravena and J.D. Neufeld. 2010. Natural attenuation of septic system nitrogen by anammox. In preparation.

Ronen, D., Y. Kanfi, and M. Magatitz. 1983. Sources of nitrate in groundwater of the coastal plain of Israel. *Water Research* 17, no. 11: 1499-1503.

Rossi, A, 2010. Nitrification and denitrification processes in groundwater studied by nitrate isotopesm Lake Joseph (ON), Canada. M.Sc. thesis, Earth Science Department. La Sapienza, University of Rome, Rome, Italy. 112 pp.

Rudolph, D.L., D.A.J. Barry, and M.J. Gross. 1998. Contamination in Ontario farmstead domestic wells and its association with agriculture: 2. Results of multilevel monitoring well installations. *Journal of Contaminant Hydrology*. 32: 295-311.

Russow, R., H.-U. Neue, and I. Sich. 1999. The formation of the trace gases NO and N_2O in soils by the coupled processes of nitrification and denitrification: results of kinetic ^{15}N tracer investigations. *Global Change Science.* 2: 339-366.

Ryan, M.C., MacQuarrie, K.T.B., Harman, J., McLellan, J., 2000. Field and modeling evidence for a ‘‘stagnant flow’’ zone in the upper meter of sandy phreatic aquifers. Journal of Hydrology 233 (1–4), 223–240.

Sander, R., 1999. Compilation of Henry’s Law Constants for Inorganic and Organic Species of Potential Importance in Environmental Chemistry, Air Chemistry Department, Max-Planck Institute of Chemistry, Germany. http://www.mpch-mainz.mpg.de/~sander/res/henry.html

Sebol, L. A., 2004. Evaluation shallow groundwater age tracers: Br^-, CFCs, $^3H/^3He$, SF_6, and HCFCs/HFCs, Ph.D thesis, Univ. of Waterloo, Waterloo, Ont. 190 pp.

Sebol, L.A., Robertson, W.D., Busenberg, E., Plummer, L.N., Ryan, M.C., and Schiff, S.L., 2007. Evidence of CFC degradation in groundwater under pyrite oxidizing conditions. J. Hydrol. 347:1-12

Snider, D.M., S.L. Schiff, and J. Spoelstra. 2008. $^{15}N/^{14}N$ and $^{18}O/^{16}O$ stable isotopes ratios of nitrous oxide produced during denitrification in temperate forest soils. *Geochimica et Cosmochimica Acta.* 73. no.4: 877-888.

Shearer, G.B., and D. Kohl. 1986. N_2-fixation in field settings: estimations based on natural ^{15}N abundance. *Australian Journal of Plant Physiology.* 13: 699-756.

Silva, S.R., C. Kendall, D.H. Wilkison, A.C. Zeigler, C.C.Y. Chang, and R.J. Avanzino. 2000. A new method for collection and analysis of nitrate from dilute water for nitrogen and oxygen isotopes. *J. Hydrol.* 228: 22-36.

Sørensen, P., and E.S. Jensen. 1991. Sequential diffusion of ammonium and nitrate from soil extracts to a polytetrafluoroethylene trap for ^{15}N determination. Anal. Chim. Acta 252: 201-203.

Spalding, R.F., and M.E. Exner. 1991. Nitrate contamination in the contiguous United States. In *Nitrate Contamination; Exposure, Consequence and Control*, ed. I. Bogardi, I., R.D. Kuzelka, and W.G. Ennenga, 13-48. Berlin Heidelberg: Springer-Verlag.

Stafford, K., 2008. Investigation of Pharmaceutical Compounds in Landfill and Septic System Plumes. M.Sc. thesis, Department of Earth Sciences. Univ. of Waterloo, Waterloo, Ont. 126 pp.

Stein, L.Y., and Y.L. Yung. 2003. Production, isotopic composition and atmospheric fate of biologically produced nitrous oxide. *Annu. Rev. Erath Planet. Sci.* 31: 329-356.

Strauss, E.A., N.L. Mitchell, and G.A. Lamberti. 2002. Factors regulating nitrification in aquatic sediments: effects of organic carbon, nitrogen availability, and pH. *Canadian Journal of Fisheries and Aquatic Sciences*. 59, no.3: 554-563.

Strauss, E.A., and G.A. Lamberti. 2000. Regulation of nitrification in aquatic sediments by organic carbon. *Limnology and Oceanography*. 45, no.8: 1854-1859.

Sutka, R.L., N.E. Ostrom, P.H. Ostrom, H. Gandhi, A.J. J.A. Breznak, 2003. Nitrogen isotopmer site preference of N2O produced by Nitrosomonas europaea and Mythylococcus capsulatus Bath. Rapid Communications in Mass Spectrometry. 17: 738-745.

Sutka, R.L., N.E. Ostrom, P.H. Ostrom, H. Gandhi, A.J. J.A. Breznak, 2004. Erratum Nitrogen isotopmer site preference of N2O produced by Nitrosomonas europaea and Mythylococcus capsulatus Bath. Rapid Communications in Mass Spectrometry. 18: 1141-1142.

Sutka, R.L., N.E. Ostrom, P.H. Ostrom, J.A. Breznak, H. Gandhi, A.J. Pitt, and F. Li. 2006. Distinguishing nitrous oxide production from nitrification and denitrification on the basis of isotopomer abundances. *Applied and Environmental Microbiology.* 72: 638-644.

Thuss, S. J., 2008. Nitrous oxide production in the Grand River, Ontario, Canada: new insights from stable isotope analysis of dissolved nitrous oxide. M.Sc. thesis, Department of Earth Sciences. Univ. of Waterloo, Waterloo, Ont. 185 pp.

Vandernhoff, A., 2007. Extreme N_2O production in a riparian zone with a low organic content aquifer. B.Sc. thesis, Department of Earth Sciences. Univ. of Waterloo, Waterloo, Ont. 48 pp.

Vieten, B., T. Blunier, A. Neftel, C. Alewell, and F. Conen. 2007. Fractionation factors for stable isotopes of N and O during N_2O reduction in soil depend on reaction rate constant. *Rapid Communications in Mass Spectrometry.* 21: 846-850.

Vogel, J.C., A.S. Talma and T.H.E Heaton. 1981. Gaseous nitrogen as evidence for denitrification in groundwater. *J. Hydrol.* 50, no. 1/3: 191-200.

Von der Heide, C., J. Böttcher, M. Deurer, D. Weymannn, R. Well, and W.H.M. Duijnisveld. 2008. Spatical variability of N_2O concentrations and of denitrification-related factors in the surficial groundwater of a catchment in Northern Germany. *J. Hydrol.* 360: 230-241.

Walker, W.G., J. Bouma, D.R. Keeney, P.G. Olcott. 1973. Nitrogen transformation during subsurface disposal of septic tank effluent in sands: II Ground water quality. *J. Environ. Qual.* 2: 521-525.

Wassenaar, L.I. 1995. Evaluation of the origin and fate of nitrate in the Abbotsford Aquifer using the isotopes of 15N and 18O in NO3-1. *Applied Geochemistry*. 10: 391-405.

Wrage. N., G. L. Velthof, M.L. van Beusichem, and O. Oenema. 2001. Role of nitrifier denitrification in the production of nitrous oxide. *Soil Biology & Biochemistry*. 33: 1723-1732.

Yoshida, N. 1984. Nitrogen isotope studies on the geochemical cycle of nitrous oxide. Thesis, Tokyo Institute of Technology, Tokyo, Japan. 184 pp.

Yoshida, N. 1988. ^{15}N-depleted N_2O as a product of nitrification. *Nature*. 335: 528–529.

Table 1.1. Sources of atmospheric N_2O (Adapted from Stein and Yung, 2003).

Source	Data in 1990[1]		Data in 1994[2]	
	Tg N/year	% of total	Tg N/year	% of total
Anthropogenic sources				
Agricultural soils	3.6	21.7%	4.2	23.7%
Biomass burning	0.5	3.0%	0.5	2.8%
Industrial sources	0.7	4.2%	1.3	7.3%
Cattle and feedlots	1.0	6.0%	2.1	11.9%
Subtotal	5.8	34.9%	8.1	45.8%
Natural sources				
Ocean	3.6	21.7%	3.0	16.9%
Atmosphere	0.6	3.6%	0.6	3.4%
Soils	6.6	39.8%	6.0	33.9%
Subtotal	10.8	65.1%	9.6	54.2%
Total	16.6	100%	17.7	100%

[1] Olivier et al. 1998;
[2] Mosier et al. 1998; Kroeze, 1999

Table 1.2. Calculated N_2O concentrations in groundwater in equilibrium with atmosphere (Henry's law constant for N_2O is 2.5×10^{-2} M/atm[1], partial pressure of atmospheric N_2O is 319×10^{-9} atm[1]).

Temperature (ºC)	N_2O-N concentrations (µg/L) in groundwater
8	0.37
9	0.35
10	0.34
11	0.33
12	0.32
13	0.31
14	0.30
15	0.29
16	0.28
17	0.27

[1]Forster et al., 2007

1. $K_{H_X} = \frac{[X]}{P_X}$

2. $K_H = K_H{}^{o} \cdot e^{[-\frac{\Delta H_{so\ ln}}{R}(\frac{1}{T}-\frac{1}{T^o})]}$

3. $\frac{-\Delta H_{so\ ln}}{R} = \frac{-d\ln K_H}{d(\frac{1}{T})}$

Substituting 2 and 3 into 1:

4. $[X] = P_X \cdot K_{H_X}{}^{o} \cdot e^{[\left(\frac{-d\ln K_H}{d(\frac{1}{T})}\right)(\frac{1}{T}-\frac{1}{T^o})]}$

$$\frac{-d\ln K_H}{d\left(\frac{1}{T}\right)} = 2600K$$

Equation 1, 2 from Vandenhoff (2007); 3, 4 modifeied from Vandenhoff (2007), using Henry's law Source: http://en.wikipedia.org/w/index.php?oldid=386577429.

Table 3.1. Comparison of N_2O concentrations and isotopic values at multiple field sites.

Site	Sampling Date	Water Type	N_2O –N concentrations (µg/L)	$\delta^{15}N$-N_2O (‰)	$\delta^{18}O$-N_2O (‰)	Reference
Long Point	June 2008 September 2008 2009	Groundwater	1-739 1-1071 0.4-999	-42 to +31 -45 to +25 -43 to +17	+20 to +96 +27 to +89 +20 to +91	this study this study this study
Putnam	2006 2008	Groundwater	0.8-1044 0.8-1100	-28 to +22 -32 to +9	+44 to +72 +36 to +99	Vandenhoff, 2007 Unpublished data
Fuhrberger Feld catchment	March 2005	Groundwater	3-13	/	/	Von der Heide et al., 2008
Avon streambed	2008-2009	subsurface stream water	<1-36	/	/	Elgood et al., in press
Grand River	May 2006 June 2007	Surface Water	0.2-1.2	-5 to +6	+38 to +49	Thuss, 2008

Table 3.2. Parameters used to calculate the ranges of $\delta^{15}N$ and $\delta^{18}O$ values of N_2O produced from nitrification and denitrification at Long Point Site.

	Nitrification	Denitrification
Substrate	NH_4^+	NO_3^-
Product	N_2O	N_2O
$\varepsilon^{15}N$(‰)	-45 to -66[1]	-20 to -29[2]
$\varepsilon^{18}O$(‰)	-5 to +5[4]	+32 to +48[3]
$\delta^{15}N$(‰) (substrate)	+5	0 to +48
$\delta^{18}O$(‰) (substrate)	/	-12 to +25
$\delta^{15}N$-N_2O (‰) (product)	-21 to -61(combined with soil ^{15}N-N_2O)	-29 to +28
$\delta^{18}O$-N_2O (‰) (product)	+18.5 to +28.5	+20 to +73

[1] Stein and Yung, 2003
[2] Snider et al., 2008
[3] Spoelstra, per comm
[4] $\varepsilon^{18}O_{(N_2O\text{-}O_2)}$

Table 4.1. Parameters used to calculate the ranges of $\delta^{15}N$ and $\delta^{18}O$ values of N_2O produced from nitrification and denitrification at Lake Joseph site.

	Nitrification	Denitrification
Substrate	NH_4^+	NO_3^-
Product	N_2O	N_2O
$\varepsilon\ ^{15}N$(‰)	-45 to -66[1]	-20 to -29[2]
$\varepsilon\ ^{18}O$(‰)	-5 to +5[4]	+32 to +48[3]
$\delta\ ^{15}N$(‰) (substrate)	5 to 9	-1 to +14
$\delta\ ^{18}O$(‰) (substrate)	/	-12 to +5
$\delta\ ^{15}N$-N_2O (‰) (product)	-36 to -61	-6 to -30
$\delta\ ^{18}O$-N_2O (‰) (product)	+18.5 to +28.5	+20 to +53

[1] Stein and Yung, 2003
[2] Snider et al., 2008
[3] Spoelstra, per comm
[4] $\varepsilon^{18}O_{(N_2O\text{-}O_2)}$

Table 5.1. Parameters used to calculate the ranges of $\delta^{15}N$ and $\delta^{18}O$ values of N_2O produced from nitrification and denitrification at Strathroy Site.

	Nitrification	Denitrification
Substrate	NH_4^+	NO_3^-
Product	N_2O	N_2O
$\varepsilon\ ^{15}N$(‰)	-45 to -66[1]	-20 to -29[2]
$\varepsilon\ ^{18}O$(‰)	-5 to +5[4]	32 to 48[3]
$\delta\ ^{15}N$(‰) (substrate)	0 to +2[5]	+3 to +26
$\delta\ ^{18}O$(‰) (substrate)	/	-3 to +16
$\delta\ ^{15}N$-N_2O (‰) (product)	-43 to -66	-4 to -32
$\delta\ ^{18}O$-N_2O (‰) (product)	+18.5 to +28.5	+35 to +74

[1] Stein and Yung, 2003
[2] Snider et al., 2008
[3,5] Spoelstra, per comm
[4] $\varepsilon^{18}O_{(N_2O\text{-}O_2)}$

Table 6.1. Parameters used to calculate the ranges of $\delta^{15}N$ and $\delta^{18}O$ values of N_2O produced from nitrification and denitrification at Woodstock site.

	Nitrification	Denitrification
Substrate	NH_4^+	NO_3^-
Product	N_2O	N_2O
$\varepsilon\ ^{15}N$(‰)	-45 to -66[1]	-20 to -29[2]
$\varepsilon\ ^{18}O$(‰)	-5 to +5[4]	+32 to +48[3]
$\delta\ ^{15}N$(‰) (substrate)	0 to +2[5]	+5 to +7
$\delta\ ^{18}O$(‰) (substrate)	/	-1 to +2
$\delta\ ^{15}N$-N_2O (‰) (product)	-43 to -66	-13 to -24
$\delta\ ^{18}O$-N_2O (‰) (product)	+18.5 to +28.5	+31 to +50

[1] Stein and Yung, 2003
[2] Snider et al., 2008
[3,5] Spoelstra, per comm
[4] $\varepsilon^{18}O_{(N_2O\text{-}O_2)}$

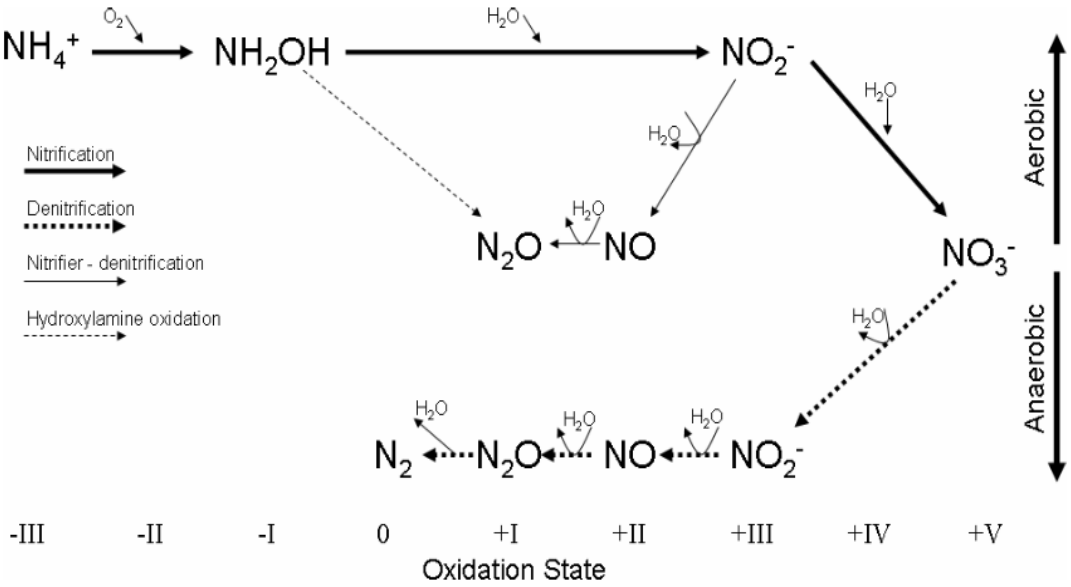

Figure 1.1. Pathways of N_2O production in the nitrogen cycle, showing that N_2O could be produced through either nitrification or denitrification and can be further consumed to produce N_2 (From Thuss, 2008).

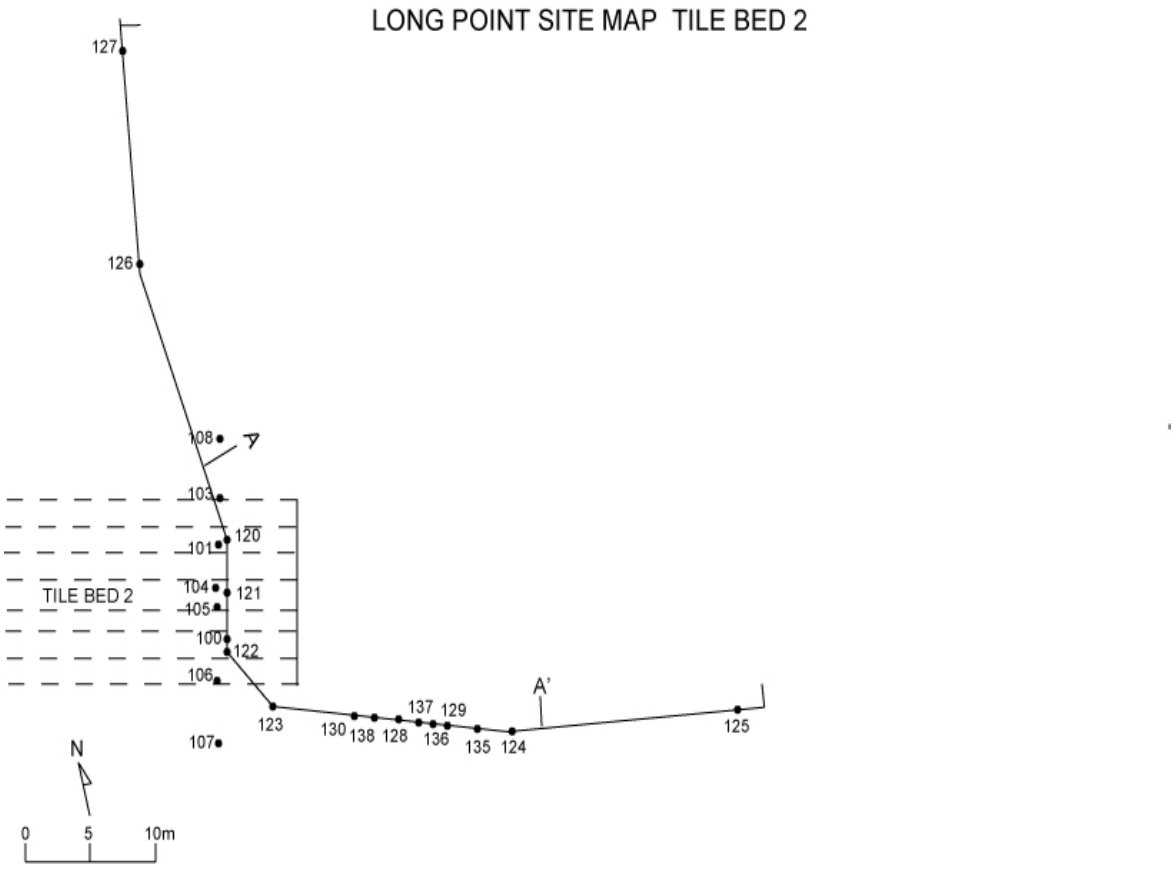

Figure 3.1. Long point Septic System Site, Ontario, showing Tile Bed 2 location., monitoring wells and Section A-A'.

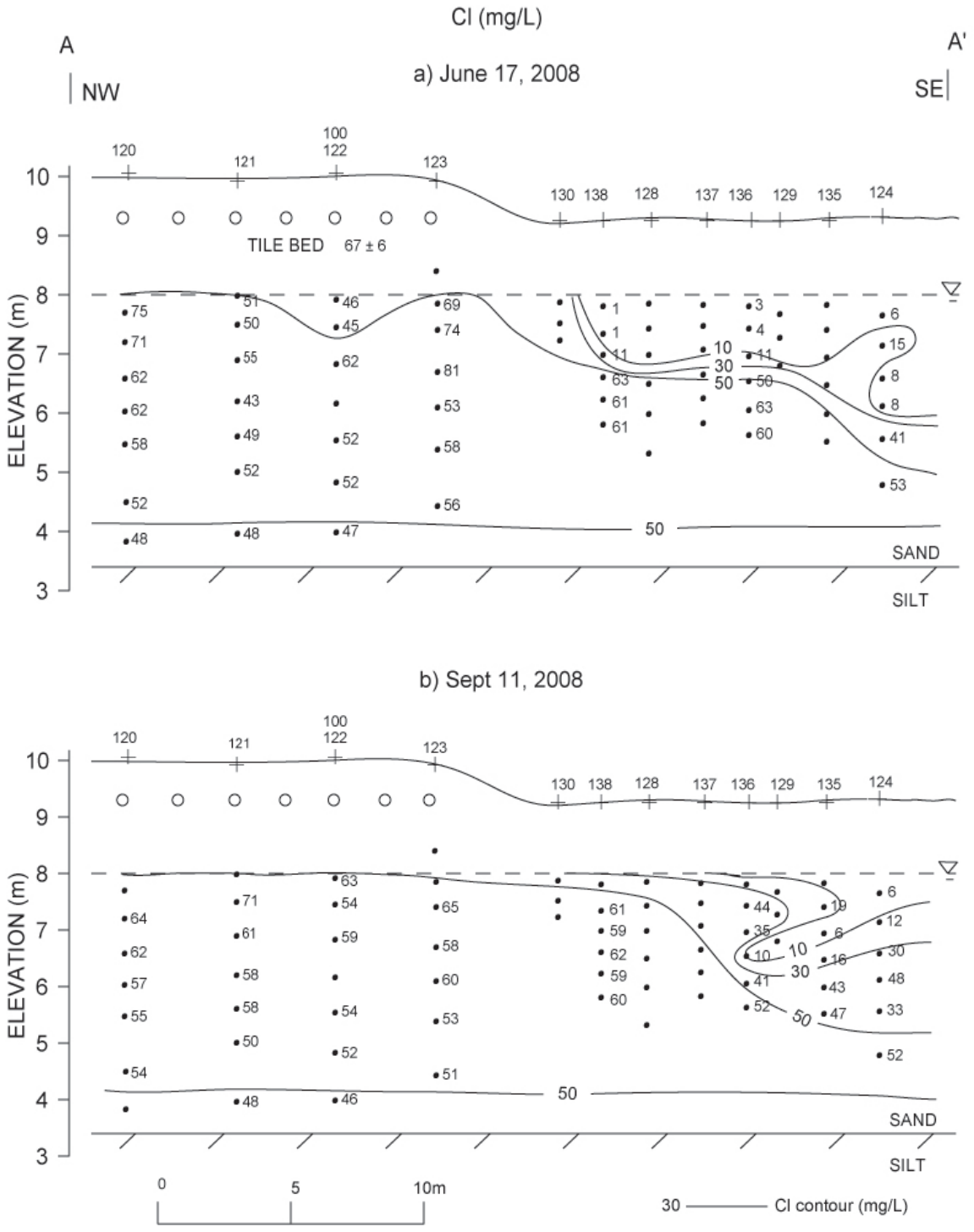

Figure 3.2. Section A-A' Tile Bed 2, showing Cl^- concentrations: a) June 2008 and b) September 2008. Septic tank effluent value is mean and standard deviation of 10 samples taken from September, 2007- June, 2010.

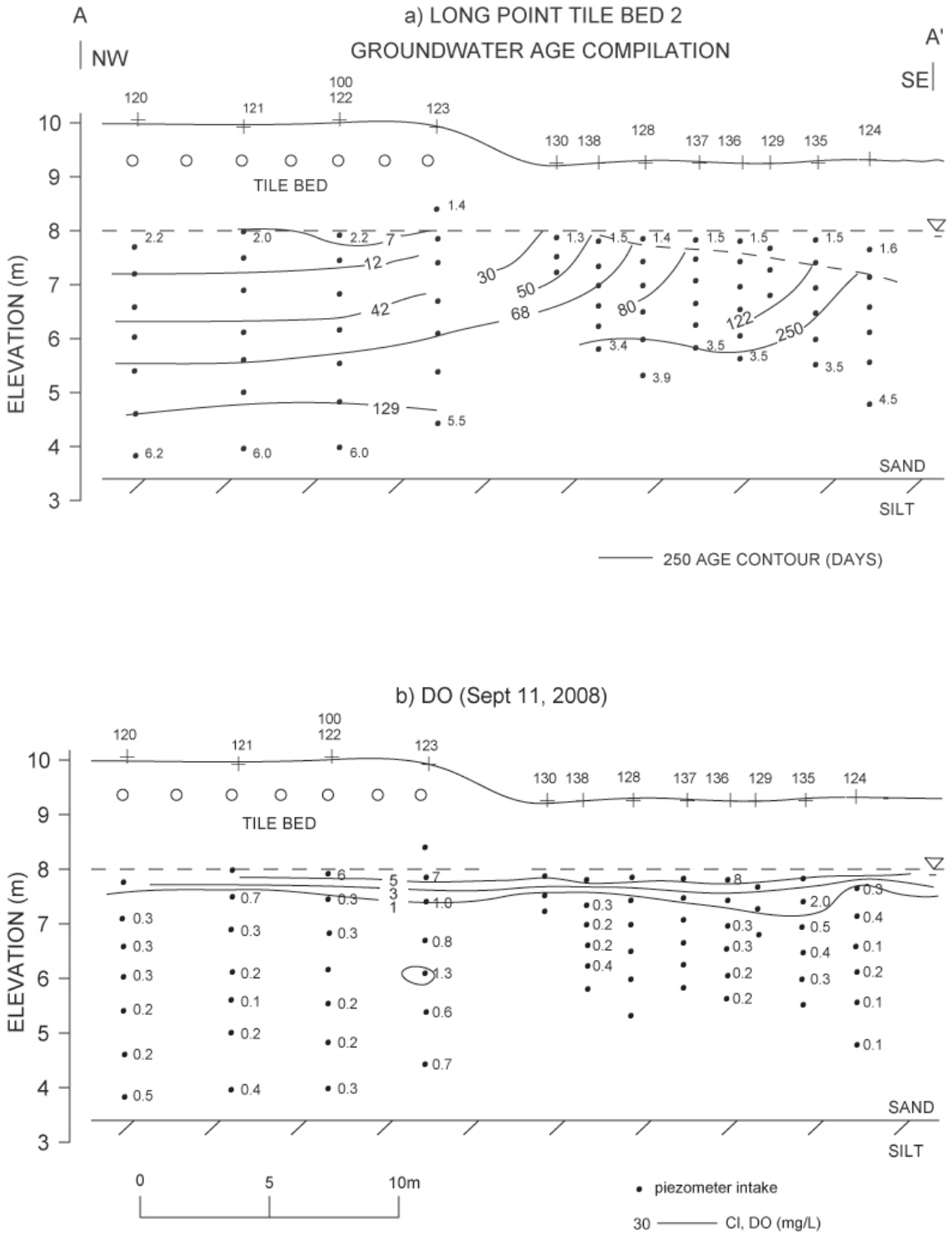

Figure 3.3. a) Groundwater age compilation from EC breakthrough and Br tracer tests; 7, 12, 129 day contours from EC breakthrough June-October, 1990; 30, 50, 80, 122 day contours from EC breakthrough June-September, 2004; 42 day from Br tracer injected September 1990; 68, 250 day contours from Br tracer injected July 4, 2008. (From Robertson et al. in prep.). b) dissolved oxygen (DO) distribution September 11, 2008 (From Robertson et al. in prep.).

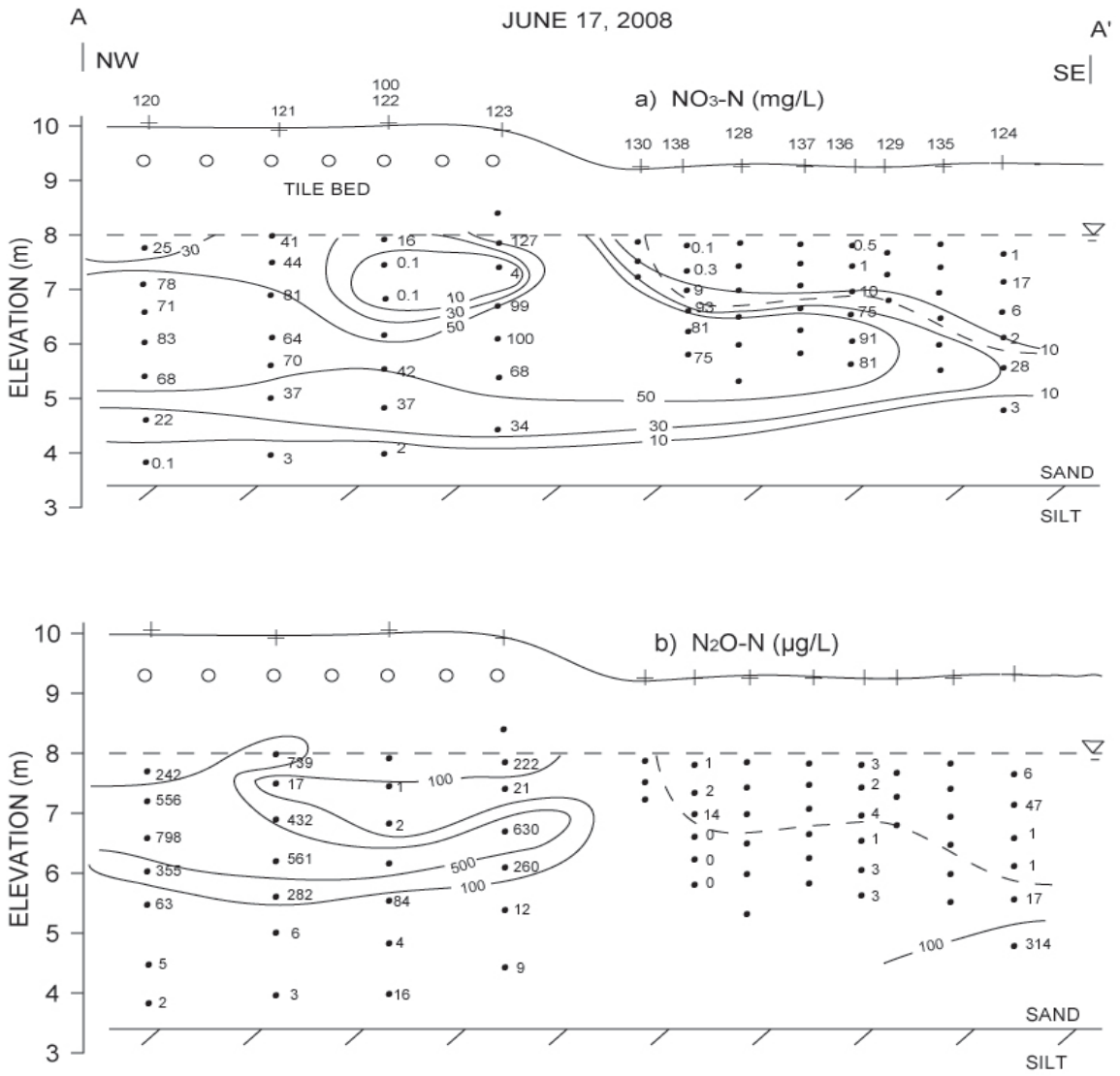

Figure 3.4. Section A-A' showing a) NO_3^--N, b) N_2O-N, Ec) $\delta^{15}N$-N_2O and $\delta^{18}O$-N_2O, d) NH_4^+-N, e) Dissolved Organic Carbon (DOC) distribution, June 17, 2008. Mean NH_4^+-N concentrations from Robertson et al., in prep.

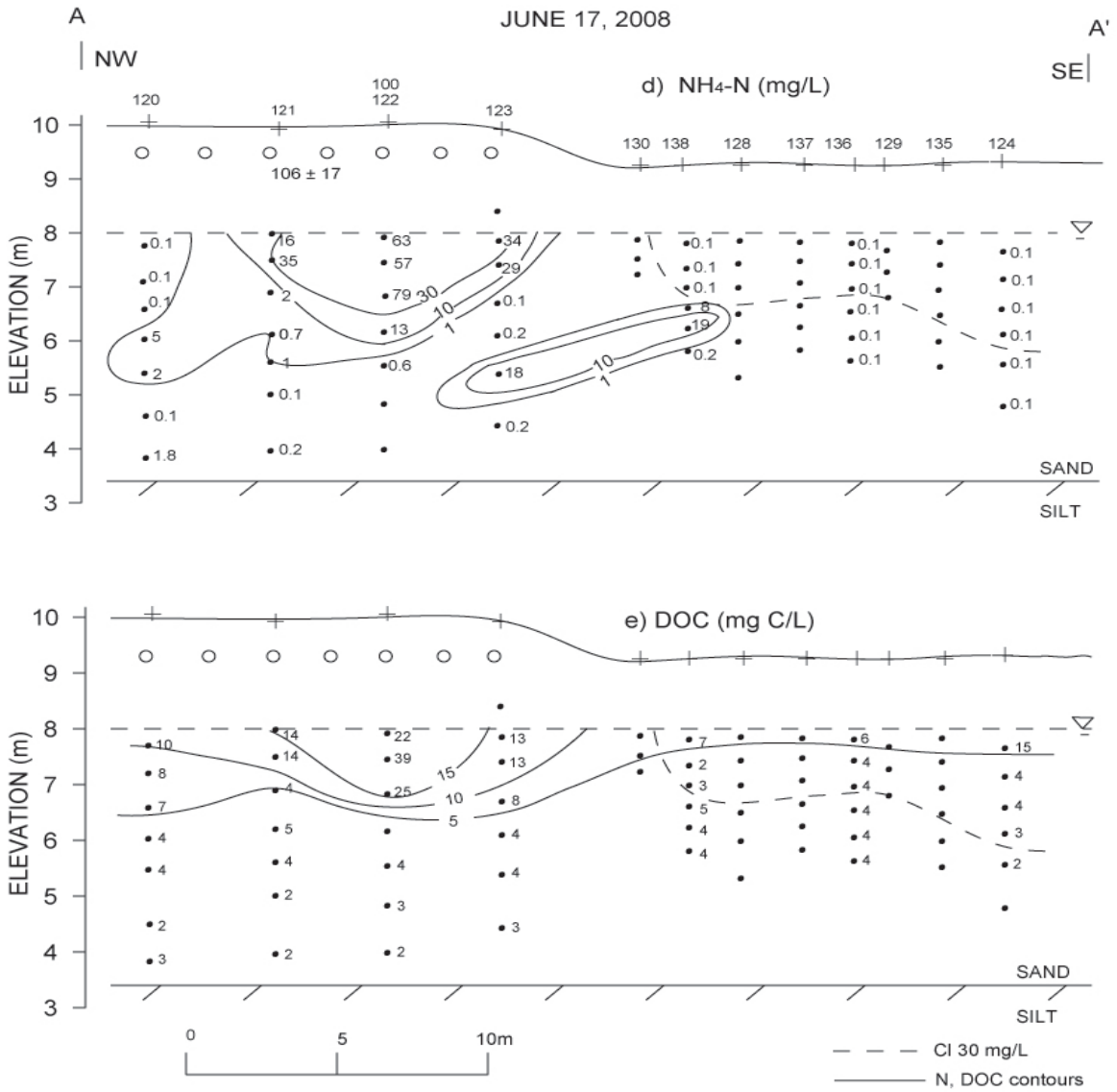

Figure 3.4 (Continued). Section A-A' showing a) NO_3^--N, b) N_2O-N, Ec) $\delta^{15}N$-N_2O and $\delta^{18}O$-N_2O, d) NH_4^+-N, e) DOC distribution, June 17, 2008. Mean NH_4^+-N concentrations from Robertson et al., in prep.

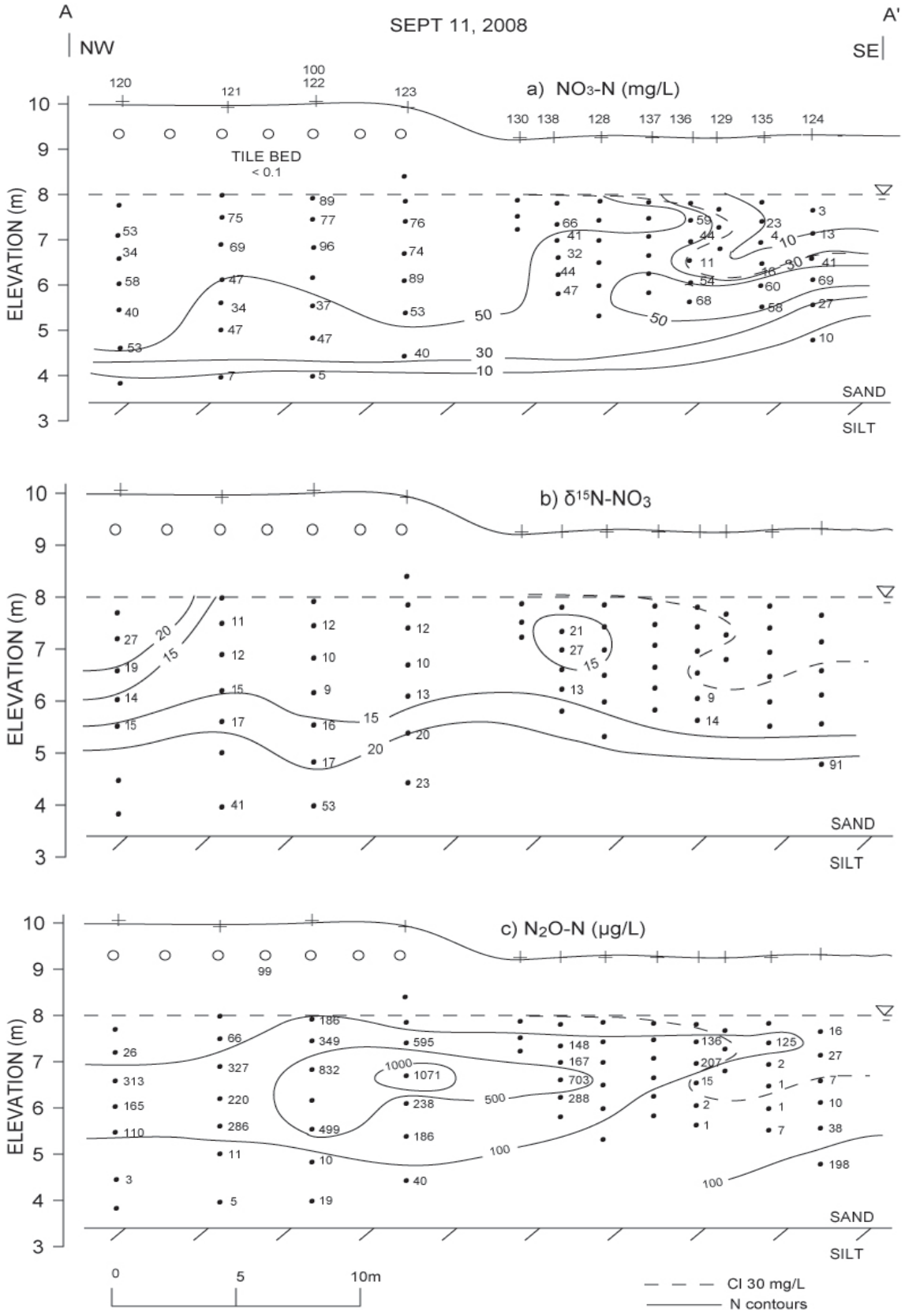

Figure 3.5. Section A-A' showing a) NO_3^--N, b) ^{15}N-NO_3^-, c) N_2O-N, Ed) $\delta^{15}N$-N_2O and $\delta^{18}O$-N_2O, e) NH_4^+-N, f) DOC distribution, Sept 11, 2008. Mean NH_4^+-N concentrations from Robertson et al., in prep.

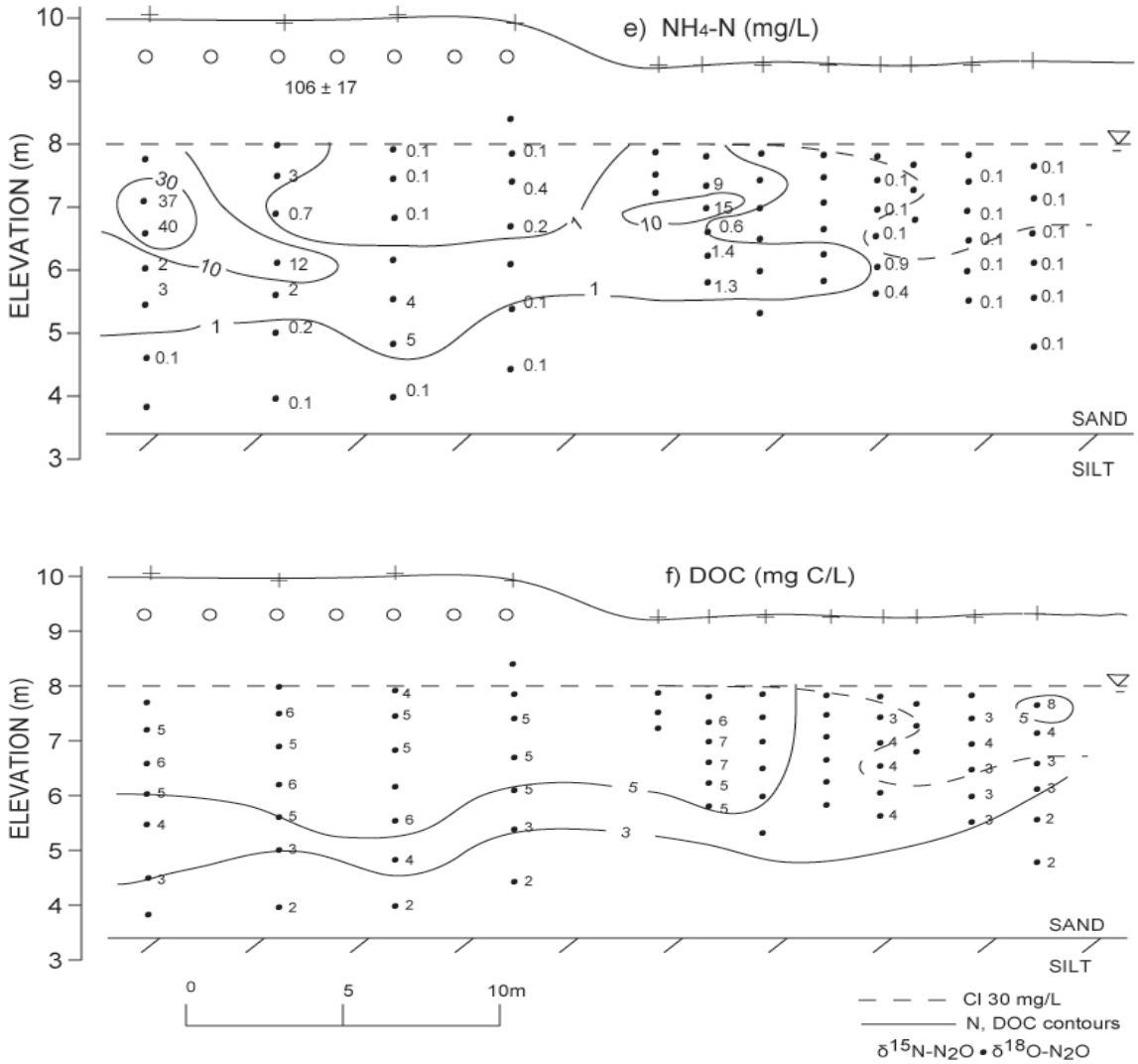

Figure 3.5 (Continued). Section A-A' showing a) NO_3^--N, b) ^{15}N-NO_3^-, c) N_2O-N, Ed) $\delta^{15}N$-N_2O and $\delta^{18}O$-N_2O, e) NH_4^+-N, f) DOC distribution, Sept 11, 2008. Mean NH_4^+-N concentrations from Robertson et al., in prep.

LP 100

a) June 2, 2009

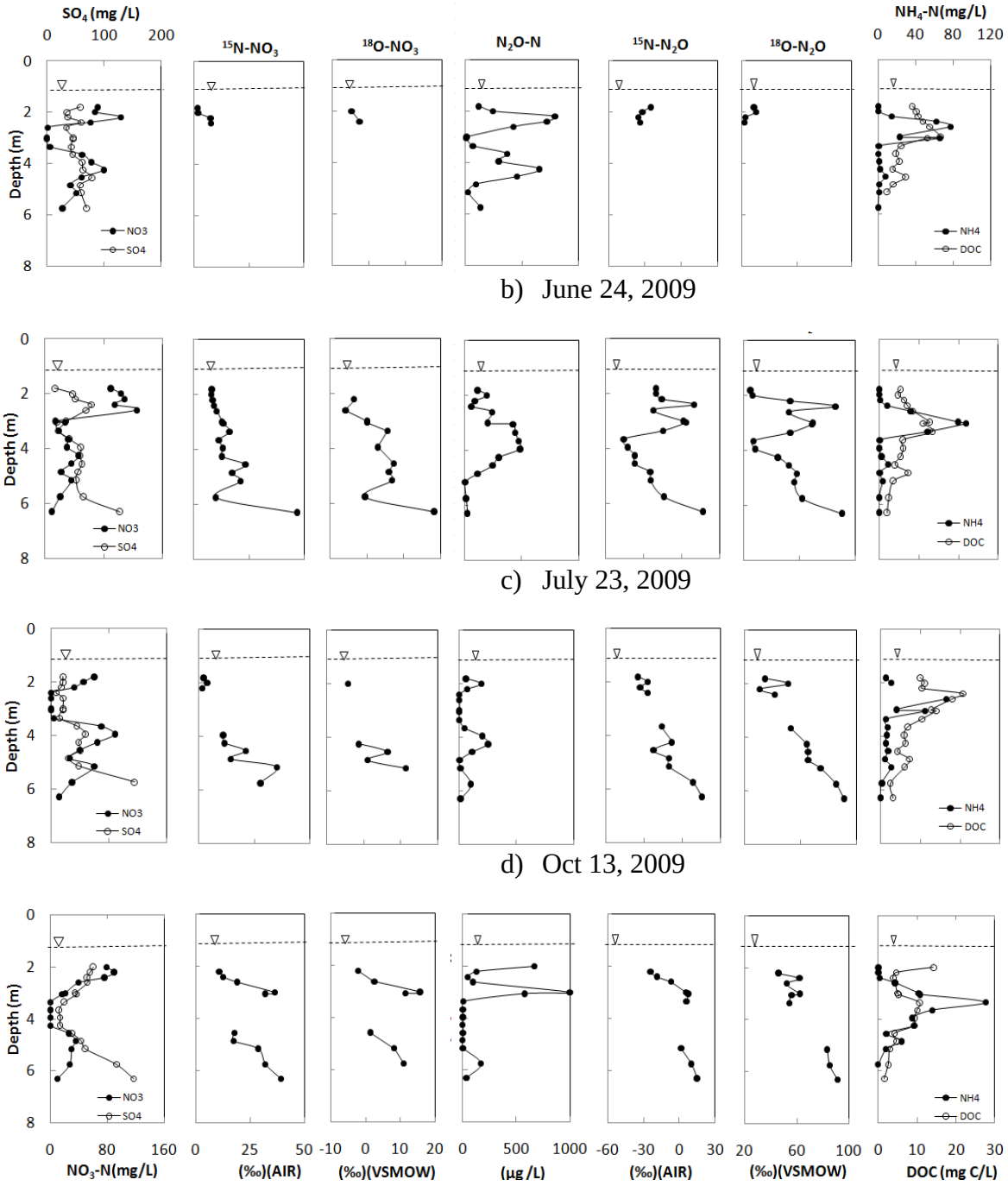

b) June 24, 2009

c) July 23, 2009

d) Oct 13, 2009

Figure 3.6. Depth profiles showing aqueous concentrations of NO_3^--N, N_2O, SO_4^{2-}, NH_4^+-N and DOC and isotopic composition of $\delta^{15}N\text{-}NO_3^-$, $\delta^{18}O\text{-}NO_3^-$, $\delta^{15}N\text{-}N_2O$ and $\delta^{18}O\text{-}N_2O$ at proximal piezometer nests LP100 on; a) June 2, 2009, b) June 24, 2009, c) July 23, 2009, d) October 13, 2009.

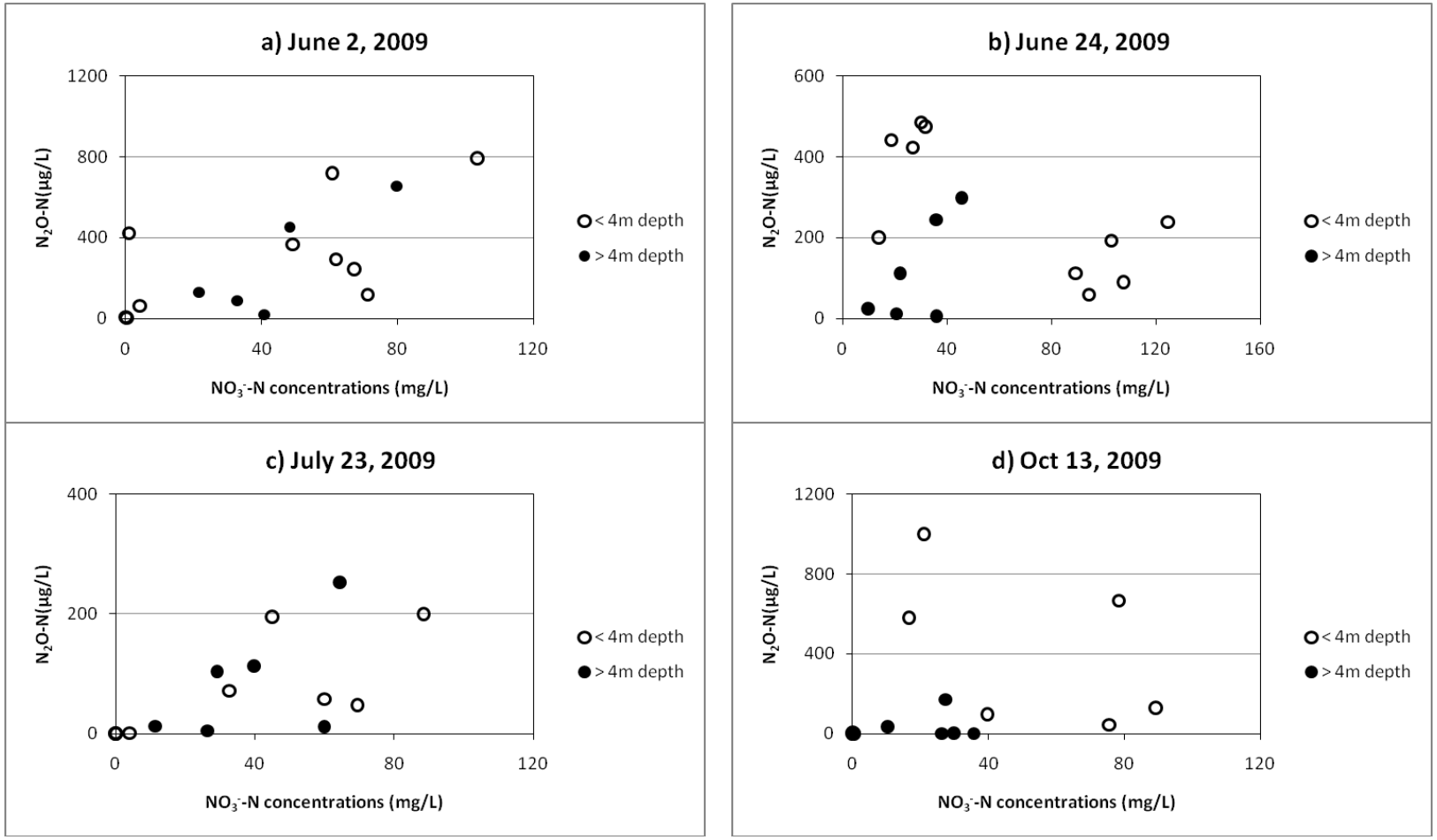

Figure 3.7. Comparison of N_2O-N versus NO_3^--N for the samples collected at LP 100 piezometer nests on four separate sampling dates: a) June 2, 2009; b) June 24, 2009; c) July 23, 2009 and d) October 13, 2009.

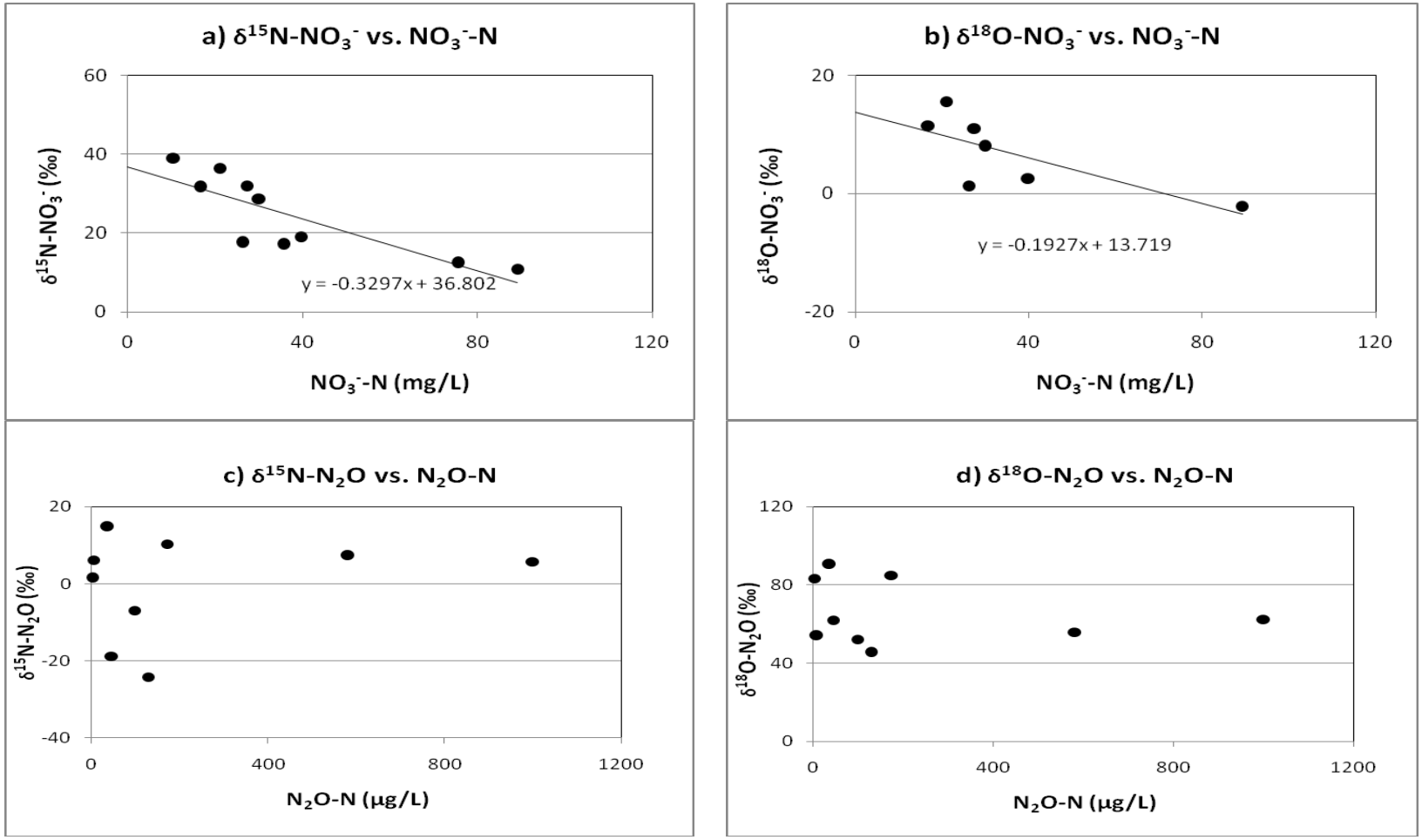

Figure 3.8. Comparison of a) $\delta^{15}N\text{-}NO_3^-$ versus NO_3^--N, b) $\delta^{18}O\text{-}NO_3^-$ versus NO_3^--N, c) $\delta^{15}N\text{-}N_2O$ versus N_2O-N, d) $^{18}\delta N\text{-}N_2O$ versus N_2O-N for the samples collected at LP 100 piezometer nests on October 13, 2009.

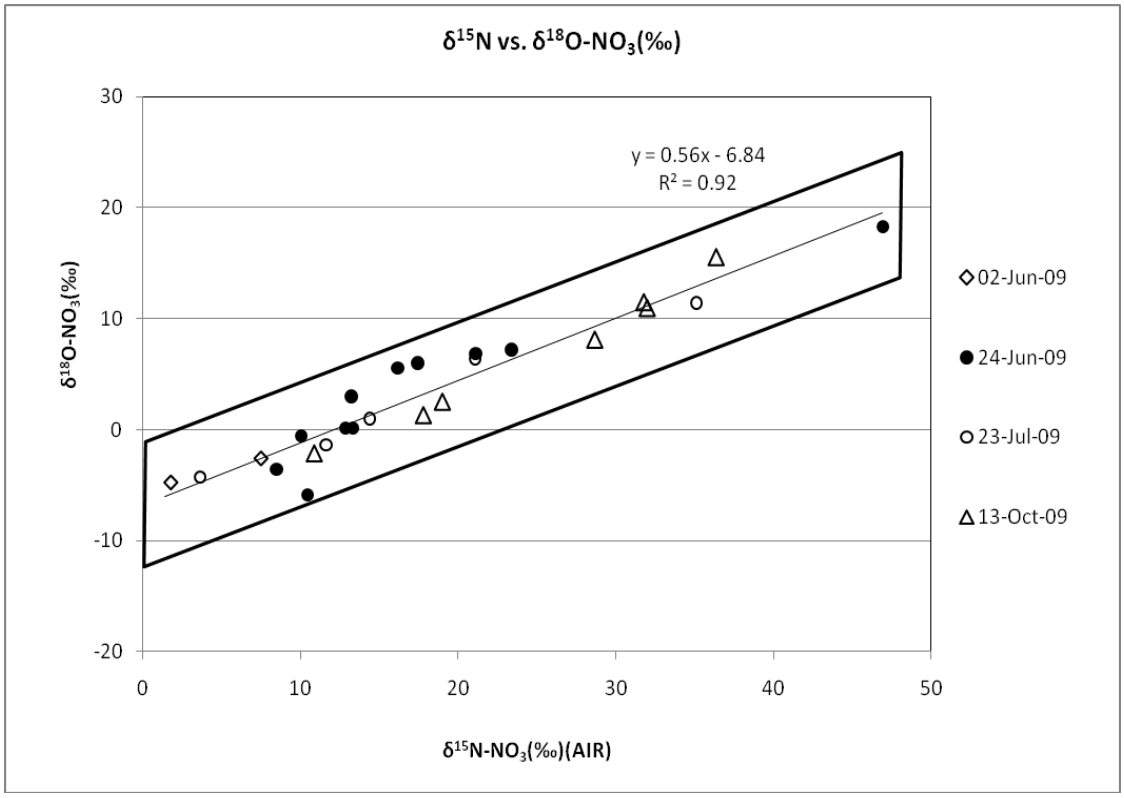

Figure 3.9. Comparison of NO_3^- $\delta^{18}O$ and $\delta^{15}N$ for the samples collected at LP 100: June 2, 2009; June 24, 2009; July 23, 2009 and October 13, 2009. Box shows the $\delta^{15}N$-NO_3^- ranges from 0 to +48‰ and $\delta^{18}O$ -NO_3^- ranges from -12 to +25‰. Line represents the isotope enrichment ratio of $\delta^{15}N$ to $\delta^{18}O$ is approximately 1.8:1.

Long Point N_2O Isotope Data (Full Transect)

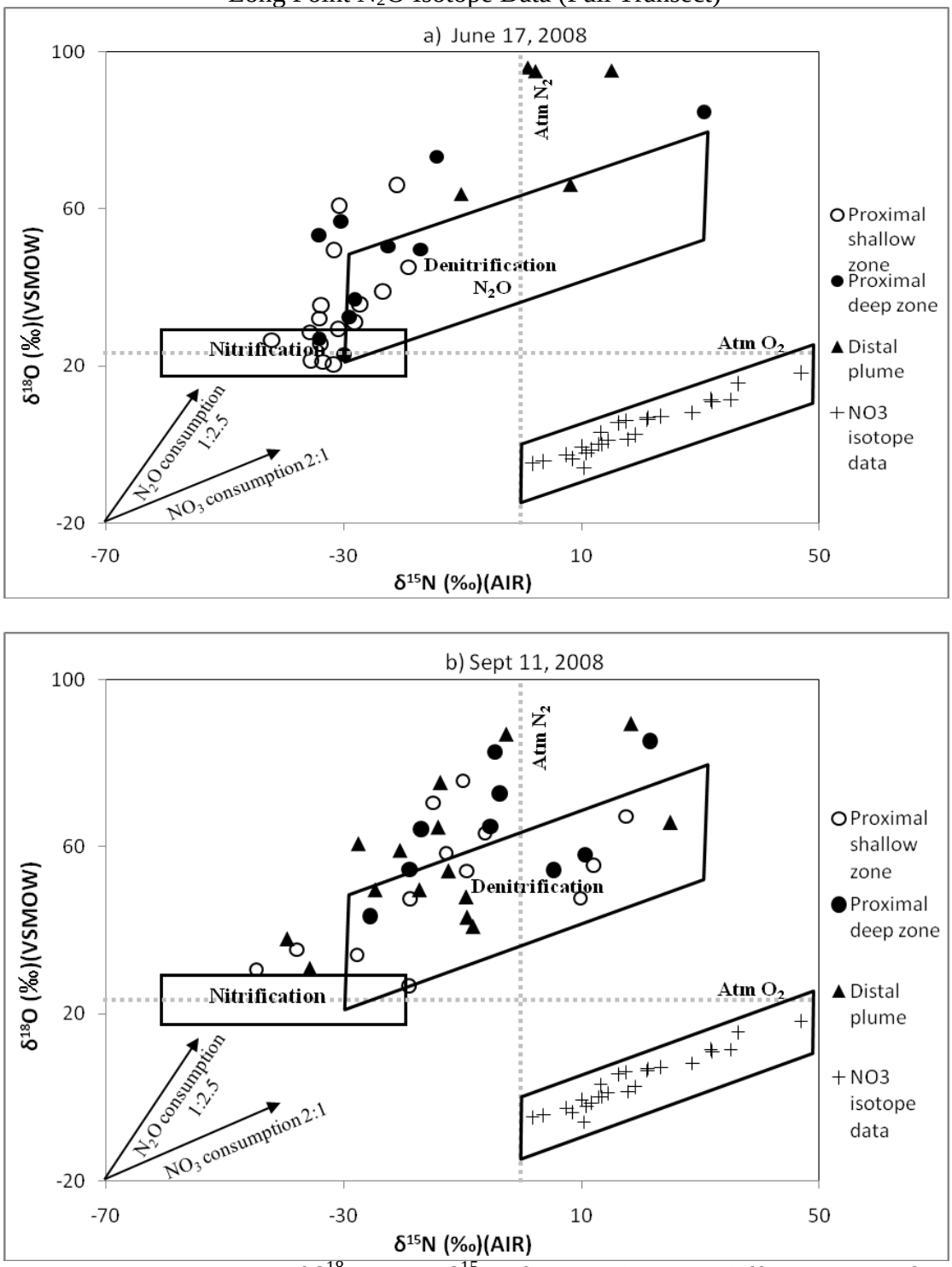

Figure 3.10. Comparison of $\delta^{18}O$ versus $\delta^{15}N$ of N_2O and NO_3^- in different zones of the Long Point plume; a) June 17, 2008, b) September 11, 2008. NO_3^- isotope box shows $\delta^{15}N$-NO_3^- ranges from 0 to +48‰ and $\delta^{18}O$ -NO_3^- ranges from -12 to +25‰ at LP. Nitrification and denitrification boxes show the calculated ranges of $\delta^{15}N$ and $\delta^{18}O$ values of N_2O produced from nitrification and denitrification (see Table 3.2 for details). Lines represent the isotope enrichment ratio of $\delta^{15}N$-N_2O to $\delta^{18}O$-N_2O is 1:2.5 for N_2O consumption and the isotope enrichment ratio of $\delta^{15}N$- NO_3^- to $\delta^{18}O$-NO_3^- is 2:1 for NO_3^- consumption. Dashed lines represent atmospheric $\delta^{18}O$-O_2 and $\delta^{15}N$-N_2 are +23.5‰ and 0‰, respectively.

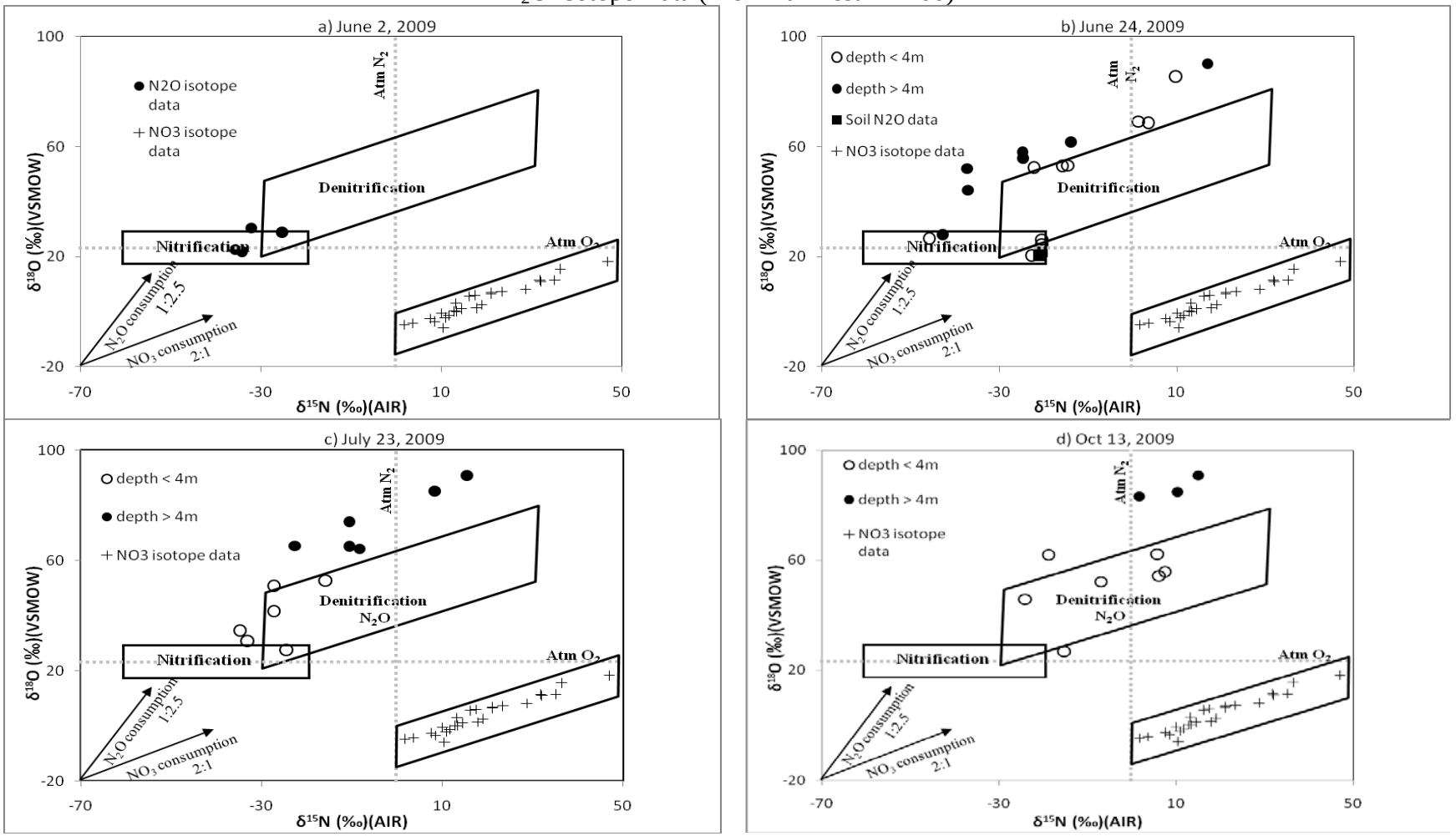

Figure 3.11. Comparison of $\delta^{18}O$ versus $\delta^{15}N$ of N_2O and NO_3^- for the samples collected at LP 100 piezometer nests on four separate sampling dates: a) June 2, 2009; b) June 24, 2009; c) July 23, 2009 and d) October 13, 2009. Mean $\delta^{15}N$-N_2O value from soil gas is -20.85±0.09‰ (n=7) and mean $\delta^{18}O$-N_2O value from soil gas is 20.84±0.09‰ (n=7).

Figure 4.1. Lake Joseph site, Ontario, showing tile bed location, monitoring wells, and section A-A' and B-B' (From Rossi, 2010).

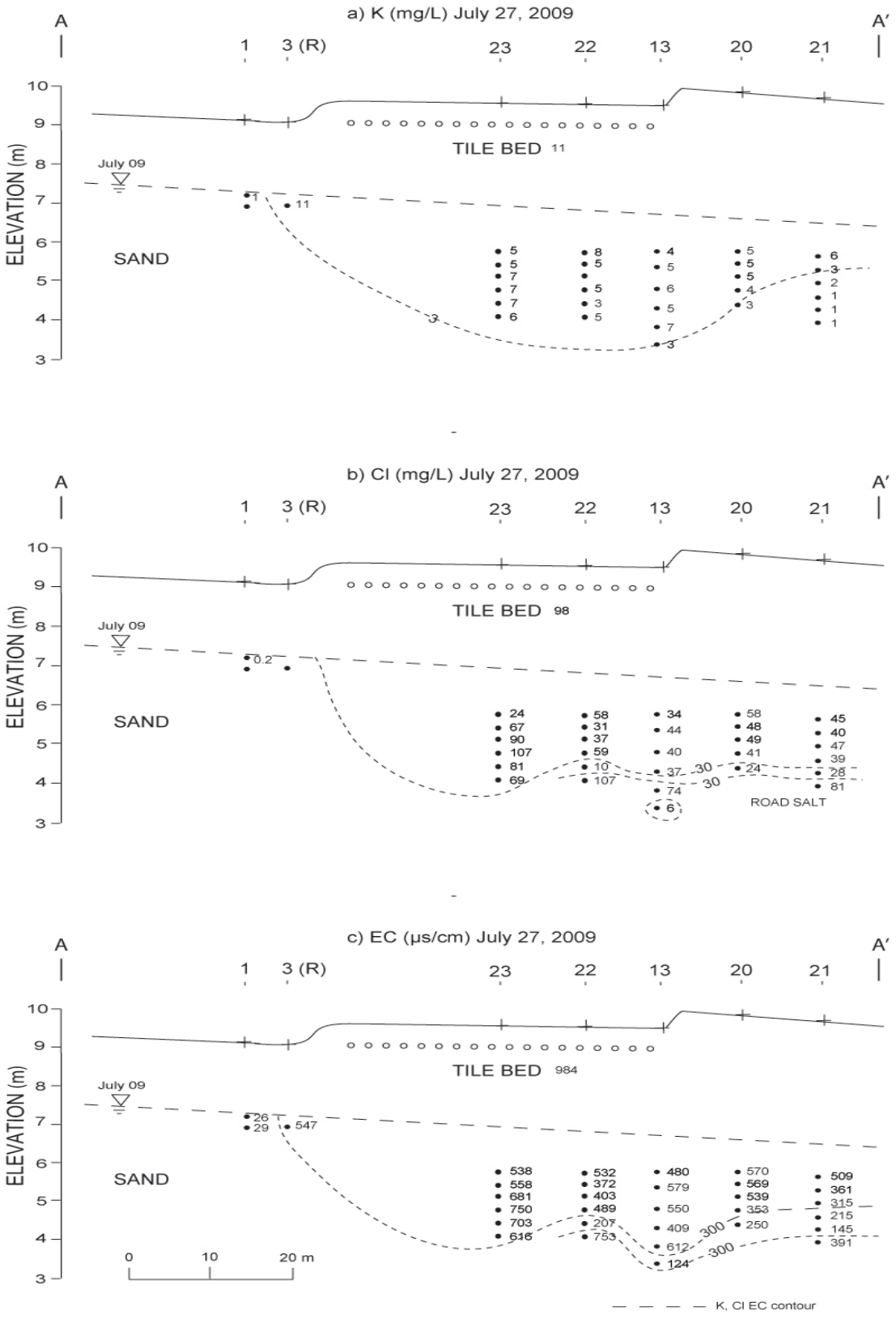

Figure 4.2. Lake Joseph Septic System, Section A-A' showing a) K^+, b) Cl^-, and c) Electrical Conductivity (EC) distribution, July 27, 2009.

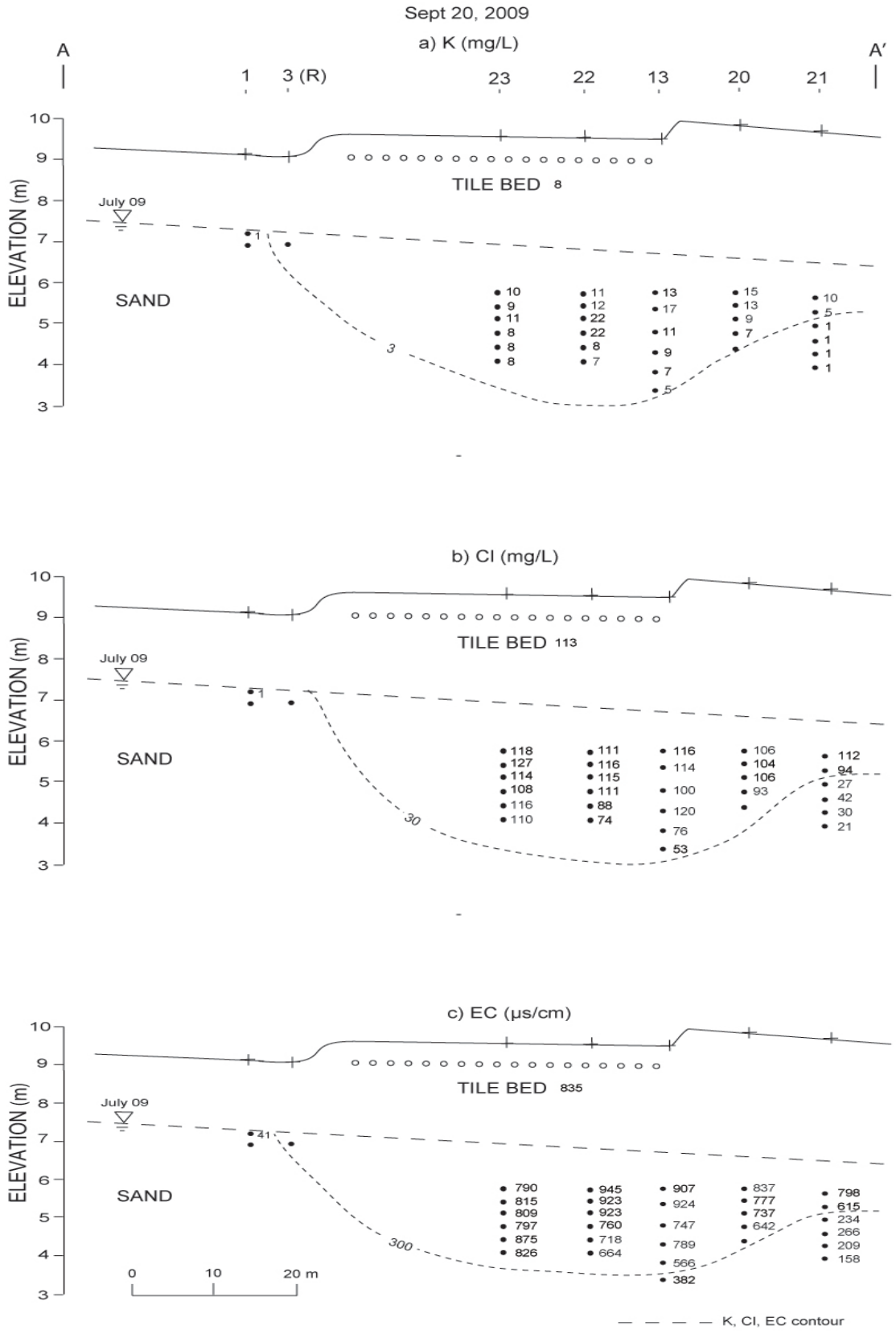

Figure 4.3. Lake Joseph Septic System, Section A-A' showing a) K^+, b) Cl^-, and c) EC distribution, September 20, 2009.

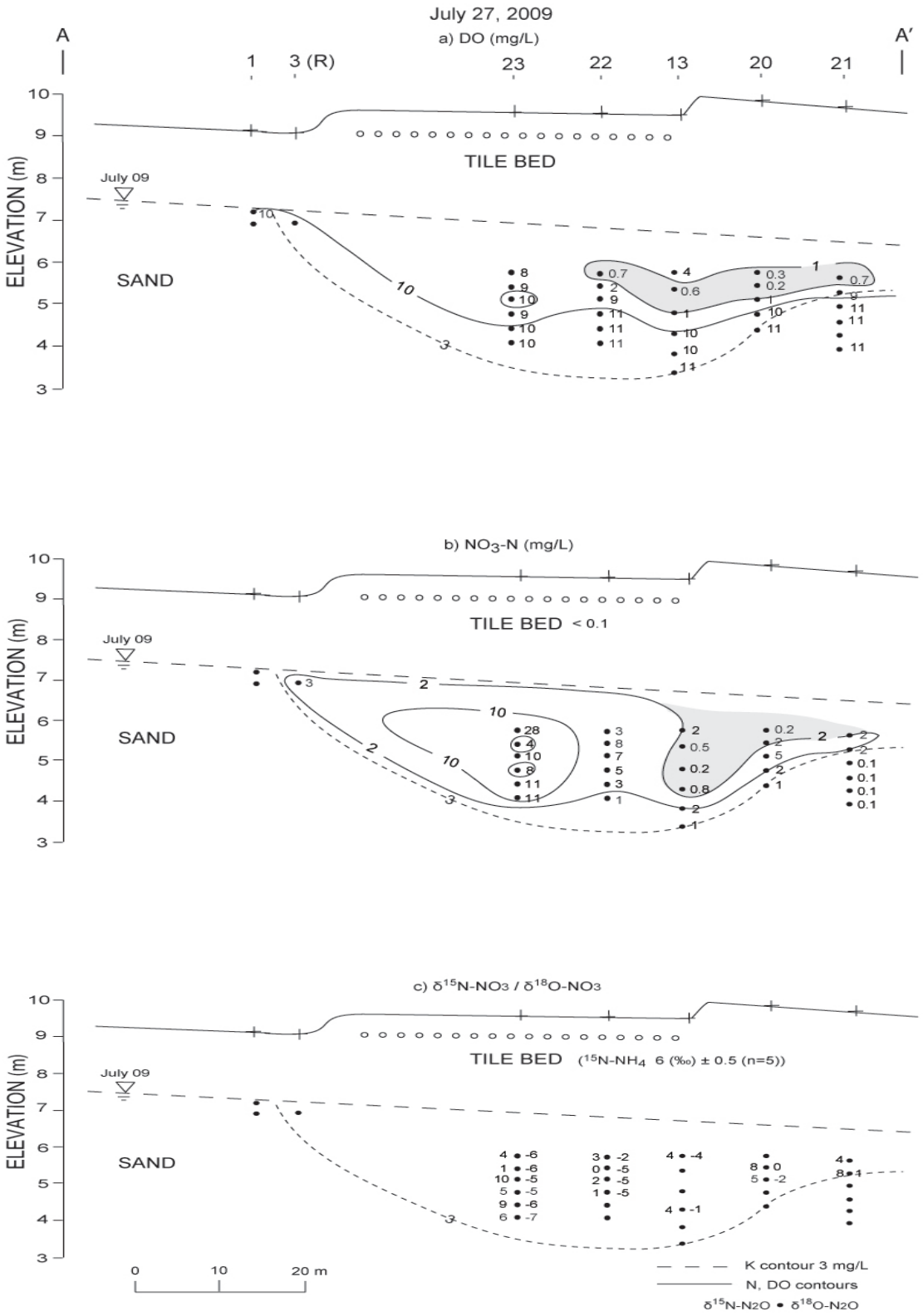

Figure 4.4. Section A-A' showing a) Dissolved Oxygen (DO), b) NO_3^--N, c) $\delta^{15}N$-NO_3^- and $\delta^{18}O$- NO_3^-, d) NH_4^+-N, e) N_2O-N,E f) $\delta^{15}N$-N_2O and $\delta^{18}O$-N_2O distribution, July 27, 2009. The plume boundary, as defined by K^+ (3 mg/L) is indicated by the dashed line.

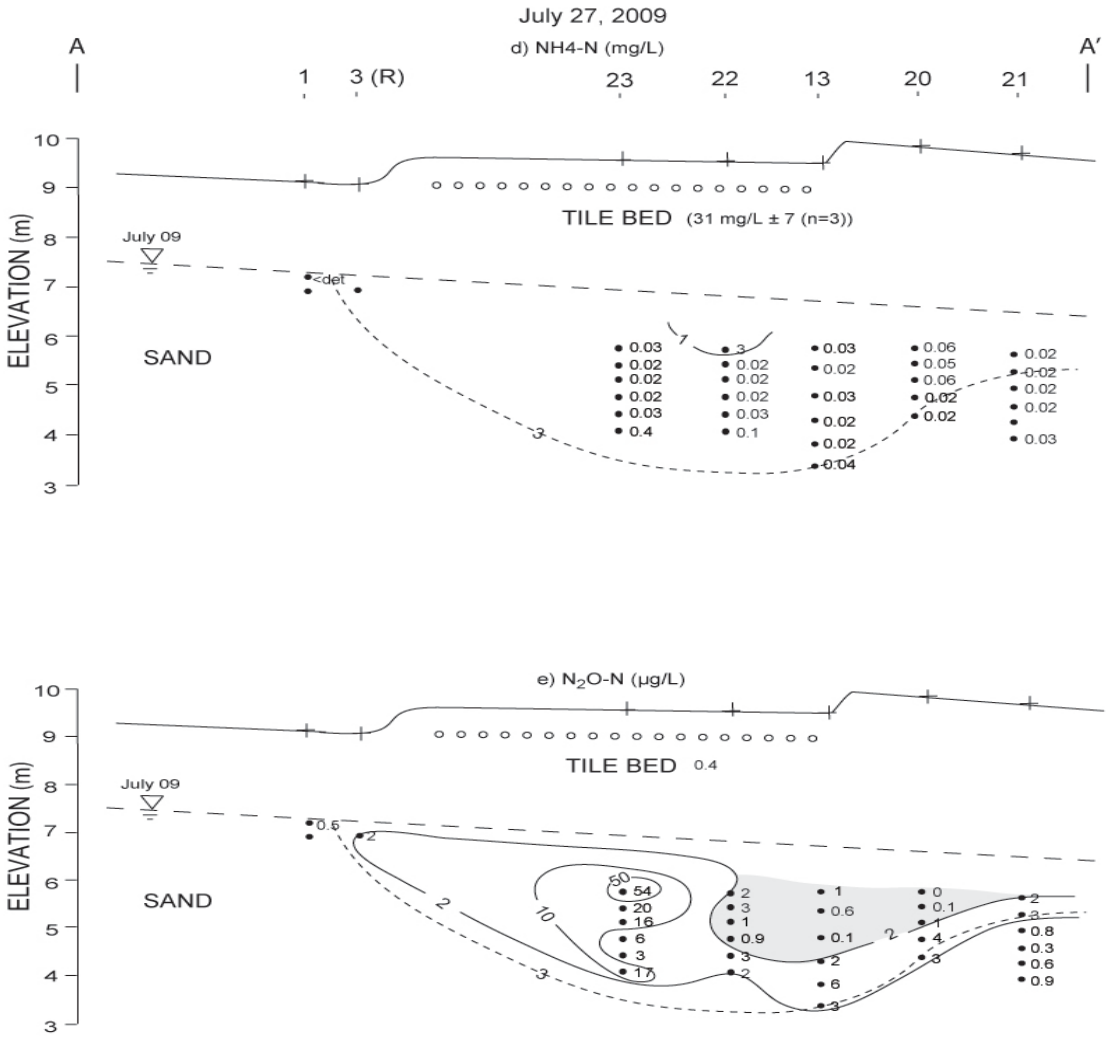

Figure 4.4 (Continued). Section A-A' showing a) Dissolved Oxygen (DO), b) NO_3^--N, c) $\delta^{15}N\text{-}NO_3^-$ and $\delta^{18}O\text{-}NO_3^-$, d) NH_4^+-N, e) N_2O-N,E f) $\delta^{15}N\text{-}N_2O$ and $\delta^{18}O\text{-}N_2O$ distribution, July 27, 2009. The plume boundary, as defined by K^+ (3 mg/L) is indicated by the dashed line. Note tank NH_4^+-N value is mean of three sampling events in 2009.

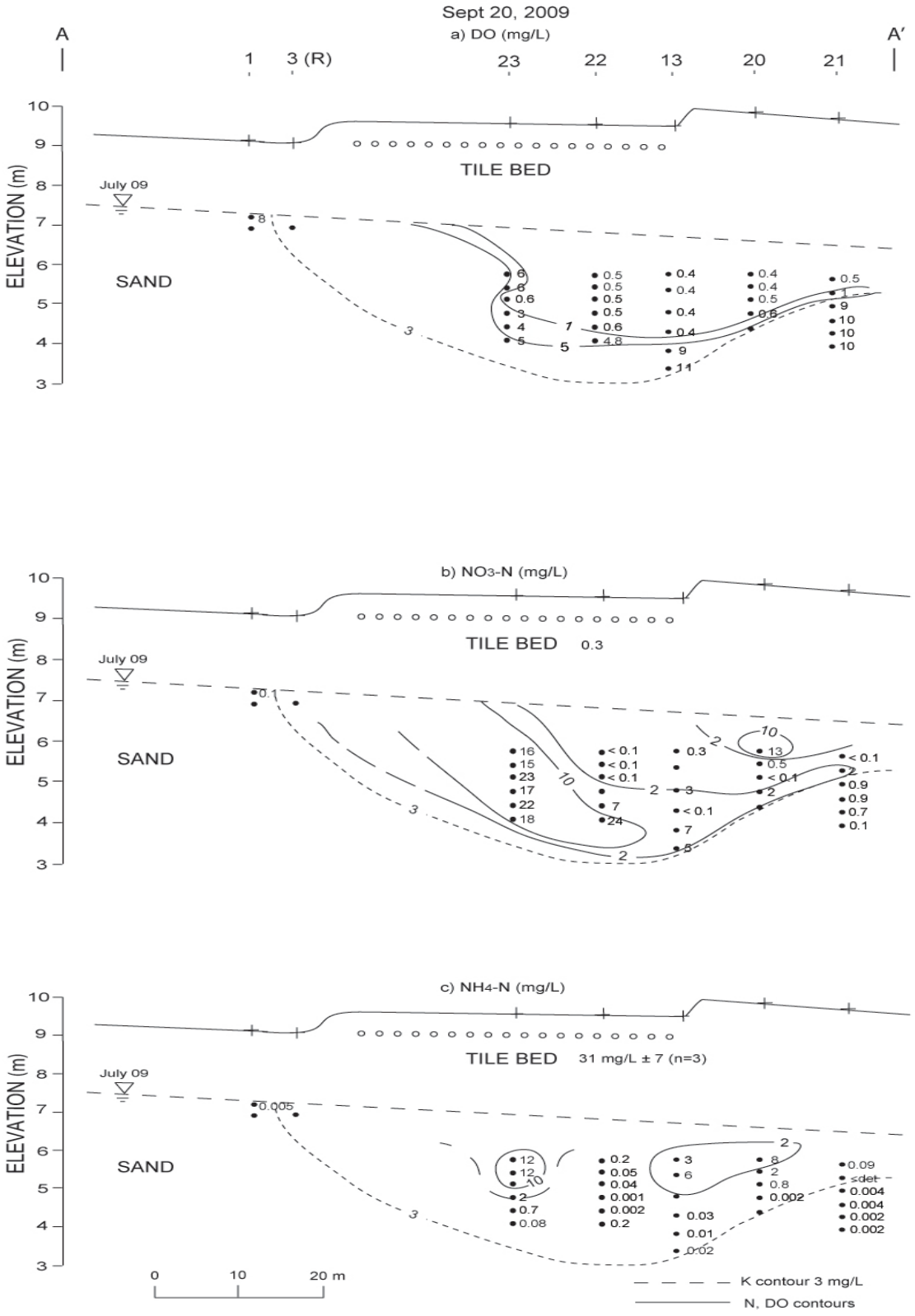

Figure 4.5. Section A-A' showing a) Dissolved Oxygen (DO), b) NO_3^--N, c) NH_4^+-N, d) N_2O-N,E e) $\delta^{15}N$-N_2O and $\delta^{18}O$-N_2O distribution, Sept 20, 2009. The plume boundary, as defined by K^+ (3 mg/L) is indicated by the dashed line. Note tank NH_4^+-N value is mean of three sampling events in 2009.

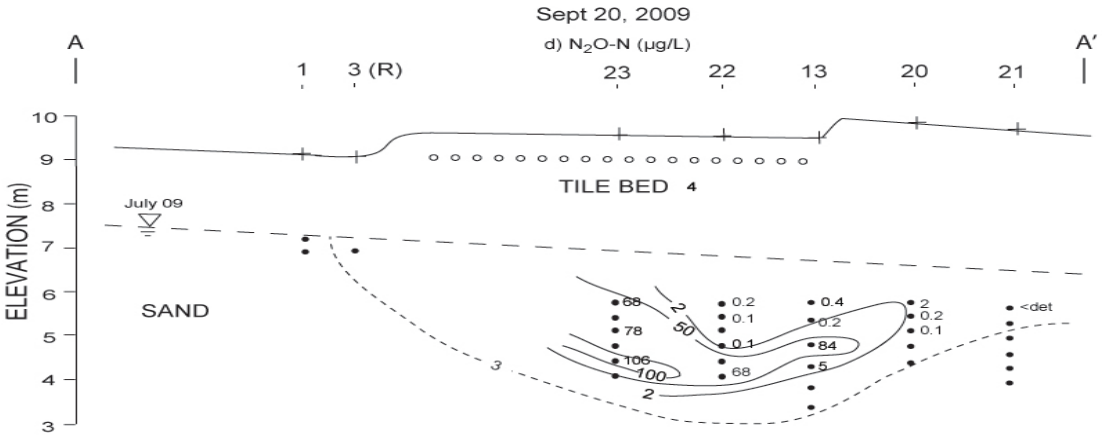

Figure 4.5 (Continued). Section A-A' showing a) Dissolved Oxygen (DO), b) NO_3^--N, c) NH_4^+-N, d) N_2O-N, E e) $\delta^{15}N$-N_2O and $\delta^{18}O$-N_2O distribution Sept 20, 2009. The plume boundary, as defined by K^+ (3 mg/L) is indicated by the dashed line.

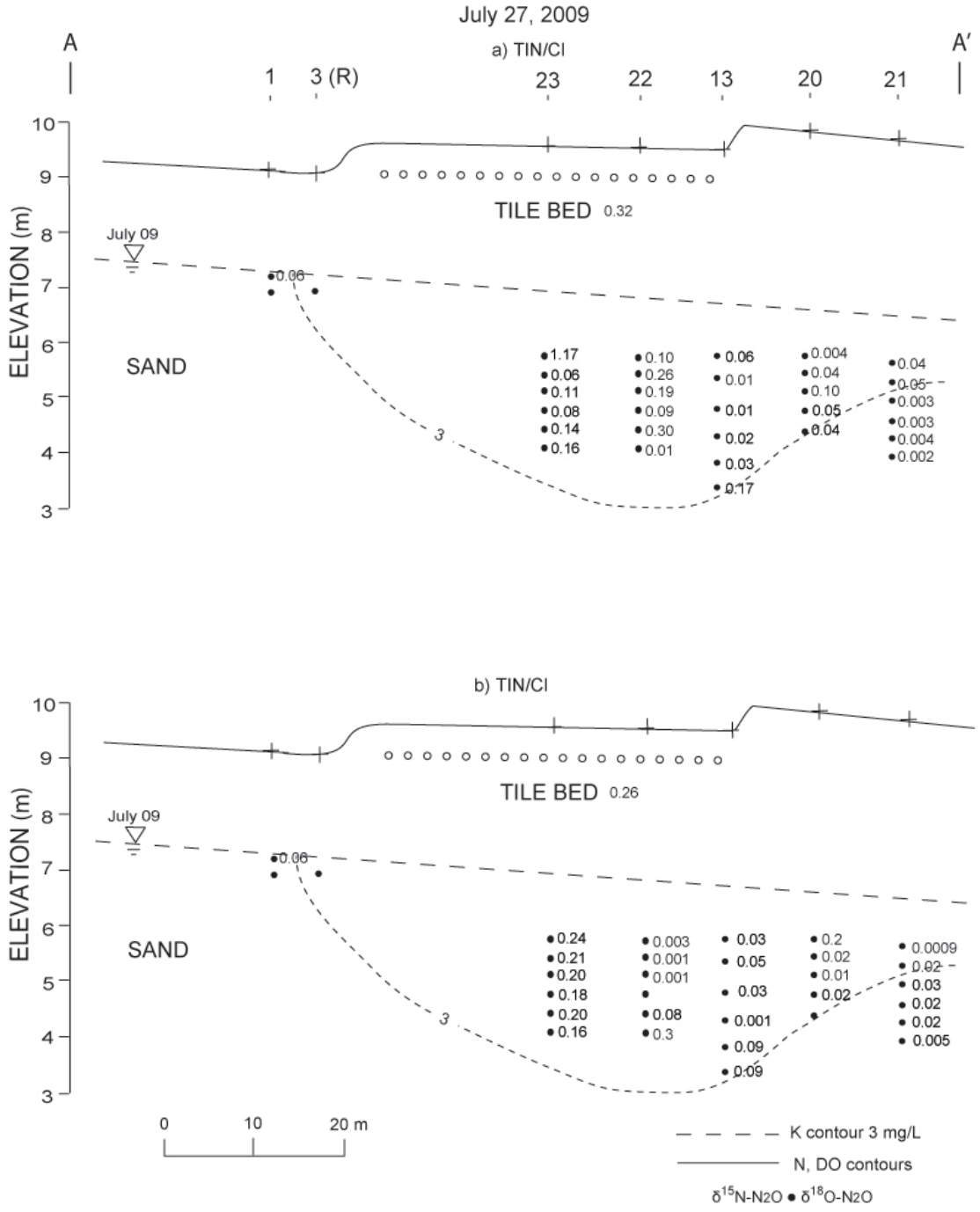

Figure 4.6. Section A-A' showing ratio of total inorganic nitrogen to Cl^- (TIN/ Cl^-) distribution on a) July 27, 2009, b) Sept 20, 2009. TIN is the sum of NO_3^--N and NH_4^+-N concentrations shown in Fig 4.4 and 4.5. Cl^- concentrations are shown in Fig.4.2 and 4.3. The plume boundary, as defined by K^+ (3 mg/L) is indicated by the dashed line. Note tank NH_4^+-N value is mean of three sampling events in 2009.

Lake Joseph Septic System Plume

a) June 9, 2009

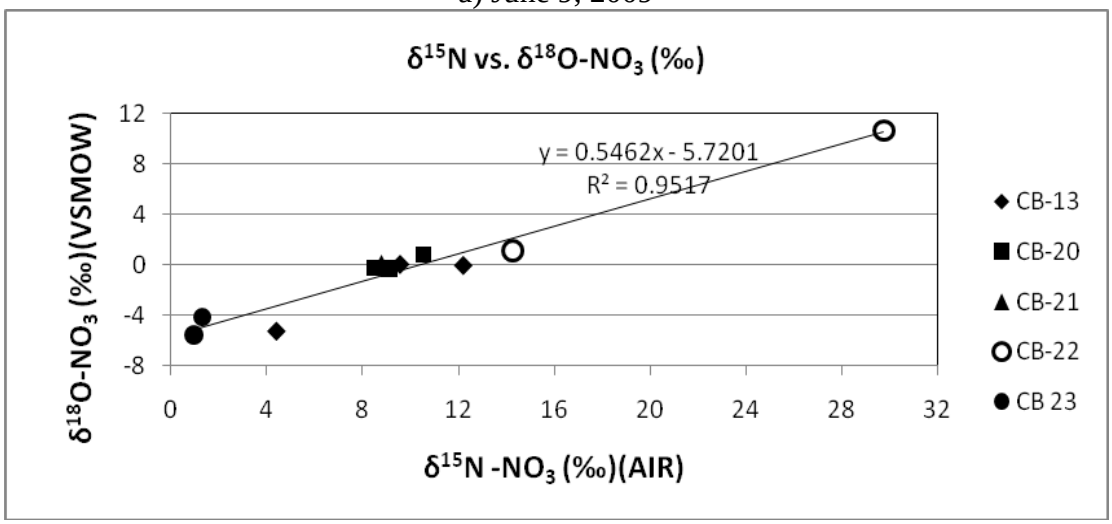

b) July 27, 2009

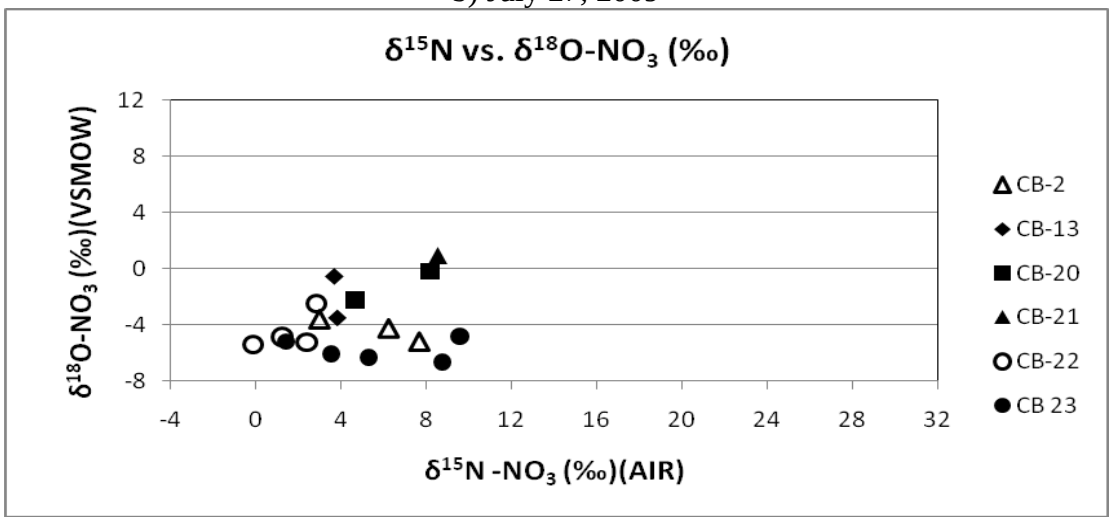

c) June 9 and July 27, 2009

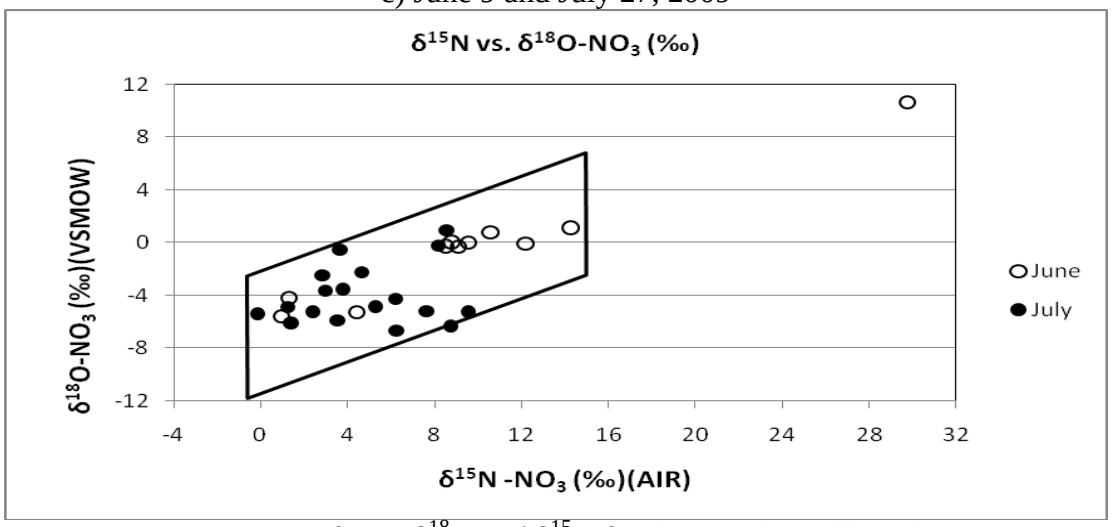

Figure 4.7. Comparison of NO_3 $\delta^{18}O$ and $\delta^{15}N$ for the samples collected at various Lake Joseph piezometer nests on a) June 9, b) July 27, 2009 and c) June 9 and July 27, 2009. Line in a) represents the isotope enrichment ratio of $\delta^{15}N$ to $\delta^{18}O$ is approximately 1.8:1. NO_3^- isotope box in c) shows $\delta^{15}N$-NO_3^- ranges from -1 to +14‰ and $\delta^{18}O$ -NO_3^- ranges from -12 to +5‰ at Lake Joseph.

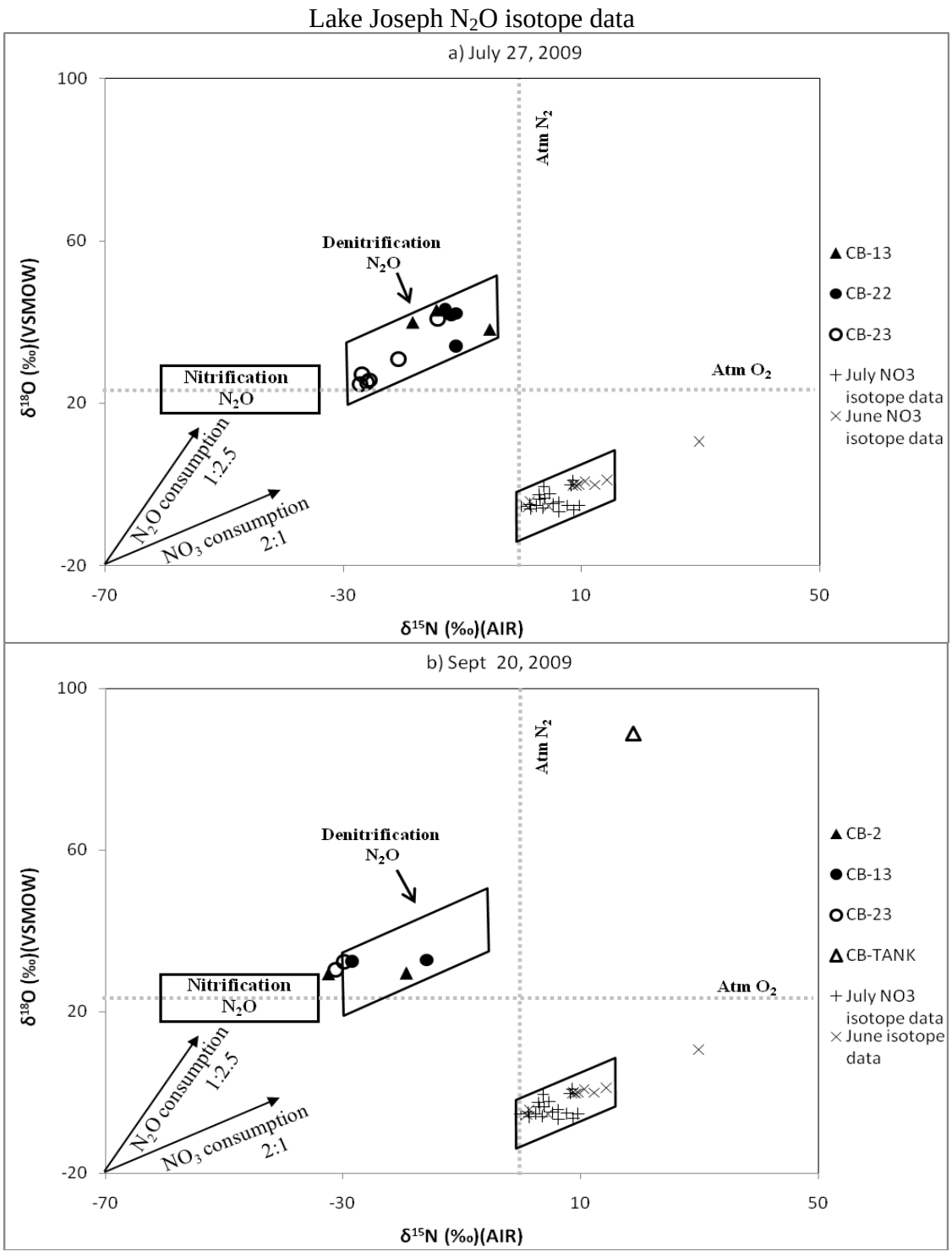

Figure 4.8. Comparison of $\delta^{18}O$ versus $\delta^{15}N$ of N_2O and NO_3^- for the samples collected at Lake Joseph Septic System plume; a)July 27, 2009, b) September 20, 2009. NO_3^- isotope box shows $\delta^{15}N$-NO_3^- ranges from -1 to +14‰ and $\delta^{18}O$ -NO_3^- ranges from -12 to +5‰. Nitrification and denitrification boxes show the calculated ranges of $\delta^{15}N$ and $\delta^{18}O$ values of N_2O produced from nitrification and denitrification (see Table 4.1 for details). Lines represent the isotope enrichment ratio of $\delta^{15}N$-N_2O to $\delta^{18}O$-N_2O is 1:2.5 for N_2O consumption and the isotope enrichment ratio of $\delta^{15}N$-NO_3^- to $\delta^{18}O$- NO_3^- is 2:1 for NO_3^- consumption. Dashed lines represent atmospheric $\delta^{18}O$-O_2 and $\delta^{15}N$-N_2 are +23.5‰ and 0‰, respectively.

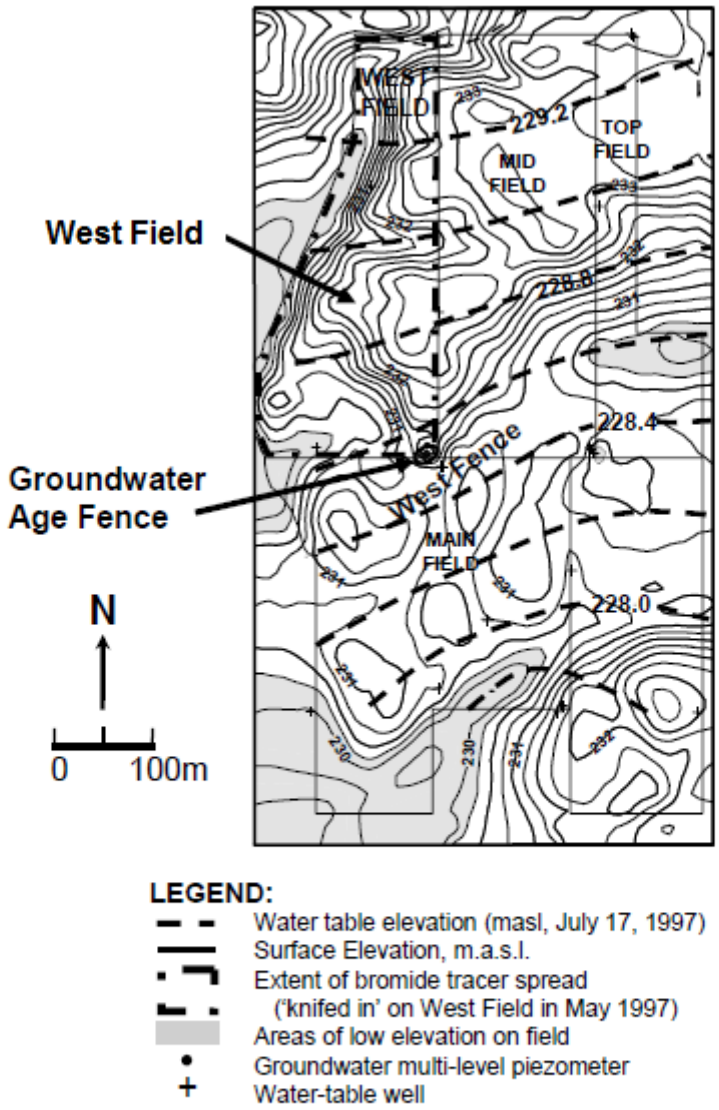

Figure 5.1. Strathroy site, Ontario, showing water table, West Field and West Fence (From Sebol, 2004).

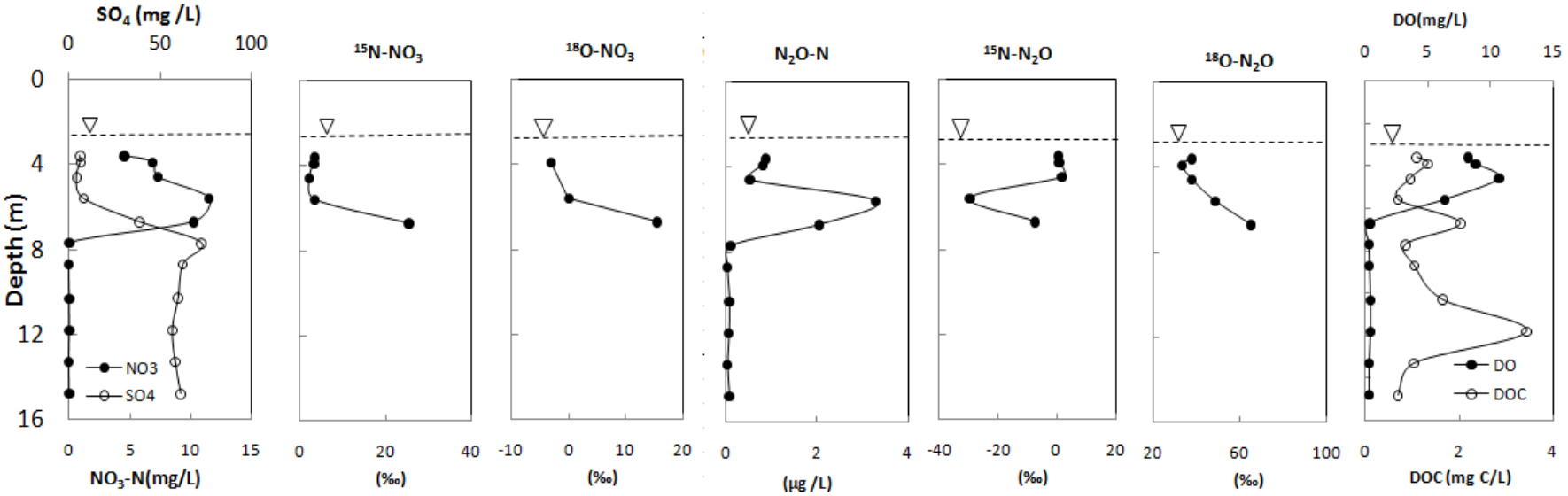

Figure 5.2. Depth profiles showing NO_3^--N, SO_4^{2-}, N_2O, DO and DOC and isotopic composition of $\delta^{15}N\text{-}NO_3^-$, $\delta^{18}O\text{-}NO_3^-$, $\delta^{15}N\text{-}N_2O$ and $\delta^{18}O\text{-}N_2O$ at piezometer nests SR3 (West Fence) at Strathroy site, on October 15 2009.

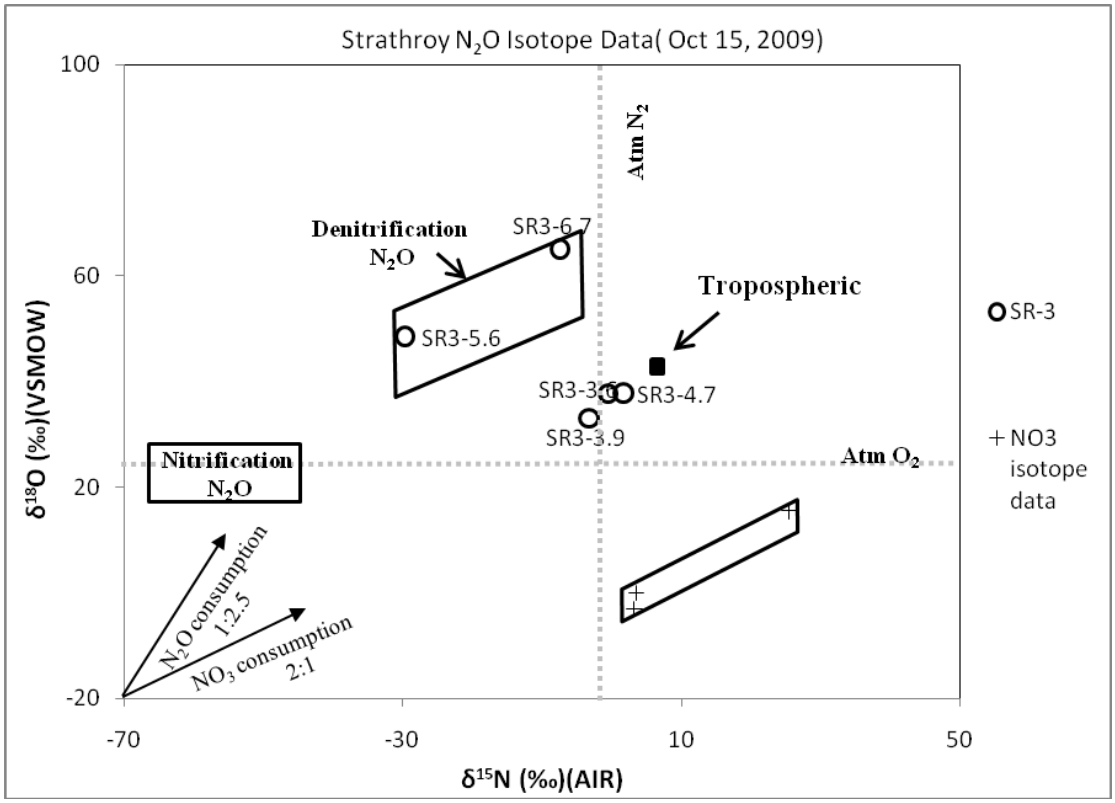

Figure 5.3. Comparison of $\delta^{18}O$ versus $\delta^{15}N$ of N_2O and NO_3^- for the samples collected from SR3 at Strathroy site on October 15, 2009. NO_3^- isotope box shows $\delta^{15}N\text{-}NO_3^-$ ranges from +3 to +26‰ and $\delta^{18}O\text{-}NO_3^-$ ranges from -3 to +16‰. The ratio of $\delta^{15}N\text{-}NO_3^-$ to $\delta^{18}O\text{-}NO_3^-$ is approximately 1.3:1. Nitrification and denitrification boxes show the calculated ranges of $\delta^{15}N$ and $\delta^{18}O$ values of N_2O produced from nitrification and denitrification (see Table 5.1 for details). Lines represent the isotope enrichment ratio of $\delta^{15}N\text{-}N_2O$ to $\delta^{18}O\text{-}N_2O$ is 1:2.5 for N_2O consumption and the isotope enrichment ratio of $\delta^{15}N\text{-}NO_3^-$ to $\delta^{18}O\text{-}NO_3^-$ is 2:1 for NO_3^- consumption. Dashed lines represent atmospheric $\delta^{18}O\text{-}O_2$ and $\delta^{15}N\text{-}N_2$ are +23.5‰ and 0‰, respectively.

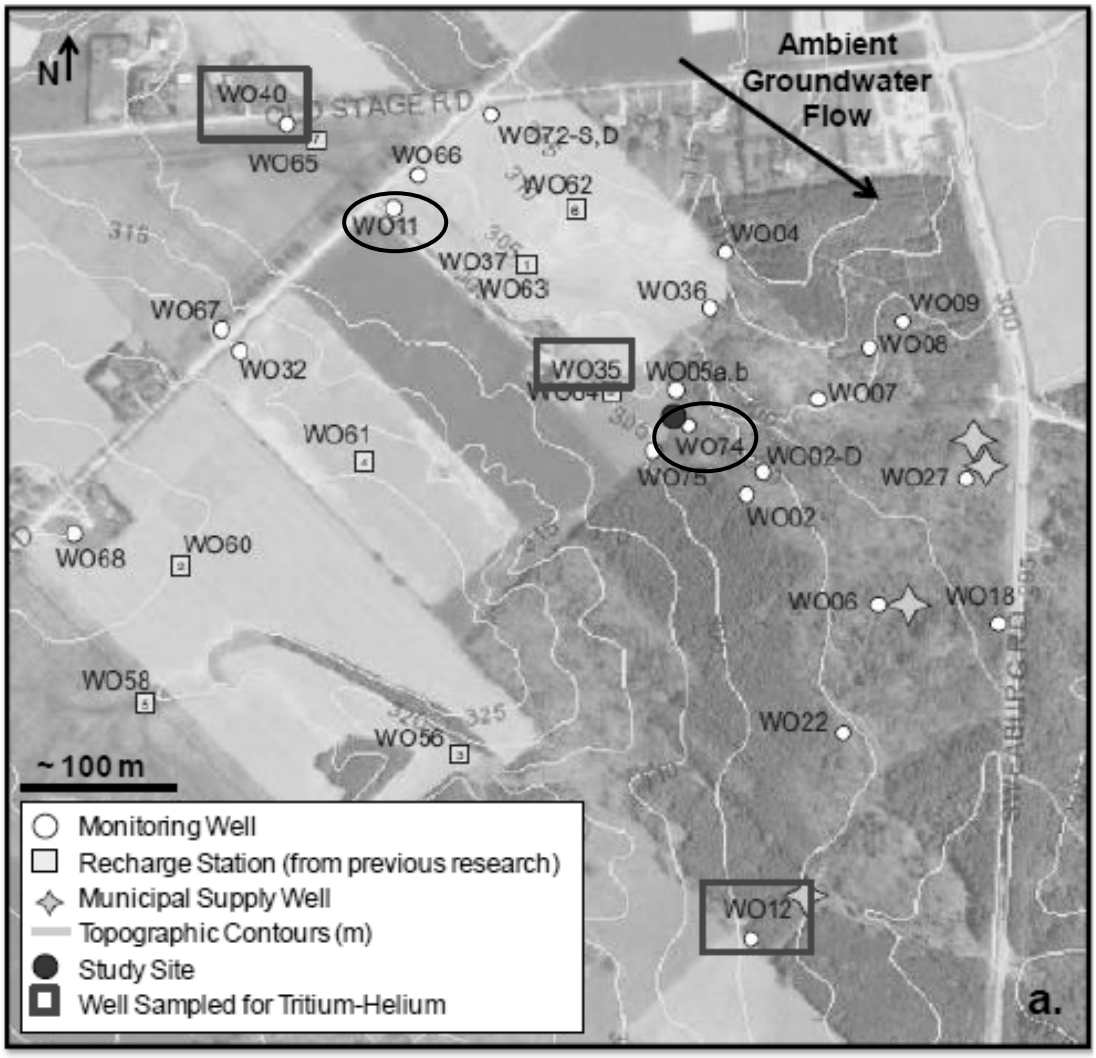

Figure 6.1. Woodstock Site, Ontario, showing monitoring well locations. Groundwater sampling was undertaken from WO 11 and WO74.

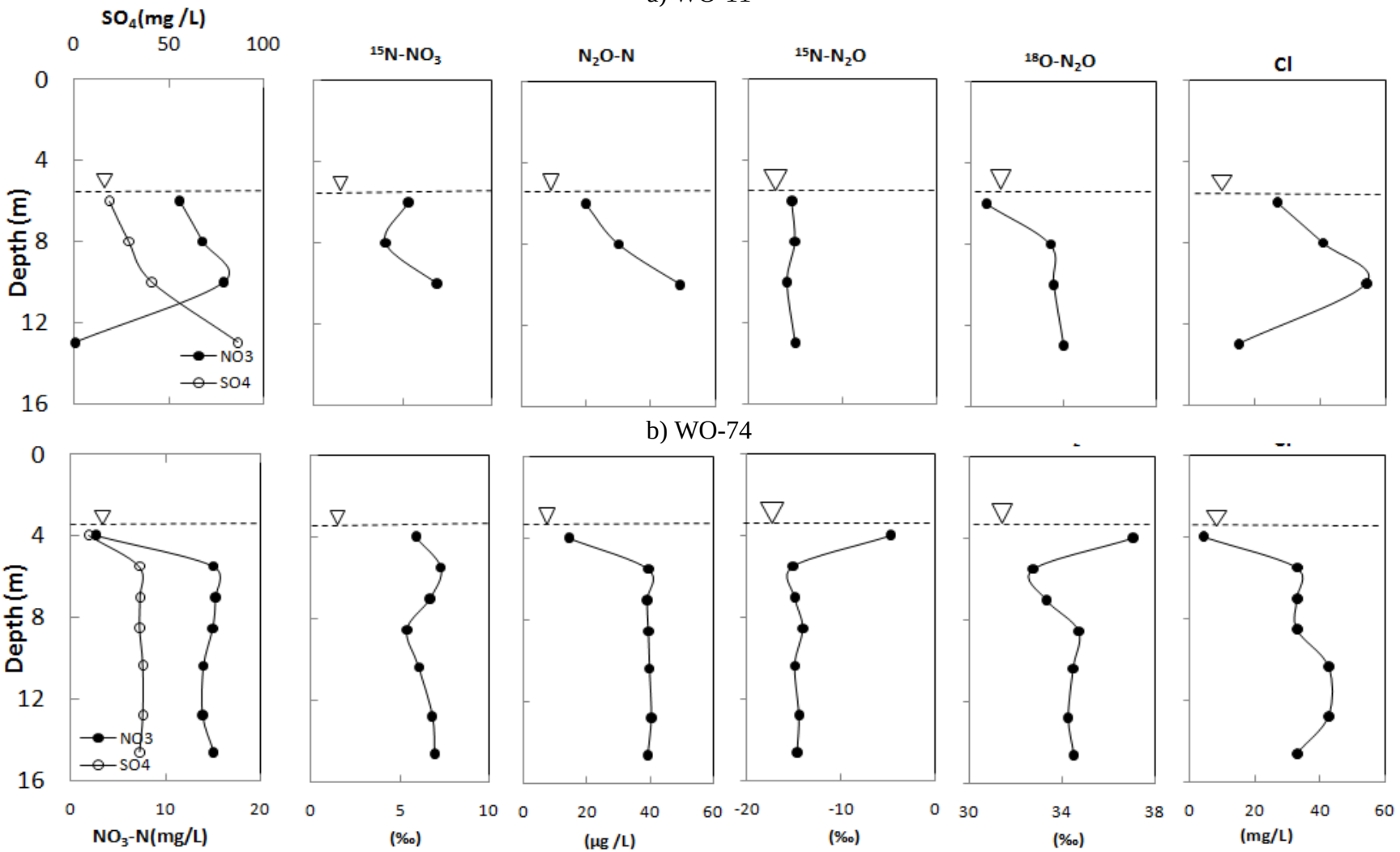

Figure 6.2. Depth profiles showing aqueous concentrations of NO_3^--N, SO_4^{2-}, N_2O, Cl^- and isotopic composition of $\delta^{15}N\text{-}NO_3^-$, $\delta^{15}N\text{-}N_2O$ and $\delta^{18}O\text{-}N_2O$ at piezometer nests a) WO-11 b) WO-74 on July 4 at Woodstock site, 2008.

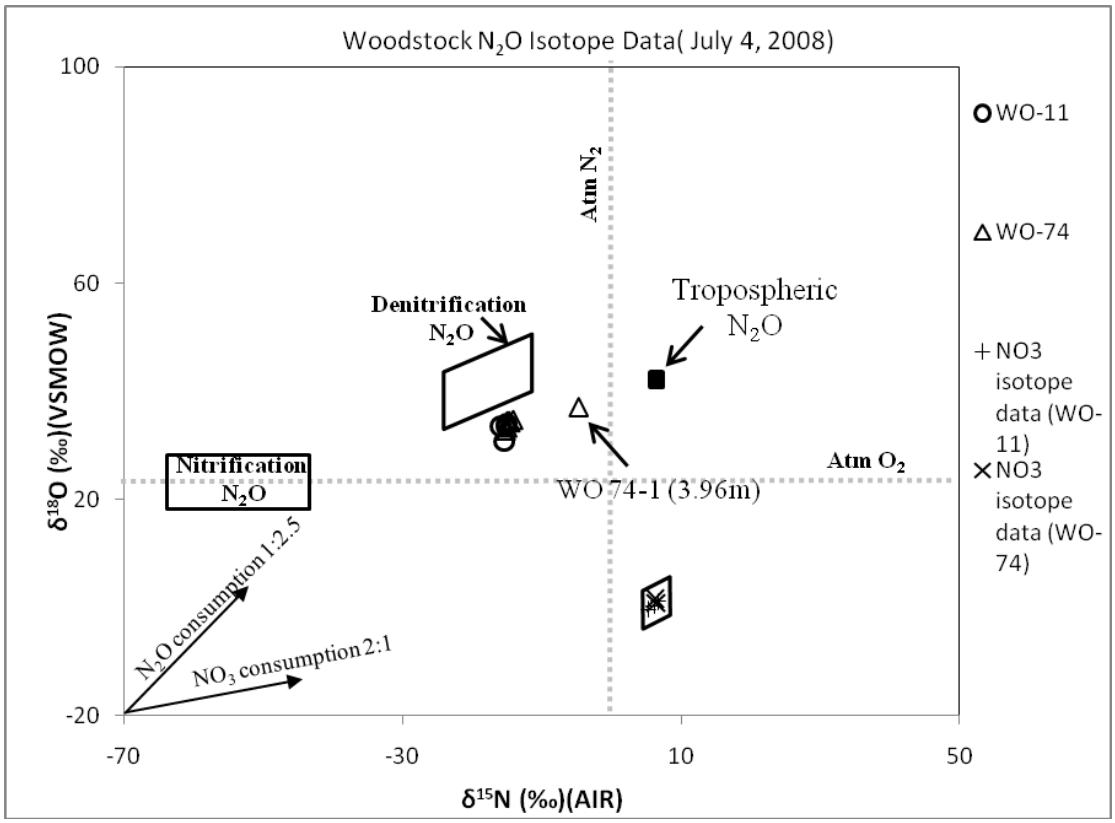

Figure 6.3. Comparison of $\delta^{18}O$ versus $\delta^{15}N$ of N_2O and NO_3^- for the samples collected from WO-11 and WO-74 from Woodstock site on July 4, 2009 (Nitrate isotope values from Koch, 2009). NO_3^- isotope box shows $\delta^{15}N$-NO_3^- ranges from +5 to +7‰ and $\delta^{18}O$ -NO_3^- ranges from -1 to +2‰. Nitrification and denitrification boxes show the calculated ranges of $\delta^{15}N$ and $\delta^{18}O$ values of N_2O produced from nitrification and denitrification (see Table 6.1 for details). Lines represent the isotope enrichment ratio of $\delta^{15}N$-N_2O to $\delta^{18}O$-N_2O is 1:2.5 for N_2O consumption and the isotope enrichment ratio of $\delta^{15}N$- NO_3^- to $\delta^{18}O$- NO_3^- is 2:1 for NO_3^- consumption. Dashed lines represent atmospheric $\delta^{18}O$-O_2 and $\delta^{15}N$-N_2 are +23.5‰ and 0‰, respectively.

Appendix A

Detailed geochemistry and Isotope Data at Long Point Site
from June 17, 2008 to November 9, 2009.

Appendix A1. Detailed Geochemistry at Long Point Site on June 17, 2008.

Well ID-depth(m)	EC (µs/cm)	NO3-N (mg/L)	NO3-N (mg/L)*	NH4-N (mg/L)	N2O-N (µg/L)	Cl (mg/L)	SO4 (mg/L)	DOC (mg/L)
LP 120-2.2	2050	28.6	25	0.1	242	75.1	31	10.1
LP 120-2.8	2190	73.3	78	0.1	556	70.8	37	8.3
LP 120-3.4	2810	66.3	71	5.0	798	62.2	80	6.8
LP 120-3.9	2740	77.5	83	2.0	355	62.0	109	4.1
LP 120-4.6	2500	64.3	68	0.1	63	57.5	77	3.5
LP 120-5.2	2040	25.1	22	0.1	5	52.2	97	2.5
LP 120-6.2	1844	0.1	0.1	1.8	2	47.9	135	2.0
LP 121-2.0	2120	39.1	41	16.0		51.0	20	14.1
LP 121-2.6	2310	40.7	44	35.0	17	50.0	50	14.1
LP 121-3.2	2300	76.5	81	2.0	432	54.7	68	4.4
LP 121-3.8	2200	60.4	64	0.7	561	42.8	76	5.0
LP 121-4.4	2280	65.9	70	1.0	282	48.9	66	3.8
LP 121-5.0	2090	34.8	37	0.1	6	51.7	69	2.5
LP 121-6.0	1890	3.1	3	0.2	3	48.0	131	1.7

Well ID-depth(m)	EC (µs/cm)	NO3-N (mg/L)	NO3-N (mg/L)*	NH4-N (mg/L)	N2O-N (µg/L)	Cl (mg/L)	SO4 (mg/L)	DOC (mg/L)
LP 122-2.0					739			
LP 122-2.2	2170	18.7	16	63.0	300	46.0	14	22.0
LP 122-2.8	2410	0.0	0.0	57.0	1	44.6	4	39.4
LP 122-3.4	2190	0.0	0.0	79.0	2	62.4	15	25.2
LP 122-4.2				13.0				
LP 122-4.6	2190	39.5	42	0.6	84	51.8	65	3.5
LP 122-5.2	2090	34.5	37	0.7	4	52.2	77	2.6
LP 122-6.3	1860	2.1	1.9	0.1	16	47.4	128	1.9
LP 123-2.0	3580	119.2	127	34.0	222	68.7	60	13.4
LP 123-2.6	2440	4.7	4	29.0	21	74.1	34	12.6
LP 123-3.2	3300	92.7	99	0.1	630	80.8	54	8.0
LP 123-3.8	2490	94.5	100	0.2	260	53.4	75	4.4
LP 123-4.5	2430	64.2	68	18.0	12	57.8	55	3.5
LP 123-5.5	2160	31.9	34	0.2	9	56.3	83	2.7

Well ID-depth(m)	EC (µs/cm)	NO3-N (mg/L)	NO3-N (mg/L)*	NH4-N (mg/L)	N2O-N (µg/L)	Cl (mg/L)	SO4 (mg/L)	DOC (mg/L)
LP 124-1.6		1.2	1	0.1	6	6.0	58	15.2
LP 124-2.1		19.1	17	0.1	47	14.5	23	4.5
LP 124-2.6		6.6	6	0.1	1	7.8	15	3.9
LP 124-3.1		2.2	2	0.1	1	7.7	26	3.3
LP 124-3.6		32.3	28	0.1	17	40.7	88	2.2
LP 124-4.5		3.0	3.0	0.1	314	53.4	124	
LP 125-1.0		<0.1		0.1	0	2.2	<0.3	
LP 125-1.5		<0.1		0.1	0	1.1	3	
LP 125-2.2		<0.1		0.1	0	1.0	10	2.5
LP 125-3.3		<0.1		0.1	0	47.6	32	1.8
LP 125-3.9		0.0		0.4	0	50.1	32	1.5
LP 128-1.9								
LP 128-2.4								
LP 128-2.9								
LP 128-3.4								
LP 128-3.9								

Well ID-depth(m)	EC (µs/cm)	NO3-N (mg/L)	NO3-N (mg/L)*	NH4-N (mg/L)	N2O-N (µg/L)	Cl (mg/L)	SO4 (mg/L)	DOC (mg/L)
LP 135-1.9								
LP 135-2.3								
LP 135-2.7								
LP 135-3.1								
LP 135-3.5								
LP 136-1.5		0.6		0.1	3	2.8	13	6.2
LP 136-1.9		1.6		0.1	2	4.1	26	4.4
LP 136-2.3		11.6		0.1	4	10.8	25	4.3
LP 136-2.7		70.5		0.1	1	50.1	38	3.5
LP 136-3.1		85.5		0.1	3	62.9	39	4.5
LP 136-3.3		75.6		0.1	3	60.0	43	4.4
LP 136-3.5					3			
LP 138-1.5		0.1		0.1	1	1.1	3.3	6.8
LP 138-1.9		0.4		0.1	2	1.0	3	1.9
LP 138-2.3		10.7		0.1	14	10.6	17	2.8
LP 138-2.7		86.9		8.0	0	63.1	40	5.0
LP 138-3.1		75.8		19.0	0	61.2	47	3.9
LP 138-3.4		70.6		0.2	0	60.8	52	4.4

Appendix A2. Detailed Geochemistry at Long Point Site on September 11, 2008.

Well ID-depth(m)	NO3-N (mg/L)	NH4-N (mg/L)	N2O-N (μg/L)	Cl (mg/L)	Br (mg/L)	SO4 (mg/L)	DOC (mg/L)	Al (mg/L)	Mg (mg/L)	Fe (mg/L)	Ca (mg/L)	Na (mg/L)	K (mg/L)	DO (mg/L)
LP 120-2.2														
LP 120-2.8	53.0	36.5	26	64.2	0.5	122	4.8	<0.05	35.5	<0.02	179.3	44.0	25.8	0.32
LP 120-3.4	33.8	39.8	313	62.3	0.7	47	6.1	<0.005	21.6	0.04	114.1	42.0	30.8	0.25
LP 120-3.9	57.8	2.4	165	56.9	3.1	41	4.9	<10	24.8	0.01	205.9	42.8	22.4	0.33
LP 120-4.6	40.0	2.8	110	54.7	3.0	40	4.4	<0.005	24.9	<0.002	198.3	41.6	20.4	0.18
LP 120-5.2	53.0	0.08	3	53.6	1.1	88	2.5	<0.05	32.7	<0.02	228.1	38.3	17.2	0.19
LP 120-6.2														0.49
LP 121-2.0														
LP 121-2.6	75.4	2.5	66	71.0	0.8	55	5.7	<0.05	32.7	0.01	247.6	47.0	24.1	0.66
LP 121-3.2	68.9	0.7	327	61.1	0.6	42	5.1	<0.05	29.8	0.01	232.4	46.5	19.3	0.28
LP 121-3.8	47.1	11.8	220	58.1	4.2	35	5.9	<0.05	25.0	<0.02	189.4	44.8	31.8	0.16
LP 121-4.4	34.3	1.7	286	57.6	4.1	33	5.1	<0.005	28.6	<0.002	210.5	43.8	21.5	0.14
LP 121-5.0	46.9	0.2	11	49.9	0.6	56	3.3	<0.005	29.8	<0.002	212.2	38.6	20.3	0.24
LP 121-6.0	6.5	0.05	5	47.5	0.6	126	2.3	<0.05	29.8	0.3	198.9	34.4	18.1	0.4

Well ID-depth(m)	NO3-N (mg/L)	NH4-N (mg/L)	N2O-N (µg/L)	Cl (mg/L)	Br (mg/L)	SO4 (mg/L)	DOC (mg/L)	Al (mg/L)	Mg (mg/L)	Fe (mg/L)	Ca (mg/L)	Na (mg/L)	K (mg/L)	DO (mg/L)
LP 122-2.2	88.9	0.02	186	63.2	0.7	58	3.8	<0.05	30.9	0.05	217.1	47.2	25.9	6.03
LP 122-2.8	76.9	0.03	349	53.8	0.6	43	4.8	<0.005	31.2	0.02	204.3	32.6	15.7	0.33
LP 122-3.4	95.6	0.01	832	59.1	0.0	39	4.6	<0.05	33.6	<0.02	231.7	42.0	20.9	0.25
LP 122-4.2														
LP 122-4.6	37.3	4.4	499	53.9	1.4	54	5.6	<0.05	29.4	<0.02	204.2	42.0	25.7	0.24
LP 122-5.2	47.3	4.9	10	52.1	0.6	131	3.5	<0.005	24.5	<0.002	153.6	35.1	26.2	0.21
LP 122-6.3	5.2	0.02	19	46.0	0.5	43	2.2	<0.005	25.7	0.7	149.7	31.5	15.8	0.31
LP 123-2.0		0.05												6.89
LP 123-2.6	75.9	0.4	595	65.4	0.6	43	4.6	<0.05	25.2	0.04	223.9	45.8	22.3	0.99
LP 123-3.2	73.8	0.2	1071	58.4	0.0	47	4.7	<0.005	23.4	0.02	175.3	41.7	22.0	0.77
LP 123-3.8	88.8	2.3	236	59.5	3.6	30	5.3	<0.005	25.9	0.02	168.5	45.5	39.1	1.28
LP 123-4.5	53.1	0.009	186	52.9	0.5	62	3.2	<0.005	26.6	<0.002	163.8	38.1	21.2	0.58
LP 123-5.5	39.5	0.008	40	50.7	0.1	62	2.4	<0.005	25.7	<0.002	156.2	35.0	17.1	0.74
LP 124-1.6	3.1	0.01	16	6.1	0.0	32	8.3	<0.005	17.4	<0.002	98.4	3.5	4.8	0.25
LP 124-2.1	12.5	0.0	27	11.8	0.1	22	4.1	<0.005	16.5	<0.002	102.7	8.4	5.5	0.35
LP 124-2.6	41.1	0.01	7	29.7	0.0	29	2.5	<0.005	23.5	<0.002	130.6	14.0	7.6	0.13
LP 124-3.1	68.5	0.02	10	47.8	0.0	35	2.7	<0.005	30.4	<0.002	162.2	27.3	12.7	0.15
LP 124-3.6	27.4	0.009	38	33.4	0.0	62	2.1	<0.005	20.9	<0.002	135.9	28.5	10.8	0.1
LP 124-4.5	10.3	0.02	198	51.7	0.3	137	1.8	<0.05	33.3	<0.02	234.6	37.0	17.1	0.1

Well ID-depth(m)	NO3-N (mg/L)	NH4-N (mg/L)	N2O-N (µg/L)	Cl (mg/L)	Br (mg/L)	SO4 (mg/L)	DOC (mg/L)	Al (mg/L)	Mg (mg/L)	Fe (mg/L)	Ca (mg/L)	Na (mg/L)	K (mg/L)	DO (mg/L)
LP 125-1.5	0.4	0.02	16	1.6	0.1	9.6	1.3	<0.005	6.5	<0.002	46.4	1.0	1.1	0.81
LP 125-2.2	0.0	0.04	2	3.5	0.1	21	1.5	<0.005	7.3	0.5	58.4	2.4	2.5	0.65
LP 125-2.7	0.0	0.05	2	37.1	0.9	35	1.8	<0.005	11.2	0.5	90.9	2.3	1.8	0.75
LP 125-3.3	0.0	0.2	1	99.2	3.1	30	1.1	<0.005	16.7	2.5	110.3	3.5	2.1	0.58
LP 125-3.9	0.0	0.3	1	25.8	0.5	29	1.5	<0.005	14.5	2.7	90.2	5.0	1.4	0.71
LP 128-1.9														
LP 128-2.4														
LP 128-2.9														
LP 128-3.4														
LP 128-3.9														
LP 135-1.9	22.9	0.01	125	18.5	0.3	18	2.5	<0.005	18.2	<0.002	112.8	9.7	5.3	2.01
LP 135-2.3	3.5	0.02	2	5.5	0.0	34	3.7	<0.005	11.4	0.01	70.1	11.0	6.1	0.5
LP 135-2.7	16.1	0.01	1	15.8	0.0	27	3.4	<0.005	14.9	<0.002	91.4	19.2	9.7	0.41
LP 135-3.1	59.5	0.02	1	42.8	0.0	38	3.0	<0.05	27.7	<0.02	176.8	38.2	15.5	0.25
LP 135-3.5	58.2	0.02	7	47.0	0.0	49	3.0	<0.05	29.7	<0.02	197.7	35.8	15.4	5.54

Well ID-depth(m)	NO3-N (mg/L)	NH4-N (mg/L)	N2O-N (μg/L)	Cl (mg/L)	Br (mg/L)	SO4 (mg/L)	DOC (mg/L)	Al (mg/L)	Mg (mg/L)	Fe (mg/L)	Ca (mg/L)	Na (mg/L)	K (mg/L)	DO (mg/L)
LP 136-1.5														7.72
LP 136-1.9	58.7	0.01	136	44.4	0.6	30	2.9	<0.05	27.2	0.03	216.5	14.7	7.5	
LP 136-2.3	43.5	0.001	207	35.0	0.1	26	3.6	<0.05	28.6	<0.02	175.4	17.5	14.3	0.3
LP 136-2.7	11.1	0.05	15	10.3	0.1	15	4.1	<0.05	12.5	0.01	89.2	15.7	15.6	0.28
LP 136-3.1	53.7	0.9	2	40.8	0.4	36	3.9	<0.05	23.3	<0.02	169.7	34.8	21.7	0.22
LP 136-3.3														
LP 136-3.5	67.6	0.4	1	52.0	0.5	43	3.8	<0.05	29.2	<0.02	207.4	39.6	21.6	0.18
LP 137-2.7														
LP 137-3.1														
LP 137-3.5														
LP 138-1.5														
LP 138-1.9	66.1	8.6	156	61.0	8.4	103	6.4	<0.05	35.9	<0.02	290.7	54.9	20.9	0.33
LP 138-2.3	41.1	15.0	167	59.0	11.1	66	6.9	<0.05	29.6	<0.02	209.5	49.0	56.1	0.2
LP 138-2.7	31.6	0.6	703	62.4	0.5	31	7.4	<0.05	30.2	<0.02	223.8	47.5	15.8	0.16
LP 138-3.1	44.0	1.4	288	58.9	0.5	43	5.3	<0.05	27.8	<0.02	217.5	42.5	20.5	0.42
LP 138-3.4	46.7	1.3		60.1	0.6	57	4.7	<0.05	28.9	<0.02	233.7	42.7	19.3	
TANK			99							0.16	110	52	33	

Appendix A3. Bromide tracer test at Long Point site.

Well ID-depth(m)	Br tracer injected on July 4,2008 Sampled on March 13,2009		
	NO2-N(mg/L)	NO3-N(mg/L)	Br(mg/L)
LP 120-2.2			
LP 120-2.8			
LP 120-3.4			
LP 120-3.9	n.a.	58.1	0.8
LP 120-4.6	0.63	30.2	0.8
LP 120-5.2	n.a.	12.3	0.1
LP 120-6.2	n.a.	0.5	1.0
LP 121-2.0			
LP 121-2.6			
LP 121-3.2			
LP 121-3.8	n.a.	43.9	1.5
LP 121-4.4	n.a.	38.9	0.9
LP 121-5.0	n.a.	43.1	1.5
LP 121-6.0	n.a.	1.3	0.6

Well ID-depth(m)	Br tracer injected on July 4,2008 Sampled on March 13,2009		
	NO2-N(mg/L)	NO3-N(mg/L)	Br(mg/L)
LP 122-2.0			
LP 122-2.2			
LP 122-2.8			
LP 122-3.4	n.a.	95.1	0.3
LP 122-4.2			
LP 122-4.6	n.a.	36.4	1.7
LP 122-5.2	n.a.	44.8	0.8
LP 122-6.3	n.a.	0.3	0.5
LP 123-2.0			
LP 123-2.6			
LP 123-3.2	1.63	82.8	0.0
LP 123-3.8	n.a.	50.0	1.5
LP 123-4.5	n.a.	37.1	1.6
LP 123-5.5	0.46	34.0	0.0

Well ID-depth(m)	Br tracer injected on July 4,2008 Sampled on March 13,2009		
	NO2-N(mg/L)	NO3-N(mg/L)	Br(mg/L)
LP 124-1.6			
LP 124-2.1			
LP 124-2.6	n.a.	8.5	n.a.
LP 124-3.1	n.a.	37.7	0.0
LP 124-3.6	n.a.	53.1	0.3
LP 124-4.5			
LP 125-1.0			
LP 125-1.5			
LP 125-2.2			
LP 125-3.3			
LP 125-3.9			
LP 128-1.9			
LP 128-2.4			
LP 128-2.9	n.a.	80.0	2.7
LP 128-3.4	n.a.	68.9	5.0
LP 128-3.9	n.a.	48.6	1.9

Well ID-depth(m)	Br tracer injected on July 4,2008 Sampled on March 13,2009		
	NO2-N(mg/L)	NO3-N(mg/L)	Br(mg/L)
LP 135-1.9			
LP 135-2.3	0.9	73.1	2.8
LP 135-2.7	1.31	85.5	4.2
LP 135-3.1	0.51	68.7	2.4
LP 135-3.5	0.37	63.8	1.7
LP 136-1.5			
LP 136-1.9			
LP 136-2.3			
LP 136-2.7	n.a.	76.7	1.6
LP 136-3.1	n.a.	73.5	4.2
LP 136-3.3	n.a.	71.5	4.1
LP 136-3.5			
LP 138-1.5			
LP 138-1.9			
LP 138-2.3	n.a.	78.1	0.8
LP 138-2.7	n.a.	82.2	0.6
LP 138-3.1	n.a.	51.3	3.4
LP 138-3.4	n.a.	54.7	2.2

Notes:
EC values were measured with conductivity meter in the field.
NH4 was analyzed at Wrilfrid Laurrier University.
Cl, SO4-S and nitrate analysis was performed by ion chromatograohy using Dionex at Elgood/Schiff lab at University of Waterloo.
*indicates nitrate concentration analysis was done at University of Guelph.
N2O concentration was conducted using Varian CP-3800 ECD (Electron Capture Detector).
DOC concentrations were conducted using Dohrmann DC-190.

Cations were done by using ICP (Inductively Coupled Plasma) at CCIW lab.

Appendix A4. Detailed Geochemistry from LP 100 at Long Point Site on May 15, 2009.

WELL ID	DEPTH(m)	EC(us/cm)	Eo	NH4-N(mg/L)	NO3-N(mg/L)	Cl(mg/L)	DO(mg/L)
LP122	2.2	429	129	0.03	21.6	37	5
LP122	2.8	877	128	0.03	61.7	15	0.5
LP122	3.4	1676	130	<0.01	85.1	67	0.5
LP122	4.0	1620	115	3.01	83.7	63	1.5
LP122	4.6	1408	114	6.95	35.5	98	0.3
LP122	5.2	1416	113	0.15	45.7	57	0.5
LP122	6.3	1220	14	0.08	5.3	60	0.5
Tank				85.70	2.8	54	

Notes:

NH4, NO3 and Cl were analyzed in Guelph lab.

DO values were measured using Chemets Kit.

Appendix A5. Detailed Geochemistry from LP 100 at Long Point Site on June 2, 2009.

WELL ID	DEPTH (m)	Ease of Pumping	EC (us/cm)	pH	NH4-N (mg/L)	NO3-N (mg/L)	DO (mg/L)	N2O-N (µg/L)	Cl * (mg/L)	NO2-N (mg/L)	Br (mg/L)	PO4-P (mg/L)	SO4-S (mg/)	DOC(mg C/L)
TANK					94.8	0.01			73.42	n.a.	2.97	8.72	19.58	69.9
LP 100-7	1.8	VG	1270	6.71	0.1	71.3	5.2	117	138.74	n.a.	2.57	8.69	11.75	9.1
LP 100-8	2.0	VG	1339	6.77	0.4	67.3	4.6	244	67.12	1.54	2.37	9.01	12.26	10.1
LP 100-9	2.2	VG	1884	6.51	14.1	103.4	0.6	792	70.65	2.66	2.39	8.15	19.86	10.6
LP 100-10	2.4	VG	1678	6.68	61.9	60.9	0.6	719	66.08	9.29	3.04	9.59	11.50	11.9
LP 100-11	2.6	VG	1509	6.93	77.0	1.0	0.86	422	68.30	0.87	3.86	11.61	15.44	13.7
LP 100-13	3.0	VG	1434	6.86	22.7	0.1	0.53	7	81.95	n.a.	5.49	8.27	15.25	16.5
LP 100B-1	3.05	VG	1590	6.93	65.9	0.31	0.37	2	76.86	n.a.	3.58	9.68	14.17	13.1
LP 100B-2	3.35	VG	1177	6.94	0.5	4.2	0.67	63	60.34	0.84	7.70	5.49	14.99	6.1
LP 100B-3	3.65	VG	1149	6.98	0.1	49.1	0.46	367	33.03	0.89	1.56	3.82	20.54	4.7
LP 100B-4	3.95	G	1180	6.95	0.9	62.0	0.48	293	32.23	0.34	0.77	3.71	21.04	5.6
LP 100B-5	4.25	G	1374	6.86	2.0	79.8	0.92	655	55.17	n.a.	1.41	4.21	26.08	3.8
LP 100B-6	4.55	P	1388	6.94	7.9	48.3	0.51	453	75.57	n.a.	1.61	2.01	19.32	7.2
LP 100B-7	4.85	F	1186	6.94	1.3	32.8	0.44	89	57.06	n.a.	3.76	4.50	19.84	3.9
LP 100B-8	5.15	G	1266	6.99	0.9	40.8	0.5	20	61.56	n.a.	2.02	3.01	23.13	2.4
LP 100B-10	5.75	G	1237	6.94	0.0	21.6	0.7	129	57.84	0.48	0.34	n.a.		17.4
LP 122	6.30	G												

Notes:
VG=VERY GOOD
G=GOOD
P=POOR
F=FAIR

DO values were measured with DO meter.
* indicates there may be analytical errors.

Appendix A6. Detailed Geochemistry from LP 100 at Long Point Site on June 24, 2009.

WELL ID	DEPTH (m)	EC (us/cm)	pH	NH4-N (mg/L)	NO3-N (mg/L)	DO (mg/L)	N2O-N (µg/L)	PO4-P (mg/L)	SO4-S (mg/L)	Cl * (mg/L)	NO2-N (mg/L)	Br (mg/L)	DOC (mg C/L)
TANK				204.2	0.1		135	4.6	5.5	69.6	0.8	0.15	73.1
LP 100-7	1.8	1180	6.70	0.0	89.2	bubble	112	3.7	15.7	51.6	n.a.	1.33	5.4
LP 100-8	2.0	1154	6.65	0.0	102.9	bubble	193	4.1	17.2	62.4	n.a.	1.26	4.7
LP 100-9	2.2	1106	6.50	0.9	107.7	<1	90	5.4	26.3	67.9	n.a.	1.58	6.3
LP 100-10	2.4	1173	6.40	8.2	94.5	<1	59	3.7	23.3	62.6	n.a.	1.60	7.1
LP 100-11	2.6	1246	6.40	31.8	124.6	<1	239	7.5	12.0	69.4	n.a.	2.43	8.5
LP 100-13	3.0	1025	6.70	79.6	13.8	<1	201	6.1	6.8	64.8	n.a.	2.49	12.7
LP 100B-1	3.05	1056	6.70	87.7	27.0	<1	423	9.7	7.4	70.3	n.a.	2.44	11.1
LP 100B-2	3.35	1023	6.80	48.8	18.7	<1	441	3.1	13.5	71.7	n.a.	3.18	13.4
LP 100B-3	3.65	938	6.80	0.5	31.8	<1	474	2.4	20.3	42.2	1.5	2.28	5.9
LP 100B-4	3.95	898	6.90	0.3	30.2	<1	485	2.5	19.6	39.7	0.8	1.80	6.1
LP 100B-5	4.25	918	6.80	2.5	45.7	<1	299	3.5	20.9	47.6	n.a.	1.79	5.4
LP 100B-6	4.55	1056	6.80	9.1	35.8	<1	244	1.6	18.6	62.2	n.a.	1.79	3.9
LP 100B-7	4.85	1077	6.80	0.6	22.1	<1	112	2.2	17.6	63.1	n.a.	3.20	7.3
LP 100B-8	5.15	1145	6.80	3.4	35.9	<1	6	2.8	21.5	56.8	n.a.	1.37	3.4
LP 100B-10	5.75	1054	6.90	0.0	20.6	<1	12	0.5	42.2	57.0	0.5	0.04	2.4
LP 122	6.30	1559	7.40	0.0	9.8	<1	24	n.a.	50.8	58.9	0.5	0.04	1.9

Notes:

DO values were measured using Chemets Kit.
* indicates there may be analytical errors.

Appendix A7. Detailed Geochemistry from LP 100 at Long Point Site on July 23, 2009.

WELL ID	DEPTH (m)	EC (us/cm)	pH	NH4-N (mg/L)	NO3-N (mg/L)	DO (mg/L)	N2O-N (µg/L)	PO4-P (mg/L)	SO4-S (mg/L)	Cl (mg/L)	NO2-N (mg/L)	Br (mg/L)	DOC(mg C/L)
TANK				113.5	0.0		0.4		4.0		n.a.		22.1*
LP 100-7	1.8	1155		5.6	60.0	2.48	58.1		7.0		0.92		10.0
LP 100-8	2.0	1164		10.8	45.0	1.36	195.3		7.0		1.08		11.1
LP 100-9	2.2	1390			32.6	0.81	71.8		6.0		1.27		10.4
LP 100-10	2.4	1588			0.0	0.77	1.3		3.0		n.a.		20.6
LP 100-11	2.6	1602		66.2	0.0	0.48	0.5		7.0		n.a.		18.0
LP 100-13	3.0	1351		16.1	0.0	0.7	0.4		7.0		n.a.		12.8
LP 100B-1	3.05	1889		44.6	0.1	0.65	0.01		7.0		n.a.		13.9
LP 100B-2	3.35	1203		5.6	4.0	0.47	0.8		5.0		n.a.		10.4
LP 100B-3	3.65	1384		7.2	69.5	0.59	47.6		15.0		n.a.		6.8
LP 100B-4	3.95	1525		6.3	88.5	0.64	200		20.0		n.a.		5.9
LP 100B-5	4.25	1446		5.4	64.4	0.69	253		16.0		n.a.		6.3
LP 100B-6	4.55	1300		7.8	39.7	0.55	112.8		17.0		n.a.		4.3
LP 100B-7	4.85	1261		4.8	26.3	0.47	5.2		10.0		n.a.		7.3
LP 100B-8	5.15	1345		10.8	59.9	0.52	11.5		16.0		n.a.		6.0
LP 100B-10	5.75	1266		1.3	29.2	0.75	103.8		48.0		0.30		2.5
LP 122	6.30	1644		0.0	11.4		12.4				n.a.		3.2

Notes:
DO values were measured with DO meter.
* indicates there may be analytical errors.

Appendix A8. Detailed Geochemistry from LP 100 at Long Point Site on Aug 13, 2009

WELL ID	DEPTH (m)	EC (us/cm)	pH	NH4-N (mg/L)	NO3-N (mg/L)	DO (mg/L)	N2O-N (µg/L)	PO4-P (mg/L)	SO4-S (mg/L)	Cl (mg/L)	NO2-N (mg/L)	Br (mg/L)
TANK				101.9								
LP 100-7	1.8			0.1	94.43				15.84	54.02		n.a.
LP 100-8	2.0			0.1	90.52				14.72	55.21		n.a.
LP 100-9	2.2			0.0	94.07				18.89	54.32		n.a.
LP 100-10	2.4			7.9	102.06				15.41	69.24		n.a.
LP 100-11	2.6			92.5	85.97				13.34	71.65		n.a.
LP 100-13	3.0			111.2	0.34					64.74		0.03
LP 100B-1	3.05			105.9	69.58				10.10	66.55		0.40
LP 100B-2	3.35			98.7	0.33					64.48		0.03
LP 100B-3	3.65			82.7	n.a.					63.73		0.03
LP 100B-4	3.95			47.4	0.00				4.36	62.02		3.92
LP 100B-5	4.25			53.2	0.20				3.20	62.58		1.65
LP 100B-6	4.55			10.2	39.44				17.17	52.88		3.22
LP 100B-7	4.85			17.9	30.54				16.91	55.16		1.48
LP 100B-8	5.15			8.9	24.26				16.72	57.23		2.02
LP 100B-10	5.75			0.0	39.81				27.71	52.27		0.65
LP 122	6.30											

Appendix A9. Detailed Geochemistry from LP 100 at Long Point Site on September 11, 2009

WELL ID	DEPTH (m)	EC (us/cm)	E°	pH	NH4-N (mg/L)	NO3-N (mg/L)	DO (mg/L)	N2O-N (µg/L)	PO4-P (mg/L)	SO4-S (mg/L)	Cl (mg/L)	NO2-N (mg/L)	Br (mg/L)
TANK													
LP 100-7	1.8												
LP 100-8	2.0				0.71	71.70							
LP 100-9	2.2				1.2	77.10							
LP 100-10	2.4				43.1	77.30							
LP 100-11	2.6				92.6	4.90							
LP 100-13	3.0				82.9	0.34							
LP 100B-1	3.05												
LP 100B-2	3.35				161.0	0.01							
LP 100B-3	3.65				82.6	0.04							
LP 100B-4	3.95				118.0	0.19							
LP 100B-5	4.25				48.0	3.30							
LP 100B-6	4.55				22.0	43.60							
LP 100B-7	4.85				0.4	11.50							
LP 100B-8	5.15				18.9	21.60							
LP 100B-10	5.75				1.5	36.00							
LP 122	6.30												

Notes:

NH4 and NO3 were analyzed at University of Guelph.

Appendix A10. Detailed Geochemistry from LP 100 at Long Point Site on October 13, 2009

WELL ID	DEPTH (m)	EC (us/cm)	E°	pH	NH4-N (mg/L)	NO3-N (mg/L)	DO (mg/L)	N2O-N (µg/L)	PO4-P (mg/L)	SO4-S (mg/L)	Cl (mg/L)	NO2-N (mg/L)	Br (mg/L)	DOC (mg C/L)
TANK					112.5	0.1		150.8	4.5	6.6	65.2	n.a.	0.9	25.7
LP 100-7	1.8													
LP 100-8	2.0				0.1	78.4		666.6	4.6	25.0	28.9	n.a.	n.a.	14.2
LP 100-9	2.2				0.1	89.2		128.8	5.7	23.0	48.4	n.a.	0.2	4.7
LP 100-10	2.4				1.7	75.6		44.5	2.5	21.2	46.2	n.a.	0.2	3.8
LP 100-11	2.6				17.4	39.7		98.4	1.5	21.6	45.4	n.a.	0.3	4.3
LP 100-13	3.0				41.6	21.1		998.8	1.4	14.5	39.2	n.a.	0.2	5.0
LP 100B-1	3.05				43.1	16.7		580.4	1.3	15.3	42.7	n.a.	0.3	5.2
LP 100B-2	3.35				110.6	0.0		5.8	3.3	8.0	52.4	n.a.	0.5	10.6
LP 100B-3	3.65				55.8	0.0		1.0	1.1	4.9	59.0	n.a.	1.1	10.1
LP 100B-4	3.95				35.0	0.5		0.9	1.1	5.8	58.3	n.a.	0.6	9.4
LP 100B-5	4.25				37.0	0.6		0.8	1.1	5.8	58.9	n.a.	0.6	9.3
LP 100B-6	4.55				8.3	26.3		1.4	0.7	12.5	55.7	n.a.	1.3	4.2
LP 100B-7	4.85				24.3	35.7		0.5	2.1	18.0	49.0	n.a.	1.6	4.8
LP 100B-8	5.15				8.1	29.9		3.2	1.4	20.4	53.3	n.a.	1.7	3.1
LP 100B-10	5.75				0.0	27.3		172.1	n.a.	38.6*	48.2	n.a.	0.1	2.7
LP 122	6.30					10.4		34.6	n.a.	48.7	47.7	n.a.	0.4	1.6

* indicates there may be analytical errors.

Appendix A11. Detailed Geochemistry from LP 100 at Long Point Site on Nov 9, 2009.

WELL ID	DEPTH (m)	EC (us/cm)	E°	pH	NH4-N (mg/L)	NO3-N (mg/L)	DO (mg/L)	N2O-N (µg/L)	PO4-P (mg/L)	SO4-S (mg/L)	Cl (mg/L)	NO2-N (mg/L)	Br (mg/L)	DOC (mg C/L)
TANK														
LP 100-7	1.8													
LP 100-8	2.0				0.0	141.5								
LP 100-9	2.2				0.9	110.1								
LP 100-10	2.4				53.2	16.8								
LP 100-11	2.6				37.4	0.1								
LP 100-13	3.0				61.8	0.0								
LP 100B-1	3.05				73.5	0.0								
LP 100B-2	3.35				49.5	0.0								
LP 100B-3	3.65				30.8	0.0								
LP 100B-4	3.95				18.7	0.4								
LP 100B-5	4.25				5.6	4.7								
LP 100B-6	4.55				5.3	24.0								
LP 100B-7	4.85				6.3	38.0								
LP 100B-8	5.15				0.8	34.5								
LP 100B-10	5.75				0.0	12.5								
LP 122	6.30													

Appendix A12. Nitrate Isotope Values at Long Point Site on Sept 11, 2008

Well ID	$\delta 15N\text{-}NO_3$(‰)
LP 120-2.8	26.7
LP 120-3.4	19.5
LP 120-3.9	13.55
LP 120-4.6	14.56
LP 121-2.6	11.29
LP 121-3.2	11.89
LP 121-3.8	15.49
LP 121-4.4	16.8
LP 121-6.0	41.16
LP 122-2.2	11.81
LP 122-2.8	9.82
LP 122-3.4	8.77
LP 122-4.6	15.93
LP 122-5.2	17.13
LP 122-6.3	52.38
LP 123-2.6	12.22
LP 123-3.2	9.67
LP 123-3.8	13.08
LP 123-4.5	19.9
LP 123-5.5	22.95
LP 124-4.5	91.28
LP 136-3.1	8.76
LP 136-centre	14.41
LP 138-1.9	21.1
LP 138-2.3	26.77
LP 138-3.1	13.32

Appendix A13. Nitrate Isotope Values for LP-100 at Long Point Site from June, 2009 to Oct, 2009.

Well ID	δ15N-NO3(‰)	δ18O-NO3(‰)	Well ID	δ15N-NO3(‰)	δ18O-NO3(‰)	Well ID	δ15N-NO3(‰)	δ18O-NO3(‰)	Well ID	δ15N-NO3(‰)	δ18O-NO3(‰)
02-Jun-09			24-Jun-09			23-Jul-09			13-Oct-09		
LP 100-7	1.50		LP 100-7	8.15		LP 100-7	2.14		LP 100-9	10.86	-2.13
LP 100-8	1.76	-4.78	LP 100-8	7.84		LP 100-8	3.63	-4.29	LP 100-10	12.58	
LP 100-9	7.48		LP 100-9	8.49	-3.57	LP 100-9	1.36		LP 100-11	19.00	2.52
LP 100-10	7.51	-2.59	LP 100-10	9.07		LP 100B-4	10.98		LP 100-13	36.37	15.55
			LP 100-11	10.44	-5.89	LP 100B-5	11.61	-1.36	LP 100B-1	31.79	11.48
			LP 100-13	12.86	0.13	LP 100B-6	21.06	6.40	LP 100B-6	17.79	1.31
			LP 100B-1	13.34	0.11	LP 100B-7	14.40	1.00	LP 100B-7	17.32	
			LP 100B-2	16.16	5.55	LP 100B-8	35.11	11.42	LP 100B-8	28.67	8.11
			LP 100B-3	11.37		LP 100B-10	27.81		LP 100B-10	31.99	10.97
			LP 100B-4	13.23	3.00				LP 122	39.01	
			LP 100B-5	12.76							
			LP 100B-6	23.37	7.22						
			LP 100B-7	17.42	6.00						
			LP 100B-8	21.10	6.87						
			LP 100B-10	10.05	-0.59						
			LP 122	46.92	18.26						

Appendix A14. NH_4 Isotope Values for LP100 at Long Point Site from June 2009 to August, 2009.

Well ID	DEPTH(m)	δ^{15}N-NH4 (‰)						
		02-Jun-09	24-Jun-09	24-Jun-09 (repeat)		23-Jul-09	13-Aug-09	13-Oct-09
TANK		5.95		4.8	5.3		7.3	
LP 100-7	1.8							
LP 100-8	2.0							
LP 100-9	2.2	29.89	24.72	40.6				
LP 100-10	2.4	11.4	34.93	35.4			10.5	
LP 100-11	2.6	7.13	20.49	20.3				
LP 100-13	3.0	7.03	7.92	7.5				
LP 100B-1	3.05		8.05	7.9			6.8	
LP 100B-2	3.35		6.96	7.3			6.1	
LP 100B-3	3.65						6.6	
LP 100B-4	3.95	27.18					9.0	
LP 100B-5	4.25	25.65	20.01	21.7			8.2	
LP 100B-6	4.55	22.29	21.00	21.5			20.7	
LP 100B-7	4.85						11.6	
LP 100B-8	5.15			19.8			10.6	
LP 100B-10	5.75							
LP 122	6.30	8.28						

Notes:
Stable isotope analyses were conducted by using Elemental Analyzer at the Envrionmental Isotope Laboratory

Samples were prepared at Schiff/Elgood lab

The isotopic composition is expressed in δ units, commonly used for measurement of natural isotope abundance variations:
$\delta^{15}N$ or $\delta^{18}O = 1000*[(R_{sample} - R_{standard})/ R_{standard})]$
where Rsample and Rstandard are the 15N/14N or 18O/16O ratios for the sample and standard. The standards for 15N and 18O are atmospheric nitrogen and VSMOW

Duplicate N2O isotope samples were took in the field. The tables above show the average isotope values of the two duplicate samples.

Appendix B

Detailed geochemistry and Isotope Data at Lake Joseph Site
from June 9, 2009 to September 20, 2009.

Appendix B1. Detailed Geochemistry at Lake Joseph Site on June 9, 2009 (from Rossi 2010, Msc. Thesis).

SAMPLE	T (°C)	EC(µS/cm)	pH	DO (mg/L)	Al (mg/L)	Fe (mg/L)	Ca^{2+}(mg/L)	K^{+}(mg/L)	Mg^{2+}(mg/L)	Na^{+}(mg/L)	NH_4^{+}-N(mg/L)
CB22- 3.7		602	6.1	0.3	<0.005	0.012	32.8	5.7	5.4	47.2	0.016
CB22- 4.0		659	6.1	0.7	<0.005	0.026	40.2	5.1	5.0	46.3	0
CB22- 4.3		579	6.2	7.5	<0.005	0.034	45.6	5.2	5.0	47.5	0.014
CB22- 4.5	9	682	6.3	8.5	<0.005	0.005	29.6	7.8	5.0	45.9	0.027
CB22- 4.9		650	6.4	8.6	<0.005	0.009	32.0	6.4	5.6	44.4	0.025
CB22- 5.2	9	648	6.4	7.6	<0.005	0.005	44.4	6.1	5.5	46.3	0.17
CB23- 3.7		602	6.3	9.3	<0.005	0.004	44.2	5.9	6.7	40.2	0.028
CB23- 4.1		659	6.3	0.4	<0.005	0.015	39.2	6.4	6.8	49.3	0.032
CB23- 4.3		579	6.4	10.8	<0.005	0.016	48.4	5.3	5.7	50.0	0.021
CB23- 4.6		682	6.4	11	<0.005	0.008	42.6	5.5	6.7	53.3	0.021
CB23- 4.9		650	6.4	11.1	<0.005	0.011	50.8	6.0	6.3	50.9	0.027
CB23- 5.2		648	6.4	10.1	<0.005	0.007	52.9	6.0	6.3	60.3	0.002
CB13- 3.5	12	596	6.1	1.1	<0.005	0.019	54.6	5.5	5.7	50.6	0.103
CB13- 4.0		580	6.1	0.6	<0.005	0.023	48.9	4.6	5.1	46.9	0.092
CB13- 4.5		524	6.1	3.5	<0.005	0.012	45.6	4.5	4.8	44.1	0.032
CB13- 5.0		601	6	2.5	<0.005	0.011	39.3	6.4	5.3	50.5	0.029
CB13- 5.4		620	6.4	7.9	<0.005	0.005	42.7	6.1	5.3	50.4	0.032
CB13- 5.9		208	6.6	10.2	<0.005	0.005	20.4	3.4	2.6	15.0	0.03
CB20- 4.3	9	477	6.4	0.7	<0.005	0.008	54.0	4.7	4.7	49.1	0.081
CB20- 4.5		474	6.3	0.5	<0.005	0.008	49.6	5.0	4.7	48.5	0.248
CB20- 4.8		479	6.3	0.3	<0.005	0.019	47.4	5.1	5.2	48.2	0.213
CB20- 5.1		364	6.4	7.2	<0.005	0.006	26.3	4.6	4.0	38.1	0.034
CB20- 5.5		309	6.7	9.4							
CB21- 4.1		560	6	2.4	<0.005	0.006	38.1	6.7	5.4	46.2	0.022

CB21- 4.4		400	6.1	6.3	<0.005	0.005	29.2	4.3	3.9	37.6	0.036
CB21- 4.7		280	6.1	8.8	<0.005	0.008	12.1	2.3	1.9	31.6	0.032
CB21- 5.0		260	5.9	9.5	<0.005	0.036	3.6	1.2	0.5	39.1	0.03
CB21- 5.3		313	5.9	10.6	<0.005	0.004	2.7	0.7	0.5	45.8	0.036
CB21- 5.6		599	5.9	9.1	<0.005	0.002	0.8	1.2	1.8	88.6	0.032
CB3-2.1 (R)	12	188	6.7	10.6	<0.005	0.011	31.8	2.3	5.7	4015.0	0.033
CB tank		820			<0.005	0.051	35.8	13.7	8.2	79.3	44

Appendix B2. Detailed Geochemistry at Lake Joseph Site on June 9, 2009 (continued) (from Rossi 2010, Msc. Thesis).

SAMPLE	F^- (mg/L)	Cl^-(mg/L)	NO_2^-(mg/L)	Br^-(mg/L)	PO_4^{3-} (mg/L)	NO_3^--N(mg/L)	SO_4^{2-}--S(mg/L)	DOC (ppm)	DIC (ppm)	N2O-N(µg/L)
CB22- 3.7	0.03	71.5	0.07	<0.02	0.14	1.4	51.4	3.3	4	0.0
CB22- 4.0	0.03	71.4	<0.01	0.1	<0.02	2.3	73.7	3.1	21	3.9
CB22- 4.3	0.03	72.3	<0.01	0.1	<0.02	2.4	73.6	3.4	13	4.8
CB22- 4.5	0.03	77.5	<0.01	0.14	0.18	2.6	70.1	2.9	10	8.7
CB22- 4.9	0.03	80.8	0.07	0.14	0.21	2.3	72.9	2.5	10	9.1
CB22- 5.2	0.03	77.3	<0.01	0.12	0.22	2.7	74.7	2.5	11	6.9
CB23- 3.7	<0.004	74.2	<0.01	<0.02	<0.02	6.2	73.1	2.5	9	6.3
CB23- 4.1	<0.004	80.3	<0.01	<0.02	<0.02	2.8	91.5	2.6	11	5.1
CB23- 4.3	<0.004	64.2	<0.01	<0.02	<0.02	5.1	76.3	2.4	13	4.3
CB23- 4.6	0.04	88.7	<0.01	0.13	<0.02	3.8	82.3	2.5	13	4.7
CB23- 4.9	<0.004	81.6	<0.01	<0.02	<0.02	4.1	89.7	2.4	12	4.3
CB23- 5.2	0.03	90.5	<0.01	0.14	0.16	3.3	77.9	2.3	11	5.9
CB13- 3.5	<0.004	70.0	<0.01	<0.02	<0.02	6.7	68.5	3.2	17	40.0
CB13- 4.0	<0.004	61.3	<0.01	<0.02	<0.02	6.0	58.7	3.6	16	10.8
CB13- 4.5	<0.004	48.9	<0.01	<0.02	0.45	5.9	49.9	3.6	18	5.6
CB13- 5.0	<0.004	71.3	<0.01	<0.02	<0.02	3.5	74.3	3.6	15	7.6
CB13- 5.4	0.04	72.7	<0.01	<0.02	<0.02	6.8	66.3	3.6	13	20.2
CB13- 5.9	0.06	14.5	<0.01	<0.02	<0.02	2.2	13.7	3.9	11	3.7
CB20- 4.3	<0.004	68.6	<0.01	<0.02	<0.02	5.8	61.2	3.4	18	0.1
CB20- 4.5	<0.004	70.6	<0.01	<0.02	<0.02	6.2	60.3	3.5	18	
CB20- 4.8	<0.004	71.3	1.26	<0.02	4.47	4.9	67.2	4	21	0.1
CB20- 5.1	<0.004	65.5	<0.01	<0.02	<0.02	3.1	43.0	2.9	11	11.0
CB20- 5.5										

CB21- 4.1	<0.004	66.1	<0.01	<0.02	<0.02	6.2	59.3	3.8	-	13.3
CB21- 4.4	<0.004	44.4	<0.01	<0.02	0.11	2.7	46.2	3.1	15	9.3
CB21- 4.7	0.04	36.6	<0.01	<0.02	0.07	1.1	24.4	2.1	12	5.9
CB21- 5.0	0.05	48.6	<0.01	<0.02	<0.02	0.1	13.9	1.1	5	0.9
CB21- 5.3	0.05	54.2	<0.01	<0.02	<0.02	0.1	22.0	1.5	3	0.9
CB21- 5.6	0.04	125.3	<0.01	0.08	0.13	0.4	24.0	1.1	2	1.7
CB3-2.1 (R)	0.04	5.3	<0.01	<0.02	<0.02	2.7	25.1	3.2	11	6.3
CB tank	0.17	110.7	<0.01	<0.02	11.62	0.0	52.0	7.8	48	0.7

Appendix B3. Detailed Geochemistry at Lake Joseph Site on July 27, 2009 (from Rossi 2010, Msc. Thesis).

SAMPLE	EC(µS/cm)	DO(mg/L)	pH	Al (mg/L)	Ca^{2+} (mg/L)	Fe (mg/L)	K^{+} (mg/L)	Mg^{2+} (mg/L)	Na^{+}(mg/L)	N-NH4(mg/L)
CB tank	984		6.9	<0.005	50.9	0.111	10.5	8.9	82.1	21.6
CB 1-2.0	26	9.5	7.1	<0.005	2.6	<0.005	1.1	0.5	1.2	0
CB 1-2.2	29		6.7							
CB 2-2.8	414	4.0	6.5	<0.005	47.9	0.741	4.6	6.3	54.4	0.04
CB 2-3.3	510	3.5	6.5	<0.005	48.9	0.023	4.3	5.8	38.2	0.02
CB 2-3.8	215	8.5	6.7	<0.005	23.3	0.008	3.2	2.9	25.3	0.02
CB 2-4.3	350	9.9	6.6							
CB 3-2.1	547		6.97	<0.005	88.7	<0.005	10.9	7.6	<0.005	0.01
CB 13-3.5	480	4.2	6.3	<0.005	42.3	0.013	4.2	4.6	41.9	0.03
CB 13-4.0	579	0.6	6.1	<0.005	48.8	0.005	5.4	5.6	51.5	0.02
CB 13-4.5	550	1.1	6.1	<0.005	50.6	0.036	5.5	5.5	50.7	0.03
CB 13-5.0	409	9.2	6.4	<0.005	34.3	<0.005	5.1	4.0	32.8	0.02
CB 13-5.4	612	10.3	6.5	<0.005	56.2	<0.005	6.8	6.5	47.4	0.02
CB 13-5.9	124	11.4	6.9	<0.005	16.8	<0.005	2.8	2.0	7913.0	0.04
CB 20-4.3	570	0.3	6.3	<0.005	48.5	0.024	5.1	5.3	52.5	0.06
CB 20-4.5	569	0.2	6.3	<0.005	49.0	<0.005	5.5	5.6	47.3	0.05
CB 20-4.8	539	1.0	6.4	<0.005	47.8	<0.005	4.8	5.4	40.8	0.06
CB 20-5.1	353	9.9	6.5	<0.005	30.2	<0.005	4.1	3.6	29.8	0.02
CB 20-5.5	250	11.1	6.5	<0.005	21.9	<0.005	3.1	2.2	17.3	0.02
CB 21-4.1	509	0.7	6.3	<0.005	46.4	0.032	6.1	5.6	41.2	0.02
CB 21-4.4	361	9.4	6.4	<0.005	29.8	0.002	3.4	3.5	32.0	0.02
CB 21-4.7	315	10.7	6.3	<0.005	18.2	<0.005	2.2	2.3	33.6	0.02

CB 21-5.0	215	10.7	6.1	<0.005	5.5	0.017	1.1	0.7	32.0	0.02
CB 21-5.3	145			<0.005	5.3	<0.005	0.7	1.2	24.1	0.02
CB 21-5.6	391	10.8	6.1	<0.005	5.8	<0.005	1.1	1.3	57.6	0.03
CB 22-3.7	532	0.7	6.6	<0.005	48.1	0.121	8.4	6.7	48.5	3
CB 22-4.0	372	1.9	6.6	<0.005	31.5	0.044	4.9	3.6	30.9	0.02
CB 22-4.3	403	9.2	6.6	<0.005	36.0	<0.005	5.1	4.2	30.1	0.02
CB 22-4.5	489	10.8	6.5	<0.005	45.5	<0.005	5.4	5.1	34.1	0.02
CB 22-4.9	207	11.3	7	<0.005	9.9	0.026	3.0	1.0	31.5	0.03
CB 22-5.2	753	10.7	6.6	<0.005	38.7	0.005	5.4	4.3	56.8	0.1
CB 23-3.7	538	8.1	6.5	<0.005	59.9	0.033	5.2	7.2	29.5	0.03
CB 23-4.1	558	8.9	6.5	<0.005	44.4	<0.005	5.5	4.9	51.5	0.02
CB 23-4.3	681	9.8	6.4	<0.005	59.0	<0.005	6.9	7.6	53.3	0.02
CB 23-4.6	750	9.3	6.4	<0.005	63.5	<0.005	7.3	7.9	56.6	0.02
CB 23-4.9	703	10.0	6.5	<0.005	61.3	0.013	6.7	7.6	55.2	0.03
CB 23-5.2	616	10.2	6.6	<0.005	54.5	0.109	6.1	6.8	49.9	0.44

Appendix B4. Detailed Geochemistry at Lake Joseph Site on July 27, 2009 (continued) (from Rossi 2010, Msc. Thesis).

SAMPLE	Cl (mg/L)	NO2-N(mg/L)	NO3-N (mg/L)	TN/Cl	SO4-S(mg/L)	DOC ppm	DIC ppm	N2O-N(µg/L)
CB tank	98.4	n.a.	< det	0.22	45.6	9.9	42	0.4
CB 1-2.0	0.2	n.a.	< det		0.7	1.4	1	0.5
CB 1-2.2								
CB 2-2.8	53.5	0.48	5.0	0.09	16.5	5.5	21	7.5
CB 2-3.3	41.1	n.a.	3.3	0.08	15.4	2.2	18	10.6
CB 2-3.8	18	n.a.	1.2	0.07	12.1	2.8	10	2.7
CB 2-4.3								
CB 3-2.1	3.6	n.a.	3.2	0.89	67.4	15.5	22	2.0
CB 13-3.5	34.2	n.a.	1.9	0.06	32.0	2.9	10	1.3
CB 13-4.0	44.4	n.a.	0.5	0.01	18.4	3.7	22	0.6
CB 13-4.5	40	n.a.	0.2	0.01	11.4	5.7	29	0.1
CB 13-5.0	36.7	n.a.	0.8	0.02	7.0	4.2	8	1.6
CB 13-5.4	73.8	n.a.	1.6	0.02	53.6	2.4	10	6.2
CB 13-5.9	5.9	n.a.	0.9	0.15	6.4	5.7	7	2.5
CB 20-4.3	58.1	n.a.	0.2	0.00	33.9	3.7	26	0.0
CB 20-4.5	47.8	n.a.	2.1	0.05	50.1	3.4	18	0.1
CB 20-4.8	48.7	n.a.	4.5	0.09	71.0	2.5	10	1.0
CB 20-5.1	40.7	n.a.	2.2	0.05	35.8	2.9	9	4.0
CB 20-5.5	23.8	n.a.	1.2	0.05	16.2	2.5	8	3.2
CB 21-4.1	44.6	n.a.	1.5	0.03	48.0	4.1	25	1.9
CB 21-4.4	39.9	n.a.	2.0	0.05	40.2	2.5	9	2.6
CB 21-4.7	46.9	n.a.	0.1	0.00	24.4	1.9	5	0.8

CB 21-5.0	39.4	n.a.	0.1	0.00	19.0	1.1	3	0.3
CB 21-5.3	27.7	n.a.	0.1	0.00	10.1	1.3	2	0.6
CB 21-5.6	80.8	n.a.	0.1	0.00	12.5	0.7	3	0.9
CB 22-3.7	57.6	n.a.	3.0	0.10	19.6	9.4	29	2.2
CB 22-4.0	30.5	n.a.	7.9	0.26	33.2	3.5	10	3.3
CB 22-4.3	37	n.a.	6.8	0.18	31.3	2.7	10	1.4
CB 22-4.5	58.6	n.a.	4.9	0.08	40.1	2.3	10	0.9
CB 22-4.9	10.2	n.a.	2.9	0.29	22.7	6.6	7	2.6
CB 22-5.2	107.1	n.a.	0.9	0.01	14.5	7.6	10	2.1
CB 23-3.7	24	n.a.	28.2	1.18	41.1	3.1	10	53.9
CB 23-4.1	66.8	n.a.	3.9	0.06	43.0	2.6	15	19.9
CB 23-4.3	89.5	n.a.	10.1	0.11	37.9	3.6	15	15.6
CB 23-4.6	107.4	n.a.	8.2	0.08	50.5	2.2	17	6.4
CB 23-4.9	81.2	n.a.	11.3	0.14	46.0	2.3	17	2.5
CB 23-5.2	68.8	n.a.	11.3	0.17	49.4	2.7	17	16.5

Appendix B5. Detailed Geochemistry at Lake Joseph Site on Aug 30, 2009 (from Rossi 2010, Msc. Thesis).

SAMPLE	F^- (mg/L)	Cl^- (mg/L)	SO4-S(mg/L)	Br^- (mg/L)	NO_3^--N (mg/L)	NH4-N (mg/L)	Al(mg/L)	Ca^{2+}(mg/L)	Fe(mg/L)	K(mg/L)	Mg^{2+}(mg/L)	Na^+(mg/L)
CB 13-3.5	0.044	87.6	5.6	0.7	2.7	0.2	<0.005	58.6	0.0	8.3	4.6	53.0
CB 13-4.0	0.052	107.5	1.0	1.5	0.0	4.7	<0.005	67.2	0.0	16.7	7.3	70.4
CB 20-4.3	0.027	105.8	8.9	0.9	2.6	0.3	<0.005	64.4	0.0	12.2	7.6	64.8
CB 20-4.5						0.7						
CB 22-3.7	2,079	120.5	0.5	3.0	0.0	26.3	<0.005	60.6	68.7	13.3	5.2	78.3
CB 22-4.0	0.119	140.1	1.2	0.1	0.1	4.7	<0.005	101.5	0.8	16.6	10.1	90.3
CB tank						27.4						

Appendix B6. Detailed Geochemistry at Lake Joseph Site on Sept 20. 2009 (from Rossi 2010, Msc. Thesis).

SAMPLE	EC(µS/cm)	DO (mg/L)	T°C	Al (mg/L)	Ca^{2+}(mg/L)	Fe (mg/L)	K^{+}(mg/L)	Mg^{2+}(mg/L)	Na^{+}(mg/L)
CB tank	835		17.5	<0.005	35.1	0.052	8.2	7.3	78.4
CB 1-2.0	41.2	8.1	16	<0.005	3.0	0.004	1.0	0.4	1.2
CB 2-3.3	718	3.7	13.3	<0.005	63.4	0.046	5.5	7.5	54.9
CB 2-3.8	706	7.8	12.9	<0.005	57.5	0.011	6.7	8.2	41.9
CB 2-4.3	240	9.0	12.8						
CB 13-3.5	907	0.4	13.5	<0.005	72.2	0.157	13.1	9.3	74.0
CB 13-4.0	924	0.4	13.6	<0.005	60.7	0.202	16.6	10.5	75.5
CB 13-4.5	747	0.4		<0.005	60.3	1,271	10.7	7.0	61.2
CB 13-5.0	789	0.4	12.6	<0.005	64.7	0.028	8.8	7.4	77.9
CB 13-5.4	566	8.5	12.4	<0.005	58.6	0.046	6.6	5.4	44.4
CB 13-5.9	382	10.5	11.6	<0.005	43.9	0.004	5.0	4.3	26.2
CB 20-4.3	837	0.4	11.2	<0.005	74.4	0.016	15.0	9.1	57.9
CB 20-4.5	777	0.4	11.3	<0.005	54.9	0.041	12.6	7.6	62.4
CB 20-4.8	737	0.5	11.2	<0.005	63.4	0.022	9.3	7.1	59.6
CB 20-5.1	642	0.6	10.9	<0.005	56.1	0.011	7.2	6.8	51.9
CB 21-4.1	798	0.5	10.3	<0.005	76.9	0.408	10.0	8.2	70.5
CB 21-4.4	615	1.1	10	<0.005	52.5	0.077	5.4	6.5	51.7
CB 21-4.7	234	9.2	10.1	<0.005	14.6	0.008	1.2	1.4	24.5
CB 21-5.0	266	10.2	9.9	<0.005	9.7	<0.002	0.8	1.2	34.3
CB 21-5.3	209	10.4	9.8	<0.005	7.2	<0.002	0.6	1.0	26.9
CB 21-5.6	157.8	10.4	10.5	<0.005	2.2	<0.002	0.5	0.5	24.5
CB 22-3.7	945	0.5	17	<0.005	42.9	31	10.6	4.8	73.7

CB 22-4.0	923	0.5	16.2	<0.005	49.6	24	12.4	5.8	76.9
CB 22-4.3	923	0.5	17	<0.005	51.6	0.101	21.7	6.7	72.7
CB 22-4.6	760	0.5	16	<0.005	45.3	0.046	22.4	5.3	69.8
CB 22-4.9	718	0.6	15.4	<0.005	68.1	0.005	7.8	8.0	51.3
CB 22-5.2	664	4.8	15.9	<0.005	64.3	<0.002	7.0	7.3	39.8
CB 23-3.7	790	6.4	16.5	<0.005	63.6	0.002	10.1	7.2	65.3
CB 23-4.1	815	5.7	15.8	<0.005	57.1	0.007	9.3	5.9	79.4
CB 23-4.3	809	0.6	15.8	<0.005	60.4	0.005	10.6	6.2	72.8
CB 23-4.6	797	3.4	15.9	<0.005	57.8	0.003	8.2	6.2	70.6
CB 23-4.9	875	4.3	15.1	<0.005	66.4	<0.002	8.2	7.7	73.6
CB 23-5.2	826	5.1	14.5	<0.005	65.1	0.011	7.7	7.9	64.3

Appendix B7. Detailed Geochemistry at Lake Joseph Site on Sept 20. 2009 (continued) (from Rossi 2010, Msc. Thesis).

SAMPLE	Cl^-(mg/L)	SO_4^{2-}-S(mg/L)	Br^-(mg/L)	NO_3^--N(mg/L)	NH_4^+-N(mg/L)	TN/Cl	DOC ppm	DIC ppm	N2O-N (µg/L)
CB tank	113.1	9.55	1.19	0.3	12	0.11	20	34	3.7
CB 1-2.0	1.2	0.74	n.a.	0.1	0.005	0.06	1.3	1	
CB 2-3.3	94.7	12.3	0.58	13.5	0.786	0.15	2.5	30	42.6
CB 2-3.8	93.5	12.29	0.41	19.7	0	0.21	2.4	17	47.5
CB 2-4.3									
CB 13-3.5	116.1	2.15	1.2	0.3	3	0.03	19.9	58	0.4
CB 13-4.0	113.9	1.46	0.08	n.a.	6		31.8	67	0.2
CB 13-4.5	100.1	7.93	0.89	3.1	-		6.2	45	83.6
CB 13-5.0	119.5	2.27	2.47	0.0	0.034	0.00	5.8	57	5.3
CB 13-5.4	76	14.74	0.42	7.4	0.001	0.10	2.6	17	
CB 13-5.9	50.3	9.53	n.a.	4.6	0.002	0.09	2.7	10	
CB 20-4.3	105.8	8.95	0.77	12.9	8	0.20	4.7	44	2.2
CB 20-4.5	104	4.54	1.11	0.5	2	0.03	5.9	55	0.2
CB 20-4.8	105.9	4.92	2.31	0.0	0.752	0.01	4.6	48	0.1
CB 20-5.1	92.5	5.77	0.81	2.4	0.002	0.03	3.7	38	
CB 21-4.1	111.7	1.19	0.07	0.0	0.087	0.00	9.5	58	0.0
CB 21-4.4	90.4	5.23	0.78	1.5	0	0.02	4.1	42	
CB 21-4.7	27.2	4.85	n.a.	0.9	0.004	0.03	2.8	9	
CB 21-5.0	42.4	7.96	n.a.	0.9	0.004	0.02	1.3	5	
CB 21-5.3	30.1	7.57	n.a.	0.7	0.002	0.02	0.9	5	
CB 21-5.6	20.9	5.91	n.a.	0.1	0.002	0.00	1	5	
CB 22-3.7	110.6	n.a.	2.44	0.0	0.154	0.00	23	52	0.2

CB 22-4.1	115.5	1.03	0.15	0.0	0.047	0.00	33.3	58	0.1
CB 22-4.3	115.3	1.11	0.06	0.0	0.042	0.00	11.4	57	
CB 22-4.6	110.6	1.71	2.39	n.a.	0.001		6	46	0.1
CB 22-4.9	87.7	9.29	0.75	6.8	0.002		3.7	38	
CB 22-5.2	74.3	10.55	0.36	24.2	0.171		2	14	
CB 23-3.7	118.1	13.44	0.56	16.0	12	0.24	2.7	24	68.2
CB 23-4.0	127	4.79	0.67	15.3	12	0.22	3.7	34	
CB 23-4.3	113.6	8.51	0.54	22.6	-		3.1	26	77.9
CB 23-4.6	107.7	10.48	0.57	17.4	2	0.18	2.7	25	
CB 23-4.9	115.6	11.12	0.57	22.0	0.676	0.20	3	27	105.9
CB 23-5.2	109.5	12.78	0.58	18.0	0.077	0.16	3.5	25	

Appendix B8. NO3 Isotope Values at Lake Joseph Site in June, 2009 and July 2009, respectively (from Rossi 2010, Msc. Thesis).

Well ID	δ15N-NO3(‰)	δ18O-NO3(‰)	Well ID	δ15N-NO3(‰)	δ18O-NO3(‰)
09-Jun-09			27-Jul-09		
CB22- 3.7	29.77	10.62	CB 2-2.8	7.63	-5.21
CB22- 4.0	14.26	1.13	CB 2-3.3	6.2	-4.27
CB23- 3.7	0.95	-5.58	CB 2-3.8	2.98	-3.64
CB23- 4.3	1.3	-4.18	CB 13-3.5	3.78	-3.53
CB13- 3.5	12.19	-0.09	CB 13-5.0	3.64	-0.56
CB13- 4.0	9.56	-0.01	CB 20-4.5	8.16	-0.22
CB13- 5.4	4.41	-5.28	CB 20-4.8	4.65	-2.26
CB20- 4.3	10.55	0.76	CB 21-4.4	8.54	0.92
CB20- 4.5	9.1	-0.33	CB 22-3.7	2.82	-2.49
CB20- 4.8	8.52	-0.28	CB 22-4.0	-0.15	-5.41
CB21- 4.1	8.77	0.05	CB 22-4.3	2.38	-5.26
			CB 22-4.6	1.23	-4.89
			CB 23-3.7	3.52	-5.90
			CB 23-4.1	1.39	-6.09
			CB 23-4.3	9.55	-5.23
			CB 23-4.6	5.29	-4.84
			CB 23-4.9	8.74	-6.33
			CB 23-5.2	6.23	-6.68

Appendix B9. $^{15}N\text{-}NH_4$ Isotope Values at Lake Joseph Site from June 2009 to Aug, 2009 (from Rossi 2010, Msc. Thesis).

Well ID	($^{15}N\text{-}NH_4$) (‰)	Avg ($^{15}N\text{-}NH_4$) (‰)	NH_4-N (mg/L)	Date of sampling
CB tank A	5.26	4.8	44	June 12/09
CB tank B	4.33			June 12/09
CB tank C	4.82		21.6	July 28/09
CB tank D	Lost			July 28/09
CB 22-3.7A	8.4	8.1	3	July 28/09
CB 22-3.7B	7.72			July 28/09
CB tank A	6.5	6.8	27.37	Aug. 30/09
CB tank B	7.1			Aug. 30/09
CB 13-4.0 A	5.6	7.7	4.68	Aug. 30/09
CB 13-4.0 B	9.7			Aug. 30/09
CB 22-3.7 A	6.3	6.8	26.27	Aug. 30/09
CB 22-3.7 B	7.3			Aug. 30/09
CB 22-4.0 A	9.1	8.7	4.73	Aug. 30/09
CB 22-4.0 B	8.3			Aug. 30/09
CB 20-4.5 A	7	9.4	0.67	Aug. 30/09
CB 20-4.5 B	11.8			Aug. 30/09

Notes:
A, B, C, D indicates samples were repeatedly analyzed.

Notes:

Stable isotope analyses were conducted by using Elemental Analyzer at the Envrionmental Isotope Laboratory

Samples were prepared at Schiff/Elgood lab

The isotopic composition is expressed in δ units, commonly used for measurement of natural isotope abundance variations:
$\delta^{15}N$ or $\delta^{18}O = 1000*[(R_{sample} - R_{standard})/ R_{standard})]$
where Rsample and Rstandard are the 15N/14N or 18O/16O ratios for the sample and standard. The standards for 15N and 18O are atmospheric nitrogen and VSMOW

Duplicate N2O isotope samples were took in the field. The tables above show the average isotope values of the two duplicate samples.

Appendix C

Detailed geochemistry and Isotope Data at Strathroy Site on October 15, 2009.

Appendix C1. Detailed Geochemistry at Strathroy Site on Oct 15, 2009.

Well ID	DEPTH (m)	Temp (ºC)	EC (us/cm)	E°	pH	Cl (mg/L)	NO2-N (mg/L)	Br (mg/L)	NO3-N (mg/L)	DO (mg/L)	SO4-S (mg/L)	DOC (mg C/L)	N_2O % Saturation	N2O-N(µg/L)
SR 3-3.0	3.0		DRY	342										
SR 3-3.6	3.6	11.6	387	190	7.2	1.82	n.a.	0.00	4.55	8.2	2.01	1.1	141	0.9
SR 3-3.9	3.9	11.4	427	178	7.47	4.48	n.a.	0.00	6.87	8.8	2.18	1.3	246	0.8
SR 3-4.6	4.6	11.1	456	190	7.27	6.24	n.a.	n.a.	7.28	10.7	1.44	1.0	157	0.5
SR 3-5.6	5.6	10.5	551	171	7.30	2.37		0.01	11.49	6.3	2.67	0.7	974	3.3
SR 3-6.7	6.7	10.1	576	109	7.34	2.97		0.01	10.21	0.3	12.77	2.0	601	2.1
SR 3-7.7	7.7	9.8	673	-8	7.34	11.40	n.a.	0.09	0.02	0.3	24.08	0.9	30	0.1
SR 3-8.7	8.7	9.8	682	-5	7.26	17.19	n.a.	0.21	0.00	0.3	20.73	1.0	9	0.0
SR 3-10.3	10.3	9.6	693	-40	7.22	17.15	n.a.	0.08	0.04	0.4	19.85	1.6	21	0.1
SR 3-11.8	11.8	9.8	679	-46	7.26	10.32	n.a.	0.09	0.05	0.4	18.79	3.4	19	0.1
SR 3-13.3	13.3	9.6	674	-39	7.34	9.49	n.a.	0.24	0.00	0.2	19.33	1.0	9	0.0
SR 3-14.8	14.8	9.7	680	-200	7.28	9.43	n.a.	0.10	0.03	0.2	20.34	0.7	21	0.1

Appendix C2. NO3 isotope values at Strathroy Site on Oct 15, 2009.

Well ID	Averge δ15N-NO3(‰)	Averge δ18O-NO3(‰)
09-Jun-09		
SR3-3.6	3.37	
SR3-3.9	3.26	-3.02
SR3-4.6	2.22	
SR3-5.6	3.54	-0.03
SR3-6.7	25.41	15.48

Notes:

Stable isotope analyses were conducted by using Elemental Analyzer at the Envrionmental Isotope Laboratory

Samples were prepared at Schiff/Elgood lab

The isotopic composition is expressed in δ units, commonly used for measurement of natural isotope abundance variations:
$\delta^{15}N$ or $\delta^{18}O = 1000*[(R_{sample} - R_{standard})/ R_{standard})]$
where Rsample and Rstandard are the 15N/14N or 18O/16O ratios for the sample and standard. The standards for 15N and 18O are atmospheric nitrogen and VSMOW

Duplicate N2O isotope samples were took in the field. The tables above show the average isotope values of the two duplicate samples.

Appendix D

Detailed geochemistry and Isotope Data at Woodstock Site on July 4, 2008.

Appendix D1. Detailed Geochemistry and Isotope Values at Woodstock Site on July 4, 2008.

Well ID	Depth (m)	Cl (mg/L)	SO4-S (mg/L)	NO3-N (mg/L)	δ^{15}N-NO3 (‰)	N2O-N(µg/L)
WO-11-6m	6	27.1	6.2	11.1	5.32	19.93
WO-11-8m	8	41.0	9.6	13.5	4.04	29.97
WO-11-10m	10	54.1	13.6	15.7	6.92	49.02
WO-11-13m	13	15.3	28.8	0.1	7.02	45.05
WO-74-1	3.96	4.3*	3.2*	2.6*	5.90	14.57
WO-74-2	5.49	33.1	12.1	15.0	7.29	39.54
WO-74-3	7.01	33.0	12.2	15.2	6.68	39.09
WO-74-4	8.53	33.0	12.2	14.9	5.41	39.51
WO-74-5	10.36	42.9	12.7	14.0	6.06	39.91
WO-74-6	12.80	42.8	12.7	13.8	6.82	40.45
WO-74-7	14.63	33.1	12.2	15.0	6.94	39.35

Appendix D2. NO_3 isotope values at Woodstock Site (Adapted from Koch, 2009 pp.77 Table.6)

well ID	δ^{15}N-NO3 (‰)	δ^{18}O-NO3 (‰)
WO 11-6	5.32	-0.29
WO 11-8	6.13	0.24
WO 11-13	6.76	1.13
WO 74-Shallow	6.35	0.83
WO 74-Deep	6.3	1.68

Notes:
* samples re-analyzed on June 16, 2010

Stable isotope analyses were conducted by using Elemental Analyzer at the Envrionmental Isotope Laboratory

Samples were prepared at Schiff/Elgood lab

The isotopic composition is expressed in δ units, commonly used for measurement of natural isotope abundance variations:
$\delta^{15}N$ or $\delta^{18}O = 1000*[(R_{sample} - R_{standard})/ R_{standard})]$
where Rsample and Rstandard are the 15N/14N or 18O/16O ratios for the sample and standard. The standards for 15N and 18O are atmospheric nitrogen and VSMOW

Duplicate N2O isotope samples were took in the field. The tables above show the average isotope values of the two duplicate samples.